

ARMY RESEARCH LABORATORY



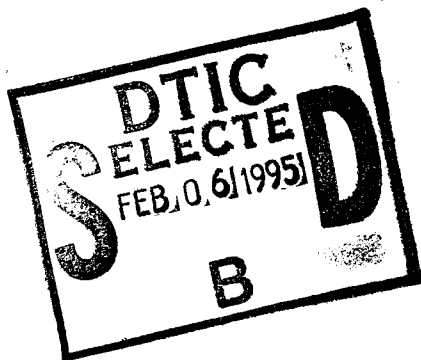
Comparison of Boundary-Layer Wind and Temperature Measurements with Model Estimations

**by Richard Okrasinski
Physical Science Laboratory**

**Robert Olsen
Arnold Tunick
Battlefield Environment Directorate**

ARL-CR-112

November 1994



19950201 072

NOTICES

Disclaimers

The findings in this report are not to be construed as an official Department of the Army position, unless so designated by other authorized documents.

The citation of trade names and names of manufacturers in this report is not to be construed as official Government indorsement or approval of commercial products or services referenced herein.

Destruction Notice

When this document is no longer needed, destroy it by any method that will prevent disclosure of its contents or reconstruction of the document.

REPORT DOCUMENTATION PAGE			Form Approved OMB No. 0704-0188	
Public reporting burden for this collection of information is estimated to average 1 hour per response, including the time for reviewing instructions, searching existing data sources, gathering and maintaining the data needed, and completing and reviewing the collection of information. Send comments regarding this burden estimate or any other aspect of this collection of information, including suggestions for reducing this burden, to Washington Headquarters Services, Directorate for Information Operations and Reports, 1215 Jefferson Davis Highway, Suite 1204, Arlington, VA 22202-4302, and to the Office of Management and Budget, Paperwork Reduction Project (0704-0188), Washington, DC 20503.				
1. AGENCY USE ONLY (Leave blank)	2. REPORT DATE November 1994	3. REPORT TYPE AND DATES COVERED Final		
4. TITLE AND SUBTITLE Comparison of Boundary-Layer Wind and Temperature Measurements with Model Estimations			5. FUNDING NUMBERS	
6. AUTHOR(S) Richard Okrasinski, Robert Olsen, and Arnold Tunick				
7. PERFORMING ORGANIZATION NAME(S) AND ADDRESS(ES) Physical Science Laboratory New Mexico State University Las Cruces, NM 88003			8. PERFORMING ORGANIZATION REPORT NUMBER ARL-CR-112	
9. SPONSORING/MONITORING AGENCY NAME(S) AND ADDRESS(ES) U.S. Army Research Laboratory Battlefield Environment Directorate ATTN: AMSRL-BE-S White Sands Missile Range, NM 88002			10. SPONSORING/MONITORING AGENCY REPORT NUMBER ARL-CR-112	
11. SUPPLEMENTARY NOTES				
12a. DISTRIBUTION / AVAILABILITY STATEMENT Approved for public release; distribution is unlimited.			12b. DISTRIBUTION CODE	
13. ABSTRACT (Maximum 200 words) Five simple models that estimate vertical profiles of wind speed or temperature in the boundary layer were evaluated by comparing the predictions with measured data. The models evaluated consist of three Monin-Obukhov similarity algorithms for predicting wind speed and temperature, a p-profile algorithm for estimating wind speed, and an inversion algorithm for estimating temperature. The data for the study was collected by towers, sodars, and radiosondes at four field experiments in 1990 and 1991. Using one or two levels of the tower measurements, wind speed, and temperatures were predicted at several measurement heights. The predicted and measured data were statistically compared. The results are presented in this report showing the comparability of the model predictions as a function of height above the surface and time of day.				
14. SUBJECT TERMS similarity, boundary layer			15. NUMBER OF PAGES 155	
			16. PRICE CODE	
17. SECURITY CLASSIFICATION OF REPORT unclassified	18. SECURITY CLASSIFICATION OF THIS PAGE unclassified	19. SECURITY CLASSIFICATION OF ABSTRACT unclassified	20. LIMITATION OF ABSTRACT SAR	

Contents

Executive Summary	9
1. Introduction	11
2. Instrument Description and Data Collection	13
3. Description of the Models	17
3.1 <i>Similarity Models</i>	17
3.2 <i>P-Profile</i>	22
3.3 <i>Inversion Model</i>	22
4. Comparison of Model Estimates with Measured Data	25
4.1 <i>Tower Data Comparison</i>	25
4.2 <i>Sodar Data Comparison</i>	51
4.3 <i>Radiosonde Data Comparison</i>	89
5. Summary	139
References	141
Distribution	143

Accession For	
NTIS GRA&I	<input checked="" type="checkbox"/>
DTIC TAB	<input type="checkbox"/>
Unannounced	<input type="checkbox"/>
Justification	
By	
Distribution/	
Availability Codes	
Dist	Avail and/or Special
A-1	

FOR OFFICIAL USE ONLY

Figures

1. Rms differences between measured 4-m wind speeds and values estimated from 2- and 8-m measurements using three Monin-Obukhov similarity algorithms	33
2. Rms differences between measured 16-m wind speeds and values estimated from 2- and 8-m measurements using three Monin-Obukhov similarity algorithms	34
3. Rms differences between measured 30-m wind speeds and values estimated from 2- and 8-m measurements using three Monin-Obukhov similarity algorithms	35
4. Rms differences between measured 4-m temperatures and values estimated from 2- and 8-m measurements using three Monin-Obukhov similarity algorithms	36
5. Rms differences between measured 16-m temperatures and values estimated from 2- and 8-m measurements using three Monin-Obukhov similarity algorithms	37
6. Rms differences between measured 30-m temperatures and values estimated from 2- and 8-m measurements using three Monin-Obukhov similarity algorithms	38
7. Rms differences between measured 4-m wind speeds and values estimated from 2- and 8-m measurements using Monin-Obukhov similarity, a linear interpolation, and a p-profile fit	45
8. Rms differences between measured 16-m wind speeds and values estimated from 2- and 8-m measurements using Monin-Obukhov similarity, a linear extrapolation, and a p-profile fit	46
9. Rms differences between measured 30-m wind speeds and values estimated from 2- and 8-m measurements using Monin-Obukhov similarity, a linear extrapolation, and a p-profile fit	47
10. Rms differences between measured 4-m temperatures and values estimated from 2- and 8-m measurements using Monin-Obukhov similarity and a linear interpolation	48
11. Rms differences between measured 16-m temperatures and values estimated from 2- and 8-m measurements using Monin-Obukhov similarity and a linear extrapolation	49
12. Rms differences between measured 30-m temperatures and values estimated from 2- and 8-m measurements using Monin-Obukhov similarity and a linear extrapolation	50
13. Rms differences between 50-m sodar wind speed measurements collected at WSMR and values estimated from 2- and 10-m mast data using Monin-Obukhov similarity and a p-profile fit	59
14. Rms differences between 100-m sodar wind speed measurements collected at WSMR and values estimated from 2- and 10-m mast data using Monin-Obukhov similarity and a p-profile fit	60

Figures (continued)

15. Rms differences between 150-m sodar wind speed measurements collected at WSMR and values estimated from 2- and 10-m mast data using Monin-Obukhov similarity and a p-profile fit	61
16. Rms differences between 200-m sodar wind speed measurements collected at WSMR and values estimated from 2- and 10-m mast data using Monin-Obukhov similarity and a p-profile fit	62
17. Rms differences between 300-m sodar wind speed measurements collected at WSMR and values estimated from 2- and 10-m mast data using Monin-Obukhov similarity and a p-profile fit	63
18. Rms differences between 400-m sodar wind speed measurements collected at WSMR and values estimated from 2- and 10-m mast data using Monin-Obukhov similarity and a p-profile fit	64
19. Rms differences between 60-m sodar wind speed measurements collected at Ft. Bliss and values estimated from 2- and 10-m mast data using Monin-Obukhov similarity and a p-profile fit	71
20. Rms differences between 110-m sodar wind speed measurements collected at Ft. Bliss and values estimated from 2- and 10-m mast data using Monin-Obukhov similarity and a p-profile fit	72
21. Rms differences between 160-m sodar wind speed measurements collected at Ft. Bliss and values estimated from 2- and 10-m mast data using Monin-Obukhov similarity and a p-profile fit	73
22. Rms differences between 210-m sodar wind speed measurements collected at Ft. Bliss and values estimated from 2- and 10-m mast data using Monin-Obukhov similarity and a p-profile fit	74
23. Rms differences between 310-m sodar wind speed measurements collected at Ft. Bliss and values estimated from 2- and 10-m mast data using Monin-Obukhov similarity and a p-profile fit	75
24. Rms differences between 410-m sodar wind speed measurements collected at Ft. Bliss and values estimated from 2- and 10-m mast data using Monin-Obukhov similarity and a p-profile fit	76
25. Rms differences between 60-m sodar wind speed measurements collected at Champaign and values estimated from 2- and 10-m mast data using Monin-Obukhov similarity and p-profile fit	83
26. Rms differences between 110-m sodar wind speed measurements collected at Champaign and values estimated from 2- and 10-m mast data using Monin-Obukhov similarity and p-profile fit	84

Figures (continued)

27. Rms differences between 160-m sodar wind speed measurements collected at Champaign and values estimated from 2- and 10-m mast data using Monin-Obukhov similarity and a p-profile fit	85
28. Rms differences between 210-m sodar wind speed measurements collected at Champaign and values estimated from 2- and 10-m mast data using Monin-Obukhov similarity and a p-profile fit	86
29. Rms differences between 310-m sodar wind speed measurements collected at Champaign and values estimated from 2- and 10-m mast data using Monin-Obukhov similarity and a p-profile fit	87
30. Rms differences between 410-m sodar wind speed measurements collected at Champaign and values estimated from 2- and 10-m mast data using Monin-Obukhov similarity and a p-profile fit	88
31. Rms differences between day radiosonde wind speed measurements collected at WSMR and data estimated from tower measurements using Monin-Obukhov similarity and p-profile fit	96
32. Rms differences between night radiosonde wind speed measurements collected at WSMR and data estimated from tower measurements using Monin-Obukhov similarity and p-profile fit	97
33. Rms differences between day radiosonde temperature measurements collected at WSMR and data estimated from tower measurements using Monin-Obukhov similarity and inversion algorithms	102
34. Rms differences between night radiosonde temperature measurements collected at WSMR and data estimated from tower measurements using Monin-Obukhov similarity and inversion algorithms	103
35. Rms differences between day radiosonde wind speed measurements collected at Ft. Bliss and data estimated from tower measurements using Monin-Obukhov similarity and p-profile fit	108
36. Rms differences between night radiosonde wind speed measurements collected at Ft. Bliss and data estimated from tower measurements using Monin-Obukhov similarity and p-profile fit	109
37. Rms differences between day radiosonde temperature measurements collected at Ft. Bliss and data estimated from tower measurements using Monin-Obukhov similarity and inversion algorithms	114
38. Rms differences between night radiosonde temperature measurements collected at Ft. Bliss and data estimated from tower measurements using Monin-Obukhov similarity and inversion algorithms	115

Figures (continued)

39.	Rms differences between day radiosonde wind speed measurements collected at Champaign and data estimated from tower measurements using Monin-Obukhov similarity and p-profile fit	120
40.	Rms differences between night radiosonde wind speed measurements collected at Champaign and data estimated from tower measurements using Monin-Obukhov similarity and p-profile fit	121
41.	Rms differences between day radiosonde temperature measurements collected at Champaign and data estimated from tower measurements using Monin-Obukhov similarity and inversion algorithms	126
42.	Rms differences between night radiosonde temperature measurements collected at Champaign and data estimated from tower measurements using Monin-Obukhov similarity and inversion algorithms	127
43.	Absolute value of differences between radiosonde wind speed measurements and data estimated from tower measurements using Monin-Obukhov similarity	128
44.	Absolute value of differences between radiosonde wind speed measurements and data estimated from tower measurements using p-profile	129
45.	Absolute value of differences between radiosonde temperature measurements and data estimated from tower measurements using Monin-Obukhov similarity	130
46.	Absolute value of differences between radiosonde temperature measurements and data estimated from tower measurements using inversion algorithm	131
47.	Comparison of temperature data collected by a radiosonde launched July 22 at 1321 MDT with values estimated from tower measurements using inversion and Monin-Obukhov similarity algorithms	132
48.	Comparison of wind speed data collected by a radiosonde launched July 22 at 1321 MDT with values estimated from tower measurements using Monin-Obukhov similarity and a p-profile fit	133
49.	Comparison of temperature data collected by a radiosonde launched July 14 at 1727 MDT with values estimated from tower measurements using inversion and Monin-Obukhov similarity algorithms	134
50.	Comparison of wind speed data collected by a radiosonde launched July 14 at 1727 MDT with values estimated from tower measurements using Monin-Obukhov similarity and a p-profile fit	135
51.	Comparison of temperature data collected by a radiosonde launched July 14 at 2310 MDT with values estimated from tower measurements using inversion and Monin-Obukhov similarity algorithms	136

Figures (continued)

52. Comparison of wind speed data collected by a radiosonde launched July 14 at 2310 MDT with values estimated from tower measurements using Monin-Obukhov similarity and a p-profile fit 137

Tables

1. Statistics of differences between wind speed and temperature measured on a 30-m tower and values estimated from 2- and 8-m measurements using three Monin-Obukhov similarity algorithms 27
2. Statistics of differences between wind speed and temperature measured on a 30-m tower and values estimated from 2- and 8-m measurements using Monin-Obukhov similarity and linear and p-profile fits 39
3. Statistics of differences between wind speeds measured by sodar at WSMR and values estimated from 2- and 10-m mast data using Monin-Obukhov similarity algorithm and p-profile fit 53
4. Statistics of differences between wind speeds measured by sodar at Ft. Bliss and values estimated from 2- and 10-m mast data using Monin-Obukhov similarity algorithm and p-profile fit 65
5. Statistics of differences between wind speeds measured by sodar at Champaign and values estimated from 2- and 10-m mast data using Monin-Obukhov similarity algorithm and p-profile fit 77
6. Statistics of differences between day radiosonde wind data collected at WSMR and data estimated from 2- and 10-m measurements using Monin-Obukhov similarity 92
7. Statistics of differences between day radiosonde wind data collected at WSMR and data estimated from 2- and 10-m measurements using p-profile fit 93
8. Statistics of differences between night radiosonde wind data collected at WSMR and data estimated from 2- and 10-m measurements using Monin-Obukhov similarity 94
9. Statistics of differences between night radiosonde wind data collected at WSMR and data estimated from 2- and 10-m measurements using p-profile fit 95
10. Statistics of differences between day radiosonde temperature data collected at WSMR and data estimated from 2- and 10-m measurements using Monin-Obukhov similarity 98
11. Statistics of differences between day radiosonde temperature data collected at WSMR and data estimated from 10-m measurements using inversion algorithm 99
12. Statistics of differences between night radiosonde temperature data collected at WSMR and data estimated from 2- and 10-m measurements using Monin-Obukhov similarity 100
13. Statistics of differences between night radiosonde temperature data collected at WSMR and data estimated from 10-m measurements using inversion algorithm 101

Tables (continued)

14.	Statistics of differences between day radiosonde wind data collected at Ft. Bliss and data estimated from 2- and 10-m measurements using Monin-Obukhov similarity	104
15.	Statistics of differences between day radiosonde wind data collected at Ft. Bliss and data estimated from 2- and 10-m measurements using p-profile fit	105
16.	Statistics of differences between night radiosonde wind data collected at Ft. Bliss and data estimated from 2- and 10-m measurements using Monin-Obukhov similarity	106
17.	Statistics of differences between night radiosonde wind data collected at Ft. Bliss and data estimated from 2- and 10-m measurements using p-profile fit	107
18.	Statistics of differences between day radiosonde temperature data collected at Ft. Bliss and data estimated from 2- and 10-m measurements using Monin-Obukhov similarity	110
19.	Statistics of differences between day radiosonde temperature data collected at Ft. Bliss and data estimated from 10-m measurements using inversion algorithm	111
20.	Statistics of differences between night radiosonde temperature data collected at Ft. Bliss and data estimated from 2- and 10-m measurements using Monin-Obukhov similarity	112
21.	Statistics of differences between night radiosonde temperature data collected at Ft. Bliss and data estimated from 10-m measurements using inversion algorithm	113
22.	Statistics of differences between day radiosonde wind data collected at Champaign and data estimated from 2- and 10-m measurements using Monin-Obukhov similarity	116
23.	Statistics of differences between day radiosonde wind data collected at Champaign and data estimated from 2- and 10-m measurements using p-profile fit	117
24.	Statistics of differences between night radiosonde wind data collected at Champaign and data estimated from 2- and 10-m measurements using Monin-Obukhov similarity	118
25.	Statistics of differences between night radiosonde wind data collected at Champaign and data estimated from 2- and 10-m measurements using p-profile fit	119
26.	Statistics of differences between day radiosonde temperature data collected at Champaign and data estimated from 2- and 10-m measurements using Monin-Obukhov similarity	122
27.	Statistics of differences between day radiosonde temperature data collected at Champaign and data estimated from 10-m measurements using inversion algorithm	123
28.	Statistics of differences between night radiosonde temperature data collected at Champaign and data estimated from 2- and 10-m measurements using Monin-Obukhov similarity	124
29.	Statistics of differences between night radiosonde temperature data collected at Champaign and data estimated from 10-m measurements using inversion algorithm	125

Executive Summary

Five simple models that estimate vertical profiles of wind speed or temperature in the boundary layer were evaluated by comparing their predictions with measured data. The models evaluated consist of three Monin-Obukhov similarity algorithms for predicting wind speed and temperature, a p-profile algorithm for estimating wind speed, and an inversion algorithm for estimating temperature. Data for the study were collected by the U.S. Army Research Laboratory to support acoustic propagation experiments at Ft. Bliss, TX in June 1990, at Champaign, IL in July and August 1990, and at White Sands Missile Range (WSMR), NM in July and August 1991. All three locations were instrumented with a 10-m mast, a radiosonde station, and a Doppler sodar in close proximity. A 30-m tower was also situated at WSMR within approximately 1 km of the other instrumentation.

Fifteen-minute averaged tower data collected at one or two heights were fed into the models to predict wind speed and temperature at other measurement heights. The 2- and 8-m data collected on the 30-m tower was used to predict data at the other three tower heights of 4, 16, and 30 m, and the 2- and 10-m mast data was used to predict data at the radiosonde and sodar heights. Statistics of the differences between the measured and predicted data were computed to determine the accuracy of the model predictions as a function of altitude and time of day.

Little difference was found among the predictions of the three similarity models at any time of day at the 30-m tower heights. Between 0900 and 1900 MDT, there was good agreement between the similarity model predictions and the measured tower, sodar, and radiosonde data up to several hundred meters above the surface. By comparison, the p-profile predictions were almost the same at 4 and 16 m, somewhat worse at 30 m, and considerably worse at 50 m and above. The day inversion model estimates were much less comparable at all radiosonde heights within the first several hundred meters.

At night, the similarity and p-profile models gave good predictions only at 4 and 16 m, and the similarity model did not converge to a solution about half of the time. The night inversion algorithm comparabilities were better at all radiosonde heights above 200 m at WSMR and above 50 m at Ft. Bliss and Champaign.

1. Introduction

A knowledge of the vertical structure of wind speed and temperature in the atmospheric boundary layer is required for many applications. This information is often obtained by merging available in situ measurements collected on a mast or tower with upper-air data collected by balloons or remote sensors. There may be gaps in the data depending on the instrumentation used. For example, there is usually a 50- to several-hundred-meter difference between the highest tower measurement and the lowest upper-air measurement. Data at some heights may have to be estimated from measurements at other altitudes.

Five models that can be used for this purpose were evaluated in this study. Three models use the similarity hypothesis of Monin and Obukhov [1] to predict temperature and wind speed, one model is a p-profile for estimating wind speed, and another is an inversion algorithm for estimating temperature. The models were evaluated using tower, sodar, and radiosonde measurements collected at four field experiments. Vertical profiles of wind speed and temperature, generated by the models using one or two levels of the tower data, were statistically compared to the other measured data to determine the relative accuracies of the model predictions as a function of altitude and time of day.

2. Instrument Description and Data Collection

The data used in these analyses were collected by the U.S. Army Research Laboratory to support four acoustic propagation experiments. The first experiment was conducted June 4 to 25, 1990, at Ft. Bliss, TX, the second was held near Champaign, IL July 23 to August 3, 1990; and the other two were conducted at Dirt Site in the extreme southeast corner of White Sands Missile Range (WSMR), NM July 11 to 29 and August 19 to 29, 1991.

WSMR is located in the south, central part of the state within a broad basin between two mountain ranges. The climate and vegetation are typical of the southwestern U.S. desert. The main Dirt Site test range, consisting of a rectangle approximately 200-m wide and 2-km long, has been plowed several times in the past 15 years to support earlier experiments, so the area is rather flat with vegetation generally less than 1-m high. It is surrounded by mesquite-covered sand hills between 1.5- and 2.5-m high. The site elevation is about 1260-m above sea level.

The Ft. Bliss site is approximately 15 km east of the WSMR location. Vegetation and topography are similar to the unplowed portion of the WSMR site. The elevation is somewhat higher at about 1390-m above sea level.

Champaign, IL is situated in the prairie regions of the east, central portion of the state. The test area is a flat, mostly treeless plain with thick grass approximately .6-m high. Site elevation is about 210 m.

It was very warm and dry during the Ft. Bliss experiment. The average daily maximum 2-m temperature was approximately 36 °C, and the average dewpoint was about 4 °C. It was somewhat cooler and more humid at the other two tests. Mean maximum daily temperatures were 31 °C at WSMR and 27 °C at Champaign, and the average dewpoints were approximately 14 and 16 °C at WSMR and Champaign, respectively.

All three locations were instrumented with a 10-m tower, a radiosonde station, and a Doppler sodar in close proximity. At WSMR, there was also a 30-m tower approximately 1 km south of the other equipment.

The 30-m tower was instrumented at 2, 4, 8, 16, and 30 m with temperature sensors and propeller anemometers. Relative humidity was measured at 2 and 30 m. The data were averaged for 15-min periods before being recorded. During the two acoustic propagation experiments, measurements were collected only when personnel were at the site supporting the tests. Approximately 107 h of data were collected during the July test, and about 144 h were collected during the August experiment. Data were also recorded continuously and unattended between the two experiments from July 30 to August 13. A total of about 610 h of data was collected between July 11 and August 29.

The 10-m masts were instrumented at 1, 2, and 10 m. Wind speed and direction were measured by cup and vane anemometers, and temperature data were measured with thermocouples. At WSMR, 15-min averaged data were collected every day between July 9 and August 31. Except for two days, measurements were recorded 24 h per day. Fifteen-minute data were recorded 24 h per day on June 1 to 12 and June 13 to 25 at Ft. Bliss and on July 23 to 27, 30, 31, and August 1 to 3 at Champaign.

Doppler sodars were used to remotely measure wind parameters using acoustic sounding. One vertical and two tilted beams are transmitted upward. Changes in the acoustic refractive index caused by temperature fluctuations scatter some of this energy back to the antennas. Doppler shifts in the backscattered signals are used to derive wind velocities along the three beam paths. Horizontal wind speeds and directions are calculated from the radial velocities. At WSMR, 15-min averaged wind data were collected at 12 heights, 50 m apart, from 50 to 600 m above the surface on most days between July 12 and August 31. More than 23 h of data were recorded during 43 of the 51 days. At Ft. Bliss and Champaign, 15-min averaged data were collected at 15 heights, 50 m apart, from 60 to 760 m above the surface. Data were collected during 14 days between June 4 and June 25 at Ft. Bliss and every day between July 21 and August 2 at Champaign. Approximately 244 and 279 h of sodar data were collected at Champaign and Ft. Bliss, respectively.

Two different radiosonde systems were used. For the Ft. Bliss, Champaign, and July WSMR experiment, an automatic radio theodolite system was deployed consisting of a 1680-MHz sonde tracked by an automatic radio

theodolite using a phase array antenna. Height, temperature, humidity, and balloon-to-ground azimuth and elevation angles were recorded for every 4 to 5 s of flight. Wind data were computed using the height and angle data for 1-min layers. For the last experiment in August, an Omega Navaid system was substituted to collect data at greater heights. Measurements were provided for every 10 s of flight. The winds were calculated for 4-min layers. Fifty-eight radio theodolite soundings were flown at Ft. Bliss, 41 flights were released at Champaign, and 33 soundings were flown at the July WSMR experiment. Each flight was tracked to about 5 km. Seven Omega sondes, tracked to 15 to 20 km, were released during the August 1991 WSMR experiment.

3. Description of the Models

3.1 Similarity Models

Three models based on the Monin-Obukhov hypothesis were tested. Two of these use a linear-quartic approach named the O'KEYPS representation by Yaglom [2] from the initials of the inventors Obukhov, [3] Kanzanski and Monin, [4] Ellison, [5] Yamamoto, [6] Panofsky, [7] and Sellers. [8] Within the surface layer, the change in wind speed V and the potential temperature θ with respect to height z is

$$\frac{\partial V}{\partial z} = \frac{u_*}{kz} \phi_m \left[\frac{z}{L} \right] \quad (1)$$

$$\frac{\partial \theta}{\partial z} = \frac{\theta_*}{kz} \phi_H \left[\frac{z}{L} \right] \quad (2)$$

where

u_* = the friction velocity

T_* = a scaling temperature

k = von Karman's constant (= .4)

ϕ_m and ϕ_H = the dimensionless wind shear and temperature gradient

L = the Monin-Obukhov length.

Integrating equations (1) and (2) results in the following expressions

$$V = \frac{u_*}{k} \left[\ln \left[\frac{z}{z_o} \right] + \psi_m \left[\frac{z}{L} \right] \right] \quad (3)$$

$$\theta = \theta_o + \frac{T_*}{k} \left[\ln \left[\frac{z}{z_o} \right] + \psi_H \left[\frac{z}{L} \right] \right] \quad (4)$$

where

z_o = the roughness length.

These equations can also be expressed as a difference in wind speed and potential temperature at two levels as follows:

$$V_2 - V_1 = \frac{u_*}{k} \left[\ln \left[\frac{z_2}{z_1} \right] + \psi_m \left[\frac{z_2}{L} \right] - \psi_m \left[\frac{z_1}{L} \right] \right] \quad (5)$$

$$\theta_2 - \theta_1 = \frac{T_*}{k} \left[\ln \left[\frac{z_2}{z_1} \right] + \psi_H \left[\frac{z_2}{L} \right] - \psi_H \left[\frac{z_1}{L} \right] \right] \quad (6)$$

The Monin-Obukhov length L can be computed from

$$L = \frac{T u_*^2}{k g T_*} \quad (7)$$

where

\bar{T} = the mean temperature

g = the gravitational acceleration.

Several different investigators have developed analytic expressions for the terms ψ_m and ψ_H . In this study, these equations from Panofsky and Dutton [9] were used for stable conditions:

$$\left. \begin{aligned} \psi_m \left[\frac{z}{L} \right] &= 4.7 \left[\frac{z}{L} \right] \\ \psi_H \left[\frac{z}{L} \right] &= 4.7 \left[\frac{z}{L} \right] \end{aligned} \right\} \text{for } \frac{z}{L} > 0 \quad (8)$$

For unstable conditions, the following expressions from Paulson [10] were used:

$$\left. \begin{aligned} \psi_m \left[\frac{z}{L} \right] &= -2 \ln \left[\frac{(1+x)}{2} \right] - \ln \left[\frac{(1+x^2)}{2} \right] + 2 \tan^{-1}(x) \\ &\quad - \frac{\pi}{2} \\ \psi_H \left[\frac{z}{L} \right] &= -2 \ln \left[\frac{(1+x^2)}{2} \right] \\ x &= \left[1 - \left[15 \frac{z}{L} \right] \right]^{\frac{1}{4}} \end{aligned} \right\} \text{for } \frac{z}{L} < 0 \quad (9)$$

In both of the O'KEYPS algorithms, an iterative method is used to solve for wind speed and potential temperature. One technique, described by Wilson, [11] requires temperature data at two heights, wind speed data at one height, and an estimate of the roughness height z_0 as input. Equations (3) and (6) are first solved for u_* and T_* by assuming that the diabatic terms ψ_m and ψ_H are zero. Equation (7) is then used to compute L . The diabatic terms are calculated using equations (8) or (9) which is then used to compute u_* and T_* again using equations (3) and (6). This process is repeated until L converges. After the three scaling parameters have been determined, the wind speed and potential temperature at any selected height can then be computed using equations (3), (6), (7), (8), and (9). Generally, only a few iterations are required. Convergence is much more likely to occur during the day than at night.

The other O'KEYPS method is a modification of this technique using two levels of wind and temperature measurements. Equation (6) is used to calculate u_* instead of equation (1) eliminating the need to estimate the roughness length. Otherwise, the computation procedure is the same.

The third similarity-based technique tested was developed by Rachele et al. [12] and is named the Mariah method. In this approach, the scaling parameters are calculated directly without iteration.

The parameters u_* and θ_* are determined from the discrete form of equations (1) and (2) listed below:

$$u_* = \frac{k \Delta V}{\phi_m \Delta \ln z} \quad (10)$$

$$\theta_* = \frac{k \Delta \theta}{\phi_H \Delta \ln z} \quad (11)$$

Defining $z^* = \frac{\Delta z}{\Delta \ln z}$, ϕ_m and ϕ_H are computed for the unstable surface layer ($\frac{z^*}{L} < 0$) as follows:

$$\phi_m = \left[1 - 15 \frac{z^*}{L} \right]^{-1/4} \quad (12)$$

$$\phi_H = \left[1 - 15 \frac{z^*}{L} \right]^{-1/2} \quad (13)$$

$$L = \frac{\theta_v (\Delta V)^2}{[\Delta\theta + 0.61 \theta \Delta q] g \Delta \ln z} \quad (14)$$

where

q = the specific humidity

θ_v = the virtual potential temperature ($\theta_v = \theta(1 + .61q)$).

For stable conditions ($\frac{z^*}{L} > 0$)

$$\phi_m = \phi_H = 1 + 5 \frac{z^*}{L} \quad (15)$$

$$L = \frac{B}{2} - 5z^* \quad (16)$$

$$B = \frac{2 \theta_v (\Delta V)^2}{g [\Delta\theta + 0.61 \theta \Delta q] \Delta \ln z} \quad (17)$$

The above equations for ϕ_m and ϕ_H can be substituted into equations (1) and (2), which are then integrated to form expressions similar to equations (5), (6), (8), and (9). These are used with equations (10) through (17) to calculate wind speed and potential temperature as a function of height.

This method for determining the similarity scaling constants is new, although based on traditional concepts of similarity. It will be shown that the results obtained by using Mariah are equivalent to those using the O'KEYPS method. The advantages of employing the Mariah approach are (1) the algorithm executes quickly without laborious iterative schemes imbedded into the program, (2) as many or as few levels of tower data as are available can be used to determine layer-averaged, similarity profile structure, and (3) while in use, the similarity premise of stationarity is preserved.

3.2 P-Profile

The vertical profile of wind speed with height was also estimated with p-profile curves. This concept was first postulated by Frost. [13] The wind speed S at level z is defined as

$$S = S_o \left[\frac{z}{z_o} \right]^p \quad (18)$$

where

S_o = the wind speed at the height z_o .

The exponent p is fitted to the measured wind speeds at two selected heights.

3.3 Inversion Model

This model was developed by Hopfer and Blanco [14] to predict upper-air temperatures and pressure using 24 h of in situ tower measurements. Only the temperature predictions were considered in this study. An estimated temperature profile is created by applying a boundary layer correction to a U.S. Standard Atmosphere profile adjusted to the mean 24-h temperature. The equation is as follows:

$$T(z,t) = T_{std}(z) + \Delta T(z,t) \quad (19)$$

where

T_{std} = the adjusted standard atmosphere

$\Delta T(z,t)$ = the correction.

In the version used in this study, this boundary-layer offset is determined as follows:

$$\Delta T(z,t) = Ce^{-az}$$

$$a = \left[\frac{\pi}{24K} \right]^{\frac{1}{2}} \quad (20)$$

$$C = \sum_{n=1}^{n=4} A_n \cos \left[\frac{2\pi nt}{24} - az \right] + B_n \sin \left[\frac{2\pi nt}{24} - az \right]$$

where

K = the heat exchange coefficient
 A_n and B_n = Fourier coefficients fitted to 24 h of 10-m tower temperature measurements.

4. Comparison of Model Estimates with Measured Data

4.1 Tower Data Comparison

The relative accuracies of the p-profile and similarity models at heights close to the surface were investigated using the 15-min averaged 30-m tower data collected at WSMR. Wind speed and temperature measured at 2 and 8 m were used to predict the same parameters at the other three tower levels at 4, 16, and 30 m. Means, standard deviations, and root-mean-squares (rms) of the differences between these predictions and the measured data at the three levels were computed for each 2-h period of the day.

Statistics for the three similarity models are shown in table 1. The rms differences are also plotted versus time of day in figures 1 through 6. The O'KEYPS technique, using two levels of wind speed and temperature, is labeled Similarity #1. The other O'KEYPS algorithm, using temperature at 2 and 8 m, wind speed at 2 m, and a roughness height estimate of .15 m, is named Similarity #2. Similarity #3 is the Mariah method using wind speed and temperature at 2 and 8 m and relative humidity and pressure at 2 m. Only data in which all three methods converged to a solution were used in this analysis, so that the statistics for each method were computed using the same measurements. Little difference was found among the predictions of the three techniques. In particular, the Mariah and Similarity #1 statistics were almost identical. Therefore, in all the other analyses described in this paper only the Similarity #1 method was tested and is referred to simply as the similarity method.

The same statistical comparison among the similarity, p-profile, and linear fit algorithms is shown in table 2 and figures 7 through 12. The linear fit is simply an interpolation or extrapolation along a line drawn between the 2 and 8-m measurements. Again, the three sets of statistics were computed using the same data.

The best estimates were given by the similarity model. The rms wind speed and temperature differences between the predicted and measured data were

.2 to .3 m s⁻¹ and .1 to .3 °C, respectively, at 4 m; and .4 to .7 m s⁻¹ and .2 to .4 °C, respectively, at 16 m. There was not much diurnal variation at these two heights. At 30 m, however, the night statistics were considerably poorer than the day statistics. Rms wind speed differences were .5 to 1.0 m s⁻¹ during the day and approximately 1.5 m s⁻¹ at night. Temperature rms differences at 30 m were .4 to .6 °C and 1.0 to 1.5 °C during the day and night, respectively. These results indicate that the night similarity estimates are not very accurate above 16 m because of the shallowness of the surface boundary layer during those times. Another problem at night is the fact that the similarity algorithm often fails to converge to a solution. In this study, a solution was obtained about 50 percent of the time during the early morning hours before dawn and 90 to 96 percent of the time during midday.

Agreement between the p-profile predictions and the measured data was somewhat poorer. Compared to the similarity rms differences, the p-profile rms differences were about the same at 4 m, slightly greater at 16 m, and as much as .5 m s⁻¹ higher at 30 m. The statistics of both models had a similar diurnal variation.

The linear fit estimates were less comparable to the measured data than either the p-profile or similarity estimates for all heights and times of day. Linear interpolations to 4 m were only slightly worse than the other predictions, but the linear extrapolations to 16 and 30 m were considerably less accurate. The rms temperature differences between the linear fit estimates and the measured data were lowest at night and highest during the day, reversing the pattern for the similarity model.

Table 1. Statistics of differences between wind speed and temperature measured on a 30-m tower and values estimated from 2- and 8-m measurements using three Monin-Obukhov similarity algorithms

Jul 11 - Aug 29, 1991

0000 - 0200 MDT

	<u>Wind Speed (m/s)</u>			<u>Temp (°C)</u>			NPTS
	Mean	STDV	rms	Mean	STDV	rms	
4-m Sim #1 meas	.03	.34	.35	-.04	.04	.06	95
4-m Sim #2 meas	-.04	.35	.36	-.04	.04	.06	95
4-m Sim #3 meas	.02	.35	.35	-.04	.04	.06	95
16-m Sim #1 meas	.18	.61	.63	.02	.14	.14	95
16-m Sim #2 meas	.23	.59	.63	.02	.14	.14	95
16-m Sim #3 meas	.18	.61	.63	.02	.14	.14	95
30-m Sim #1 meas	.69	1.00	1.2	1.19	.29	.34	95
30-m Sim #2 meas	.77	.95	1.22	.17	.35	.39	95
30-m Sim #3 meas	.72	1.00	1.23	.20	.30	.35	95

0200 - 0400 MDT

	<u>Wind Speed (m/s)</u>			<u>Temp (°C)</u>			NPTS
	Mean	STDV	rms	Mean	STDV	rms	
4-m Sim #1 meas	-.07	.20	.21	-.07	.15	.16	73
4-m Sim #2 meas	-.14	.26	.30	-.07	.15	.17	73
4-m Sim #3 meas	-.07	.20	.21	-.07	.15	.16	73
16-m Sim #1 meas	.23	.54	.59	.06	.27	.28	73
16-m Sim #2 meas	.28	.52	.59	.05	.29	.30	73
16-m Sim #3 meas	.24	.55	.60	.06	.28	.28	73
30-m Sim #1 meas	.73	.87	1.13	.22	.72	.75	73
30-m Sim #2 meas	.81	.86	1.18	.21	.84	.86	73

Table 1. Statistics of differences between wind speed and temperature measured on a 30-m tower and values estimated from 2- and 8-m measurements using three Monin-Obukhov similarity algorithms (continued)

Jul 11 - Aug 29, 1991

0400 - 0600 MDT

	<u>Wind Speed (m/s)</u>			<u>Temp (°C)</u>			NPTS
	Mean	STDV	rms	Mean	STDV	rms	
4-m Sim #1 meas	-.02	.26	.26	-.05	.04	.06	74
4-m Sim #2 meas	-.05	.26	.27	-.04	.04	.06	74
4-m Sim #3 meas	-.03	.26	.26	-.05	.04	.06	74
16-m Sim #1 meas	.31	.51	.60	.02	.14	.14	74
16-m Sim #2 meas	.33	.46	.57	.01	.14	.14	74
16-m Sim #3 meas	.32	.51	.60	.02	.14	.14	74
30-m Sim #1 meas	.73	.78	1.07	.06	.39	.40	74
30-m Sim #2 meas	.75	.73	1.05	.04	.39	.39	74
30-m Sim #3 meas	.77	.78	1.10	.07	.39	.40	74

0600 - 0800 MDT

	<u>Wind Speed (m/s)</u>			<u>Temp (°C)</u>			NPTS
	Mean	STDV	rms	Mean	STDV	rms	
4-m Sim #1 meas	-.03	.30	.30	.09	.12	.15	100
4-m Sim #2 meas	-.05	.35	.35	.09	.12	.15	100
4-m Sim #3 meas	-.03	.30	.30	.09	.11	.14	100
16-m Sim #1 meas	.06	.42	.42	-.05	.19	.20	100
16-m Sim #2 meas	.07	.40	.41	-.05	.19	.19	100
16-m Sim #3 meas	.06	.42	.42	-.05	.20	.20	100
30-m Sim #1 meas	.12	.75	.76	-.08	.44	.45	100
30-m Sim #2 meas	.14	.69	.70	-.09	.44	.45	100

Table 1. Statistics of differences between wind speed and temperature measured on a 30-m tower and values estimated from 2- and 8-m measurements using three Monin-Obukhov similarity algorithms (continued)

Jul 11 - Aug 29, 1991

0800 - 1000 MDT

	<u>Wind Speed (m/s)</u>			<u>Temp (°C)</u>			NPTS
	Mean	STDV	rms	Mean	STDV	rms	
4-m Sim #1 meas	-.02	.20	.20	.20	.14	.24	185
4-m Sim #2 meas	-.12	.29	.31	.20	.14	.24	185
4-m Sim #3 meas	-.02	.20	.20	.18	.13	.22	185
16-m Sim #1 meas	.08	.34	.34	-.17	.18	.25	185
16-m Sim #2 meas	.16	.32	.36	-.17	.17	.24	185
16-m Sim #3 meas	.09	.34	.35	-.21	.20	.29	185
30-m Sim #1 meas	.09	.47	.48	-.14	.26	.29	185
30-m Sim #2 meas	.24	.45	.51	-.14	.26	.29	185
30-m Sim #3 meas	.10	.47	.48	-.18	.28	.33	185

1000 - 1200 MDT

	<u>Wind Speed (m/s)</u>			<u>Temp (°C)</u>			NPTS
	Mean	STDV	rms	Mean	STDV	rms	
4-m Sim #1 meas	.00	.18	.18	.27	.16	.32	186
4-m Sim #2 meas	-.12	.29	.31	.28	.16	.32	186
4-m Sim #3 meas	.00	.18	.18	.25	.16	.29	186
16-m Sim #1 meas	.04	.37	.37	-.23	.24	.33	186
16-m Sim #2 meas	.14	.35	.38	-.23	.24	.33	186
16-m Sim #3 meas	.05	.37	.37	-.29	.25	.38	186
30-m Sim #1 meas	.04	.62	.62	-.09	.32	.33	186
30-m Sim #2 meas	.22	.59	.62	-.09	.32	.33	186

Table 1. Statistics of differences between wind speed and temperature measured on a 30-m tower and values estimated from 2- and 8-m measurements using three Monin-Obukhov similarity algorithms (continued)

Jul 11 - Aug 29, 1991

1200 - 1400 MDT

	<u>Wind Speed (m/s)</u>			<u>Temp (°C)</u>			NPTS
	Mean	STDV	rms	Mean	STDV	rms	
4-m Sim #1 meas	-.03	.24	.24	.24	.19	.30	174
4-m Sim #2 meas	-.13	.32	.35	.24	.19	.31	174
4-m Sim #3 meas	-.02	.24	.24	.22	.19	.29	174
16-m Sim #1 meas	.15	.51	.53	-.20	.36	.41	174
16-m Sim #2 meas	.24	.48	.53	-.20	.35	.41	174
16-m Sim #3 meas	.16	.51	.54	-.25	.37	.45	174
30-m Sim #1 meas	.14	.66	.67	-.02	.43	.43	174
30-m Sim #2 meas	.30	.60	.67	-.02	.43	.43	174
30-m Sim #3 meas	.15	.66	.68	-.08	.44	.45	174

1400 - 1600 MDT

	<u>Wind Speed (m/s)</u>			<u>Temp (°C)</u>			NPTS
	Mean	STDV	rms	Mean	STDV	rms	
4-m Sim #1 meas	.00	.32	.32	.19	.16	.25	191
4-m Sim #2 meas	-.15	.47	.50	.20	.16	.26	191
4-m Sim #3 meas	.00	.32	.32	.17	.16	.23	191
16-m Sim #1 meas	.12	.74	.75	-.14	.25	.28	191
16-m Sim #2 meas	.25	.65	.69	-.14	.24	.28	191
16-m Sim #3 meas	.13	.74	.75	-.18	.26	.32	191
30-m Sim #1 meas	.18	1.05	1.06	.01	.36	.36	191
30-m Sim #2 meas	.41	.86	.95	-.01	.36	.36	191

Table 1. Statistics of differences between wind speed and temperature measured on a 30-m tower and values estimated from 2- and 8-m measurements using three Monin-Obukhov similarity algorithms (continued)

Jul 11 - Aug 29, 1991

1600 - 1800 MDT

	<u>Wind Speed (m/s)</u>			<u>Temp (°C)</u>			NPTS
	Mean	STDV	rms	Mean	STDV	rms	
4-m Sim #1 meas	.04	.31	.31	.07	.25	.26	192
4-m Sim #2 meas	-.11	.44	.45	.07	.26	.27	192
4-m Sim #3 meas	.04	.31	.31	.06	.25	.26	192
16-m Sim #1 meas	.06	.66	.66	-.09	.33	.35	192
16-m Sim #2 meas	.19	.58	.61	-.10	.33	.34	192
16-m Sim #3 meas	.07	.66	.66	-.12	.34	.36	192
30-m Sim #1 meas	.18	.86	.88	-.01	.57	.57	192
30-m Sim #2 meas	.42	.75	.86	-.02	.56	.56	192
30-m Sim #3 meas	.19	.86	.88	-.04	.58	.58	192

1800 - 2000 MDT

	<u>Wind Speed (m/s)</u>			<u>Temp (°C)</u>			NPTS
	Mean	STDV	rms	Mean	STDV	rms	
4-m Sim #1 meas	.03	.33	.33	.01	.14	.14	131
4-m Sim #2 meas	-.08	.42	.42	.01	.15	.15	131
4-m Sim #3 meas	.03	.33	.33	.00	.14	.14	131
16-m Sim #1 meas	.11	.74	.75	-.06	.37	.37	131
16-m Sim #2 meas	.20	.68	.71	-.06	.37	.37	131
16-m Sim #3 meas	.11	.74	.75	-.07	.37	.38	131
30-m Sim #1 meas	.31	.92	.97	-.01	.50	.50	131
30-m Sim #2 meas	.49	.84	.97	-.01	.49	.49	131

Table 1. Statistics of differences between wind speed and temperature measured on a 30-m tower and values estimated from 2- and 8-m measurements using three Monin-Obukhov similarity algorithms (continued)

Jul 11 - Aug 29, 1991

2000 - 2200 MDT

	<u>Wind Speed (m/s)</u>			<u>Temp (°C)</u>			NPTS
	Mean	STDV	rms	Mean	STDV	rms	
4-m Sim #1 meas	.05	.31	.31	-.07	.13	.15	78
4-m Sim #2 meas	-.01	.42	.42	-.07	.13	.15	78
4-m Sim #3 meas	.05	.31	.31	-.07	.13	.15	78
16-m Sim #1 meas	.15	.63	.65	-.05	.33	.33	78
16-m Sim #2 meas	.21	.61	.65	-.05	.32	.33	78
16-m Sim #3 meas	.16	.63	.65	-.05	.33	.33	78
30-m Sim #1 meas	.71	.85	1.11	.09	.60	.60	78
30-m Sim #2 meas	.81	.78	1.12	.11	.62	.63	78
30-m Sim #3 meas	.73	.86	1.13	.10	.60	.61	78

2200 - 2400 MDT

	<u>Wind Speed (m/s)</u>			<u>Temp (°C)</u>			NPTS
	Mean	STDV	rms	Mean	STDV	rms	
4-m Sim #1 meas	.06	.36	.36	-.05	.05	.07	98
4-m Sim #2 meas	-.04	.47	.47	-.05	.04	.07	98
4-m Sim #3 meas	.06	.36	.36	-.05	.05	.07	98
16-m Sim #1 meas	.20	.72	.74	-.01	.16	.16	98
16-m Sim #2 meas	.29	.61	.67	-.02	.17	.17	98
16-m Sim #3 meas	.21	.72	.75	-.01	.16	.16	98
30-m Sim #1 meas	.61	1.22	1.37	.06	.35	.36	98
30-m Sim #2 meas	.77	.96	1.23	.05	.38	.38	98

RMS DIFFERENCE BETWEEN
4M MEASURED AND PREDICTED PARAMETER
JUL 11 - AUG 29, 1991 - DIRT SITE

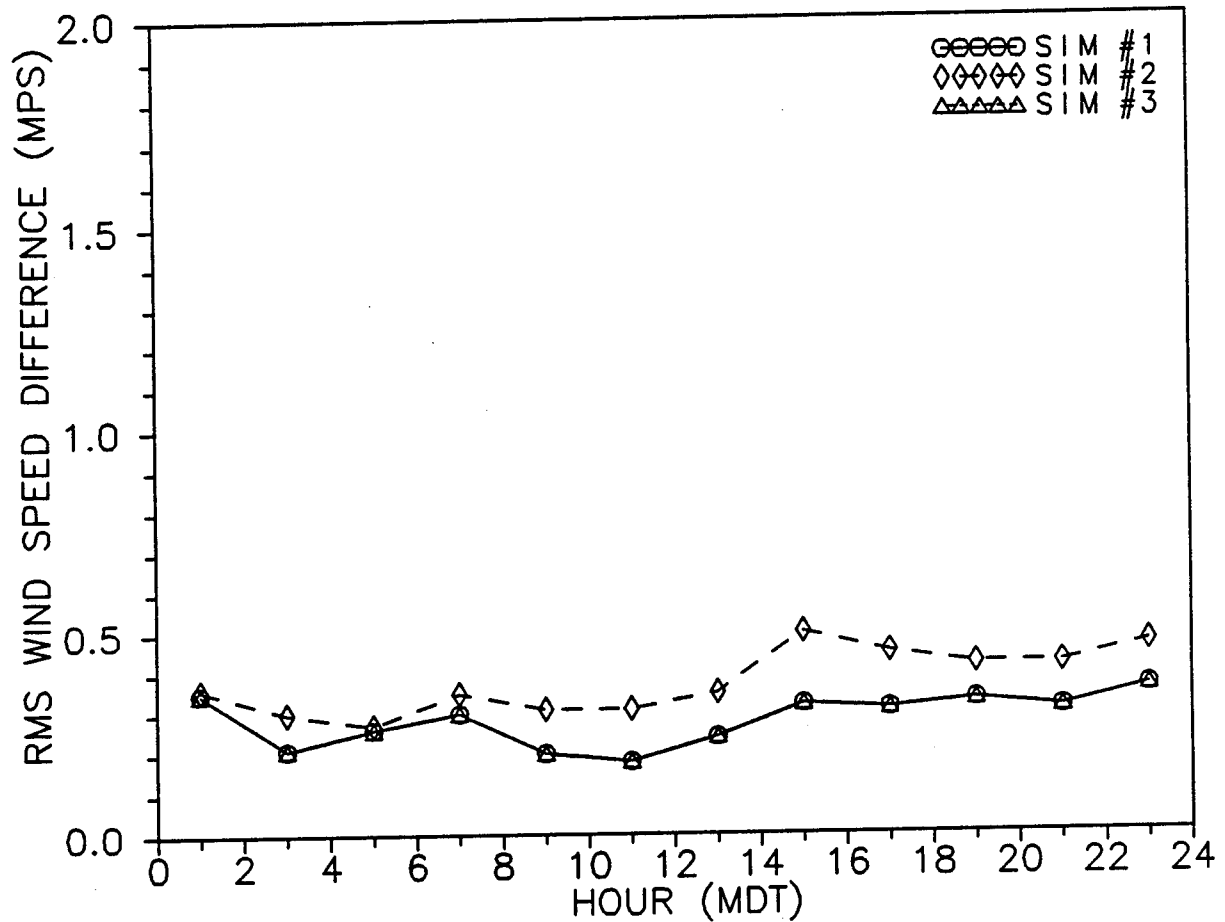


Figure 1. Rms differences between measured 4-m wind speeds and values estimated from 2- and 8-m measurements using three Monin-Obukhov similarity algorithms.

RMS DIFFERENCE BETWEEN
16M MEASURED AND PREDICTED PARAMETER
JUL 11 - AUG 29, 1991 - DIRT SITE

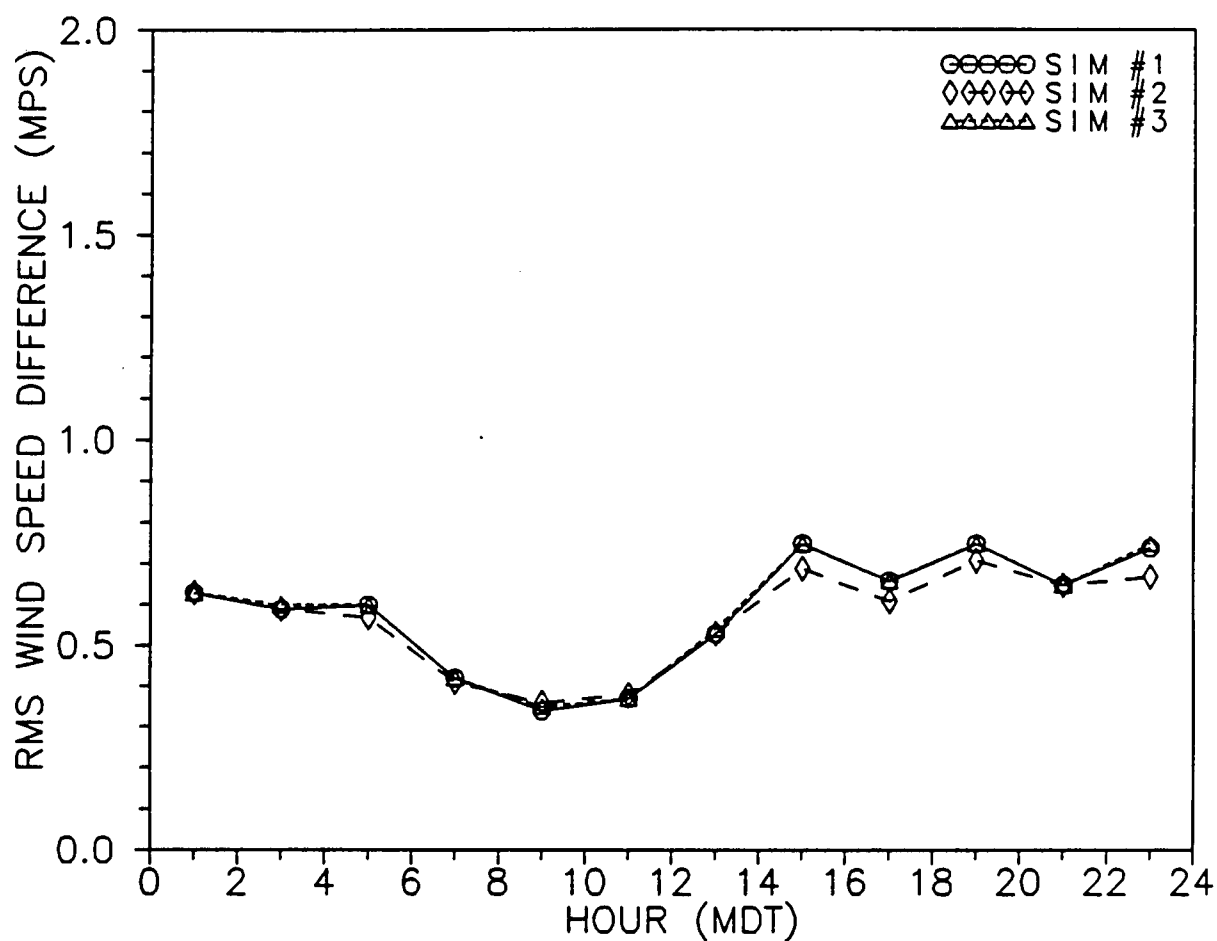


Figure 2. Rms differences between measured 16-m wind speeds and values estimated from 2- and 8-m measurements using three Monin-Obukhov similarity algorithms.

RMS DIFFERENCE BETWEEN
30M MEASURED AND PREDICTED PARAMETER
JUL 11 - AUG 29, 1991 - DIRT SITE

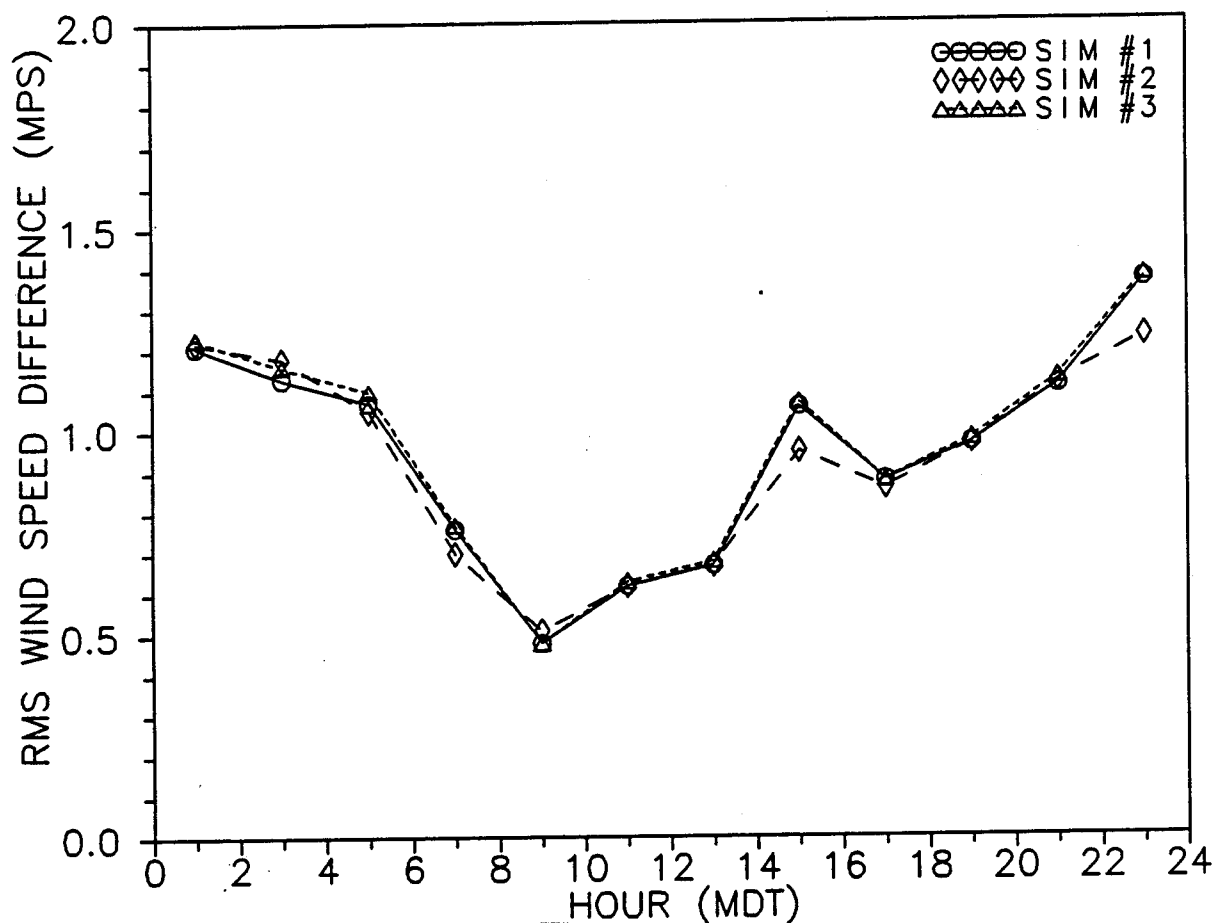


Figure 3. Rms differences between measured 30-m wind speeds and values estimated from 2- and 8-m measurements using three Monin-Obukhov similarity algorithms.

RMS DIFFERENCE BETWEEN
4M MEASURED AND PREDICTED PARAMETER
JUL 11 - AUG 29, 1991 - DIRT SITE

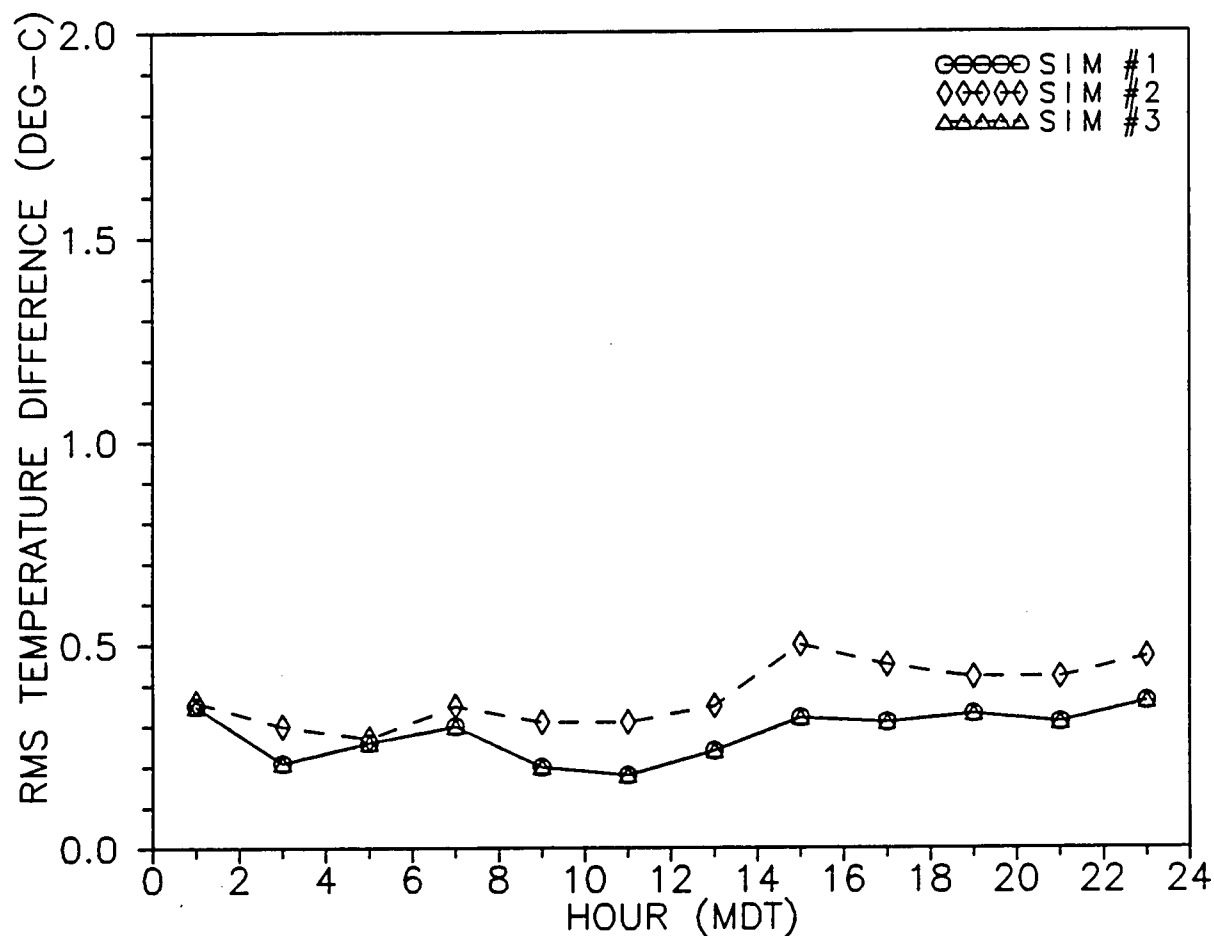


Figure 4. Rms differences between measured 4-m temperatures and values estimated from 2- and 8-m measurements using three Monin-Obukhov similarity algorithms.

RMS DIFFERENCE BETWEEN
16M MEASURED AND PREDICTED PARAMETER
JUL 11 - AUG 29, 1991 - DIRT SITE

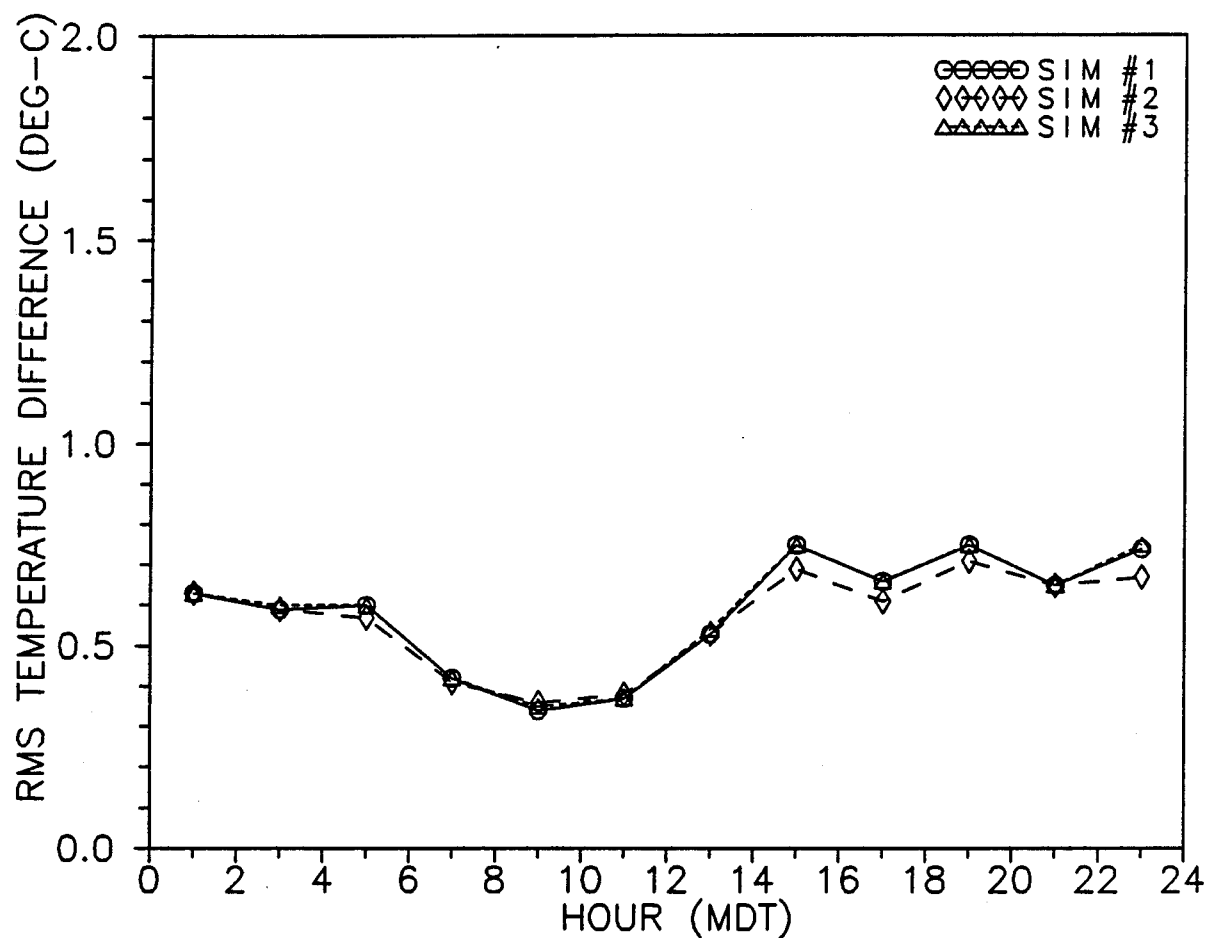


Figure 5. Rms differences between measured 16-m temperatures and values estimated from 2- and 8-m measurements using three Monin-Obukhov similarity algorithms.

RMS DIFFERENCE BETWEEN
30M MEASURED AND PREDICTED PARAMETER
JUL 11 - AUG 29, 1991 - DIRT SITE

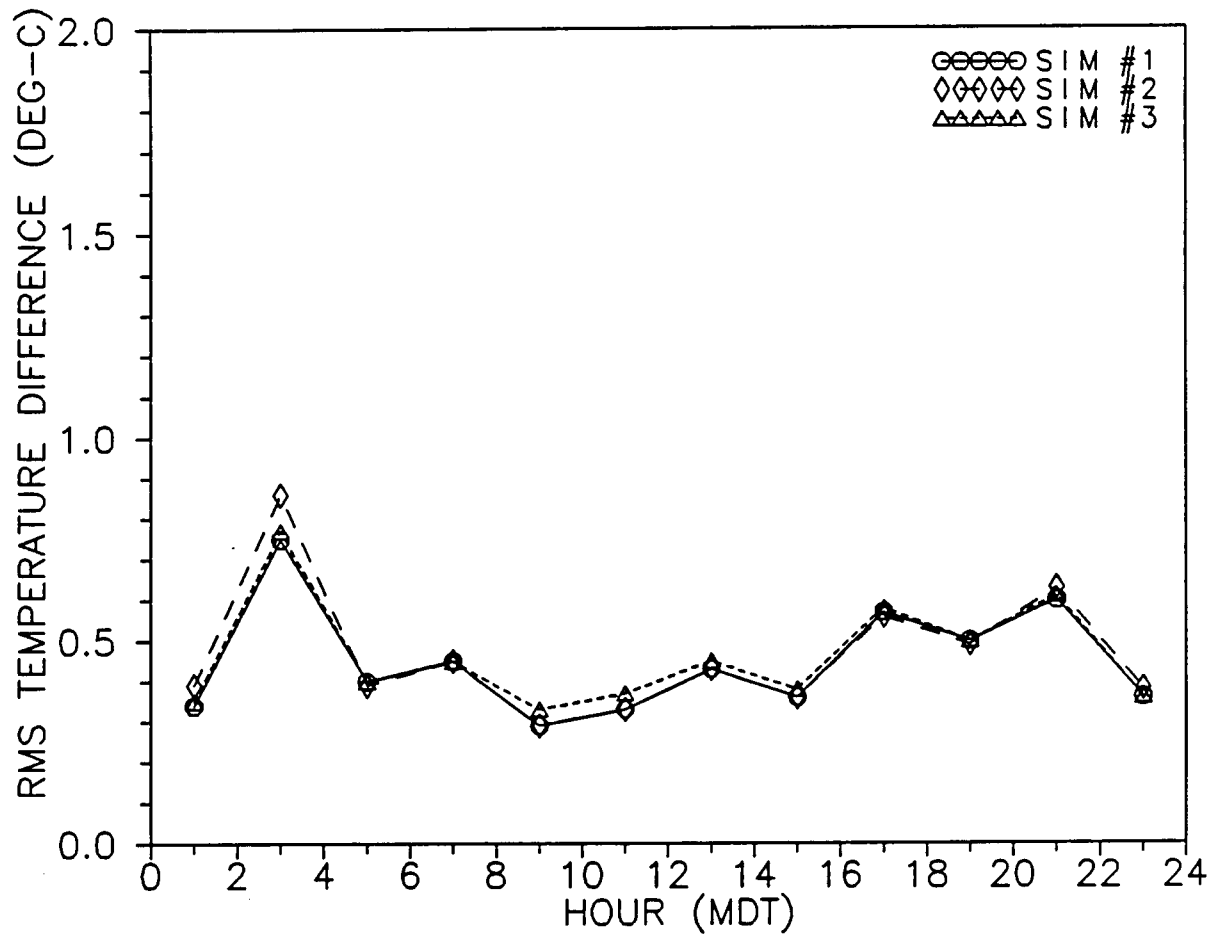


Figure 6. Rms differences between measured 30-m temperatures and values estimated from 2- and 8-m measurements using three Monin-Obukhov similarity algorithms.

Table 2. Statistics of differences between wind speed and temperature measured on a 30-m tower and values estimated from 2- and 8-m measurements using Monin-Obukhov similarity and linear and p-profile fits

Jul 11 - Aug 29, 1991

0000 - 0200 MDT

	<u>Wind Speed (m/s)</u>			<u>Temp (°C)</u>			NPTS
	Mean	STDV	rms	Mean	STDV	rms	
4-m simil meas	.01	.32	.32	-.04	.06	.07	118
4-m linear meas	-.14	.32	.35	-.08	.06	.10	118
4-m p-prof meas	-.01	.32	.32				118
16-m simil meas	.22	.63	.66	.08	.28	.29	118
16-m linear meas	.98	.84	1.29	.29	.39	.49	118
16-m p-prof meas	.24	.71	.75				118
30-m simil meas	.80	1.18	1.42	.36	.78	.86	118
30-m linear meas	3.27	2.04	3.85	1.06	1.20	1.60	118
30-m p-prof meas	.73	1.46	1.63				118

0200 - 0400 MDT

	<u>Wind Speed (m/s)</u>			<u>Temp (°C)</u>			NPTS
	Mean	STDV	rms	Mean	STDV	rms	
4-m simil meas	-.06	.22	.23	-.08	.22	.23	104
4-m linear meas	-.20	.23	.31	-.13	.24	.28	104
4-m p-prof meas	-.08	.22	.23				104
16-m simil meas	.32	.61	.69	.13	.44	.45	104
16-m linear meas	1.01	.77	1.27	.36	.56	.67	104
16-m p-prof meas	.31	.65	.72				104
30-m simil meas	.98	1.17	1.53	.54	1.38	1.49	104
30-m linear meas	3.25	1.72	3.68	1.30	1.87	2.27	104
30-m p-prof meas	.82	1.28	1.52				104

Table 2. Statistics of differences between wind speed and temperature measured on a 30-m tower and values estimated from 2- and 8-m measurements using Monin-Obukhov similarity and linear and p-profile fits (continued)

Jul 11 - Aug 29, 1991

0400 - 0600 MDT

	<u>Wind Speed (m/s)</u>			<u>Temp (°C)</u>			NPTS
	Mean	STDV	rms	Mean	STDV	rms	
4-m simil meas	-.02	.24	.24	-.05	.05	.07	98
4-m linear meas	-.17	.27	.32	-.09	.06	.11	98
4-m p-prof meas	-.05	.26	.27				98
16-m simil meas	.36	.50	.61	.10	.32	.34	98
16-m linear meas	1.09	.74	1.32	.31	.42	.52	98
16-m p-prof meas	.39	.65	.76				98
30-m simil meas	.99	1.05	1.44	.34	.95	1.01	98
30-m linear meas	3.38	1.76	3.82	1.05	1.28	1.65	98
30-m p-prof meas	.99	1.58	1.86				98

0600 - 0800 MDT

	<u>Wind Speed (m/s)</u>			<u>Temp (°C)</u>			NPTS
	Mean	STDV	rms	Mean	STDV	rms	
4-m simil meas	-.02	.28	.28	.07	.15	.16	121
4-m linear meas	-.14	.30	.33	.08	.19	.21	121
4-m p-prof meas	-.06	.28	.29				121
16-m simil meas	.16	.47	.49	.04	.30	.31	121
16-m linear meas	.72	.72	1.01	-.02	.55	.55	121
16-m p-prof meas	.25	.55	.61				121
30-m simil meas	.47	1.09	1.19	.20	.95	.97	121
30-m linear meas	2.30	2.03	3.07	.04	1.68	1.68	121
30-m p-prof meas	.68	1.29	1.46				121

Table 2. Statistics of differences between wind speed and temperature measured on a 30-m tower and values estimated from 2- and 8-m measurements using Monin-Obukhov similarity and linear and p-profile fits (continued)

Jul 11 - Aug 29, 1991

0800 - 1000 MDT

	<u>Wind Speed (m/s)</u>			<u>Temp (°C)</u>			NPTS
	Mean	STDV	rms	Mean	STDV	rms	
4-m simil meas	-.02	.20	.20	.20	.14	.24	188
4-m linear meas	-.10	.20	.22	.36	.20	.42	188
4-m p-prof meas	-.05	.19	.20				188
16-m simil meas	.08	.33	.34	-.17	.18	.25	188
16-m linear meas	.41	.53	.67	-.87	.51	1.00	188
16-m p-prof meas	.17	.39	.43				188
30-m simil meas	.08	.47	.48	-.13	.26	.30	188
30-m linear meas	1.14	1.28	1.71	-2.26	1.31	2.61	188
30-m p-prof meas	.32	.70	.77				188

1000 - 1200 MDT

	<u>Wind Speed (m/s)</u>			<u>Temp (°C)</u>			NPTS
	Mean	STDV	rms	Mean	STDV	rms	
4-m simil meas	-.01	.18	.18	.28	.17	.32	195
4-m linear meas	-.06	.17	.18	.49	.20	.53	195
4-m p-prof meas	-.03	.18	.18				195
16-m simil meas	.04	.37	.37	-.25	.27	.36	195
16-m linear meas	.28	.60	.66	-1.15	.55	1.28	195
16-m p-prof meas	.12	.41	.43				195
30-m simil meas	.05	.62	.62	-.11	.35	.37	195
30-m linear meas	.81	1.49	1.70	-2.89	1.33	3.18	195
30-m p-prof meas	.25	.78	.81				195

Table 2. Statistics of differences between wind speed and temperature measured on a 30-m tower and values estimated from 2- and 8-m measurements using Monin-Obukhov similarity and linear and p-profile fits (continued)

Jul 11 - Aug 29, 1991							
1200 - 1400 MDT							
	<u>Wind Speed (m/s)</u>			<u>Temp (°C)</u>			NPTS
	Mean	STDV	rms	Mean	STDV	rms	
4-m simil meas	-.03	.24	.24	.24	.19	.31	172
4-m linear meas	-.11	.24	.27	.44	.22	.49	172
4-m p-prof meas	-.06	.23	.24				172
16-m simil meas	.15	.51	.54	-.20	.35	.41	172
16-m linear meas	.51	.86	1.00	-1.05	.60	1.21	172
16-m p-prof meas	.26	.62	.68				172
30-m simil meas	.14	.66	.68	-.02	.43	.43	172
30-m linear meas	1.31	1.98	2.38	-2.63	1.34	2.95	172
30-m p-prof meas	.45	1.04	1.13				172
1400 - 1600 MDT							
	<u>Wind Speed (m/s)</u>			<u>Temp (°C)</u>			NPTS
	Mean	STDV	rms	Mean	STDV	rms	
4-m simil meas	-.01	.32	.32	.18	.16	.25	192
4-m linear meas	-.13	.32	.34	.37	.21	.43	192
4-m p-prof meas	-.06	.31	.32				192
16-m simil meas	.11	.74	.75	-.14	.24	.28	192
16-m linear meas	.69	1.26	1.43	-.92	.60	1.10	192
16-m p-prof meas	.27	.88	.92				192
30-m simil meas	.17	1.05	1.07	.01	.37	.37	192
30-m linear meas	2.02	2.91	3.54	-2.43	1.54	2.88	192
30-m p-prof meas	.57	1.46	1.57				192

Table 2. Statistics of differences between wind speed and temperature measured on a 30-m tower and values estimated from 2- and 8-m measurements using Monin-Obukhov similarity and linear and p-profile fits (continued)

Jul 11 - Aug 29, 1991

1600 - 1800 MDT

	<u>Wind Speed (m/s)</u>			<u>Temp (°C)</u>			NPTS
	Mean	STDV	rms	Mean	STDV	rms	
4-m simil meas	.03	.31	.31	.06	.25	.26	199
4-m linear meas	-.12	.30	.32	.17	.27	.32	199
4-m p-prof meas	-.02	.30	.30				199
16-m simil meas	.06	.65	.65	-.09	.33	.34	199
16-m linear meas	.78	1.05	1.31	-.56	.67	.88	199
16-m p-prof meas	.23	.76	.79				199
30-m simil meas	.18	.85	.87	.00	.56	.56	199
30-m linear meas	2.47	2.44	3.48	-1.47	1.68	2.23	199
30-m p-prof meas	.61	1.25	1.40				199

1800 - 2000 MDT

	<u>Wind Speed (m/s)</u>			<u>Temp (°C)</u>			NPTS
	Mean	STDV	rms	Mean	STDV	rms	
4-m simil meas	.02	.33	.33	.00	.14	.14	146
4-m linear meas	-.13	.32	.35	.02	.16	.16	146
4-m p-prof meas	-.02	.32	.32				146
16-m simil meas	.14	.72	.73	-.04	.36	.36	146
16-m linear meas	.88	1.00	1.33	-.12	.57	.59	146
16-m p-prof meas	.27	.80	.84				146
30-m simil meas	.40	.95	1.03	.07	.55	.55	146
30-m linear meas	2.81	2.20	3.57	-.16	1.32	1.33	146
30-m p-prof meas	.70	1.25	1.43				146

Table 2. Statistics of differences between wind speed and temperature measured on a 30-m tower and values estimated from 2- and 8-m measurements using Monin-Obukhov similarity and linear and p-profile fits (continued)

Jul 11 - Aug 29, 1991

2000 - 2200 MDT

	<u>Wind Speed (m/s)</u>			<u>Temp (°C)</u>			NPTS
	Mean	STDV	rms	Mean	STDV	rms	
4-m simil meas	.05	.29	.29	-.06	.12	.13	104
4-m linear meas	-.12	.28	.30	-.11	.11	.16	104
4-m p-prof meas	.01	.27	.27				104
16-m simil meas	.22	.62	.65	.03	.34	.34	104
16-m linear meas	1.07	.85	1.36	.24	.42	.49	104
16-m p-prof meas	.28	.71	.76				104
30-m simil meas	.98	1.02	1.42	.41	.86	.95	104
30-m linear meas	3.77	2.03	4.28	1.11	1.25	1.67	104
30-m p-prof meas	1.05	1.37	1.73				104

2200 - 2400 MDT

	<u>Wind Speed (m/s)</u>			<u>Temp (°C)</u>			NPTS
	Mean	STDV	rms	Mean	STDV	rms	
4-m simil meas	.03	.32	.33	-.05	.05	.07	125
4-m linear meas	-.14	.31	.34	-.09	.05	.10	125
4-m p-prof meas	.00	.31	.32				125
16-m simil meas	.23	.65	.69	.02	.19	.19	125
16-m linear meas	1.07	1.03	1.48	.21	.22	.30	125
16-m p-prof meas	.28	.76	.82				125
30-m simil meas	.70	1.15	1.34	.20	.49	.53	125
30-m linear meas	3.44	2.67	4.36	.80	.63	1.02	125
30-m p-prof meas	.74	1.59	1.75				125

RMS DIFFERENCE BETWEEN
4M MEASURED AND PREDICTED PARAMETER
JUL 11 - AUG 29, 1991 - DIRT SITE

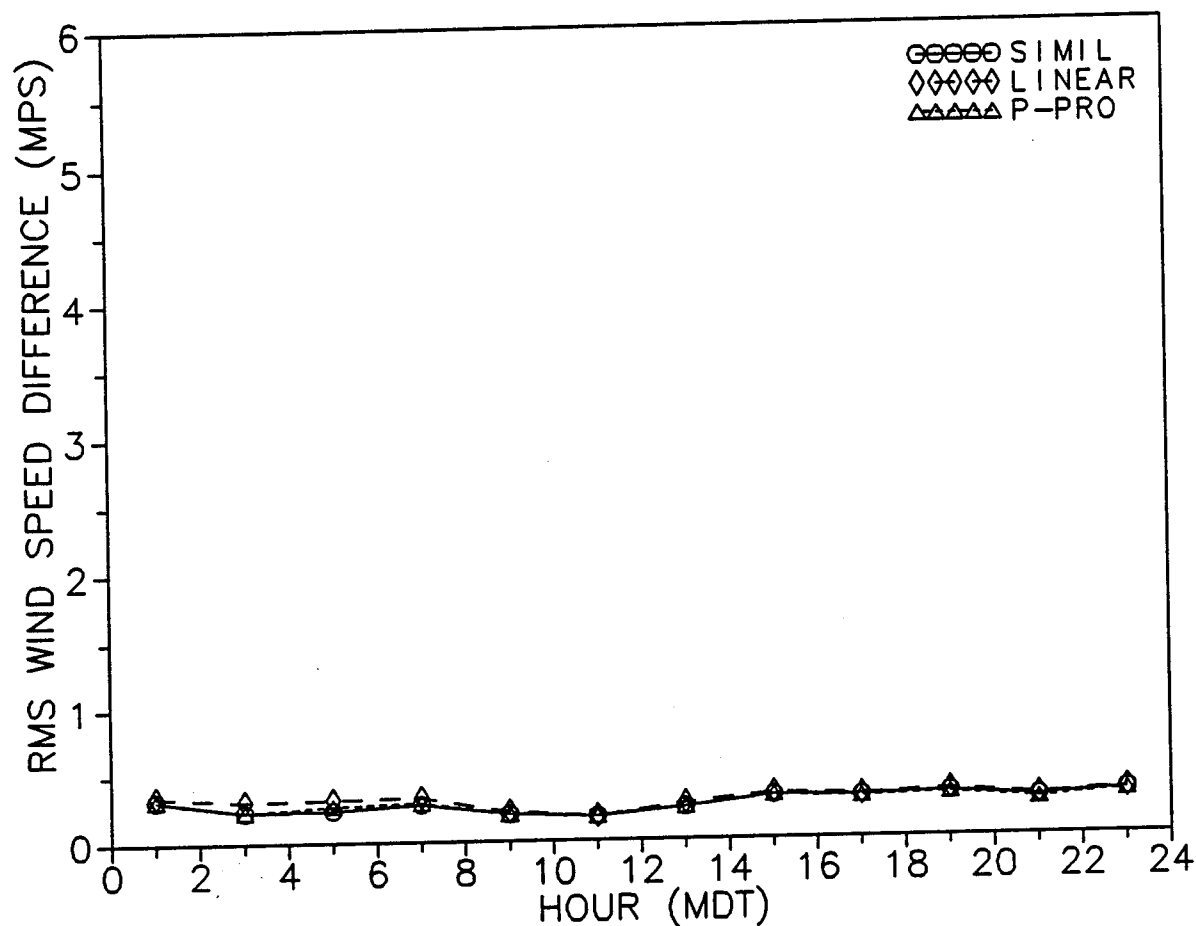


Figure 7. Rms differences between measured 4-m wind speeds and values estimated from 2- and 8-m measurements using Monin-Obukhov similarity, a linear interpolation, and a p-profile fit.

RMS DIFFERENCE BETWEEN
16M MEASURED AND PREDICTED PARAMETER
JUL 11 - AUG 29, 1991 - DIRT SITE

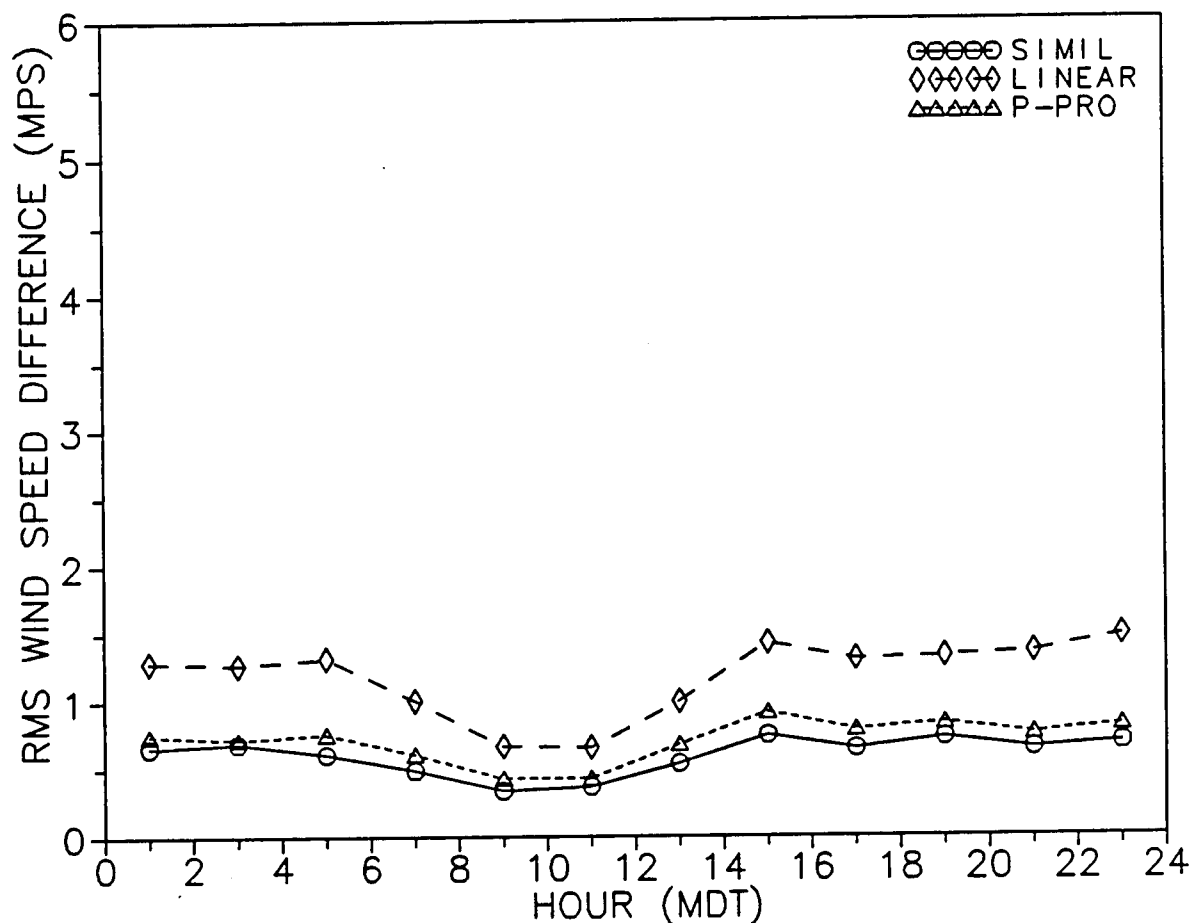


Figure 8. Rms differences between measured 16-m wind speeds and values estimated from 2- and 8-m measurements using Monin-Obukhov similarity, a linear extrapolation, and a p-profile fit.

RMS DIFFERENCE BETWEEN
30M MEASURED AND PREDICTED PARAMETER
JUL 11 - AUG 29, 1991 - DIRT SITE

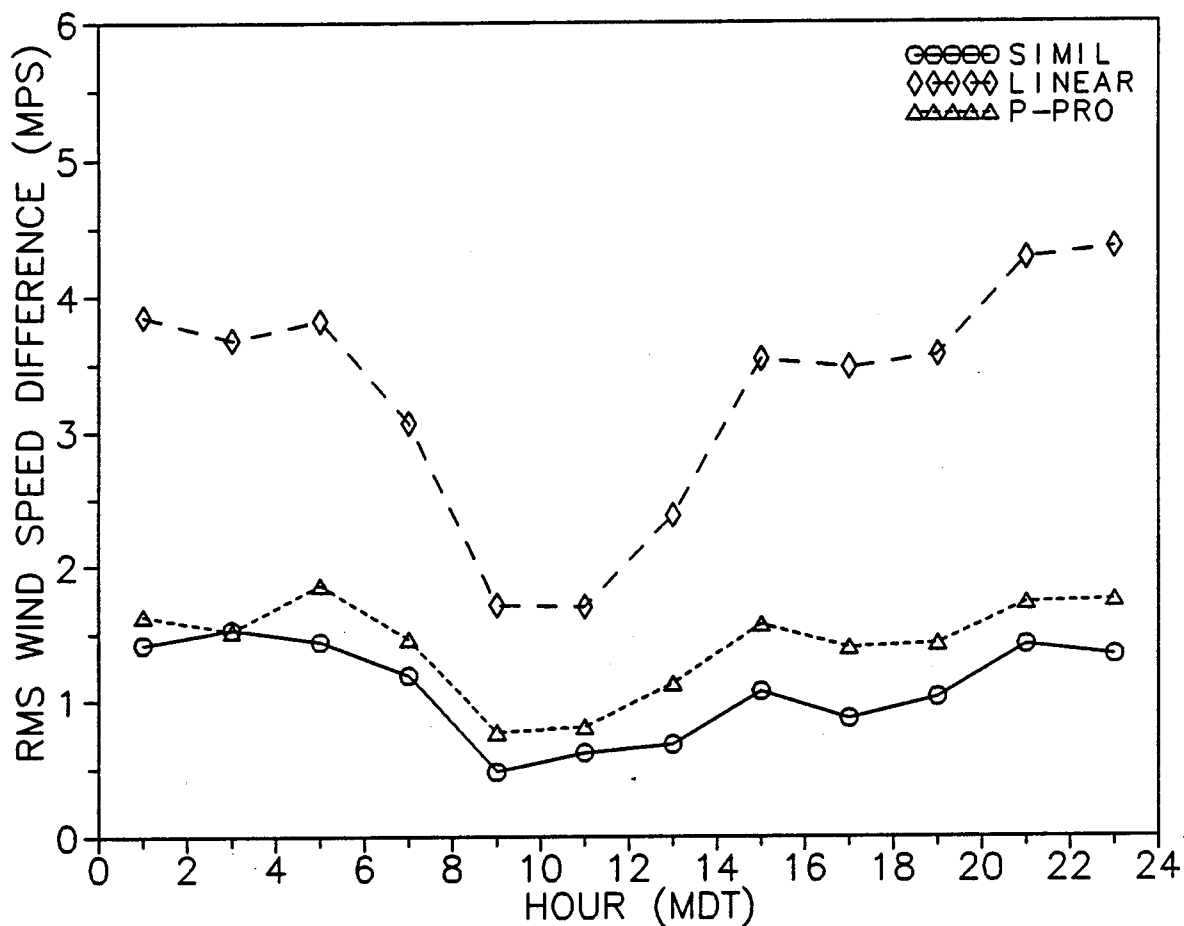


Figure 9. Rms differences between measured 30-m wind speeds and values estimated from 2- and 8-m measurements using Monin-Obukhov similarity, a linear extrapolation, and a p-profile fit.

RMS DIFFERENCE BETWEEN
4M MEASURED AND PREDICTED PARAMETER
JUL 11 - AUG 29, 1991 - DIRT SITE

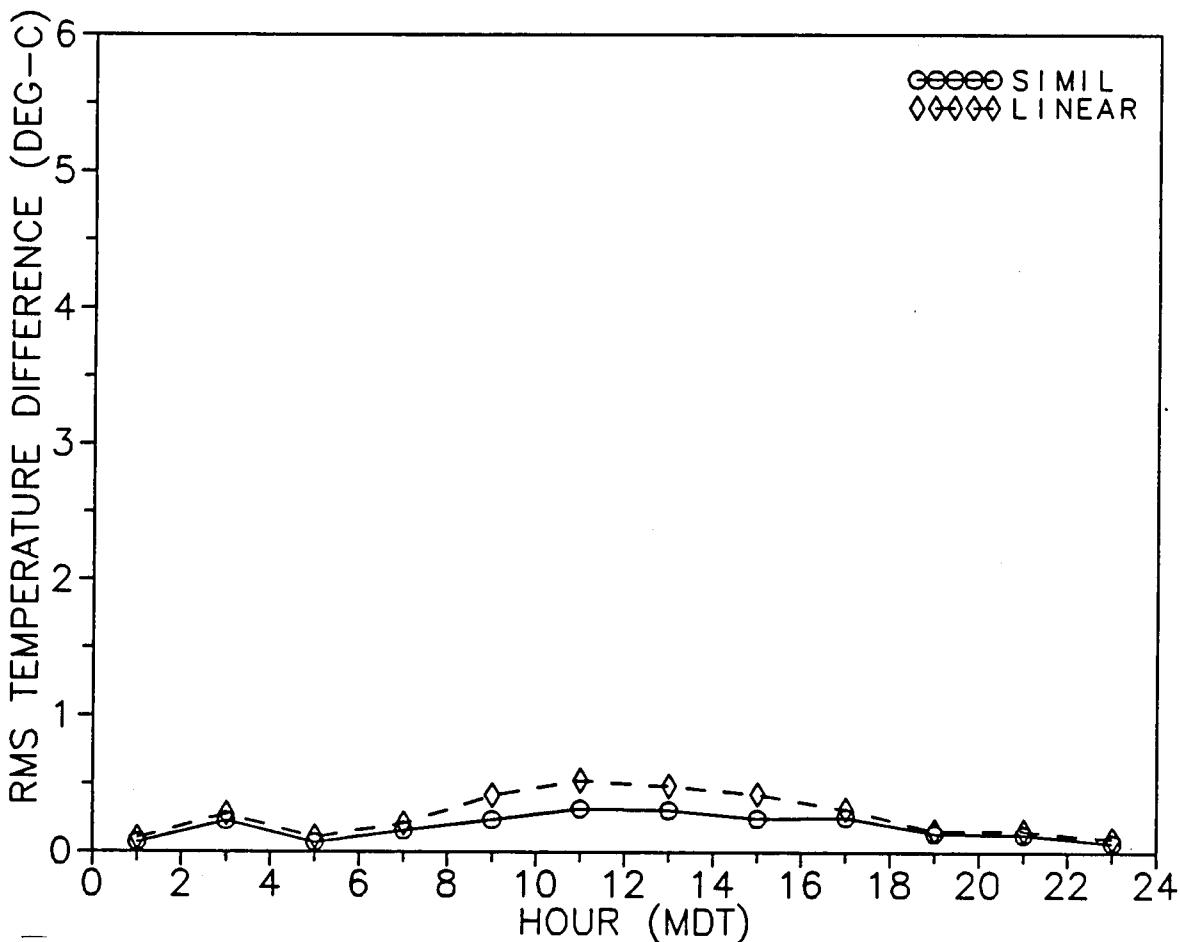


Figure 10. Rms differences between measured 4-m temperatures and values estimated from 2- and 8-m measurements using Monin-Obukhov similarity and a linear interpolation.

RMS DIFFERENCE BETWEEN
16M MEASURED AND PREDICTED PARAMETER
JUL 11 - AUG 29, 1991 - DIRT SITE

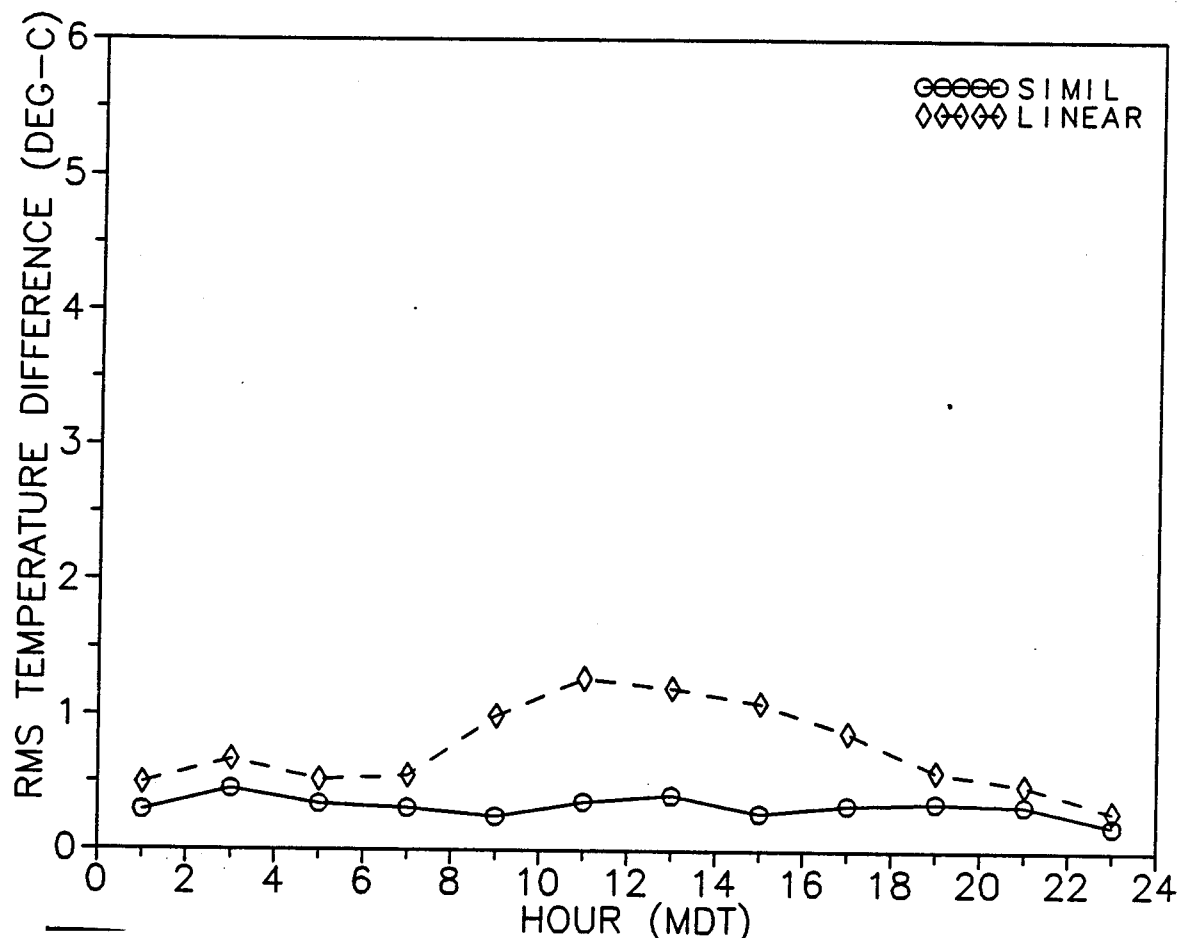


Figure 11. Rms differences between measured 16-m temperatures and values estimated from 2- and 8-m measurements using Monin-Obukhov similarity and a linear extrapolation.

RMS DIFFERENCE BETWEEN
30M MEASURED AND PREDICTED PARAMETER
JUL 11 - AUG 29, 1991 - DIRT SITE

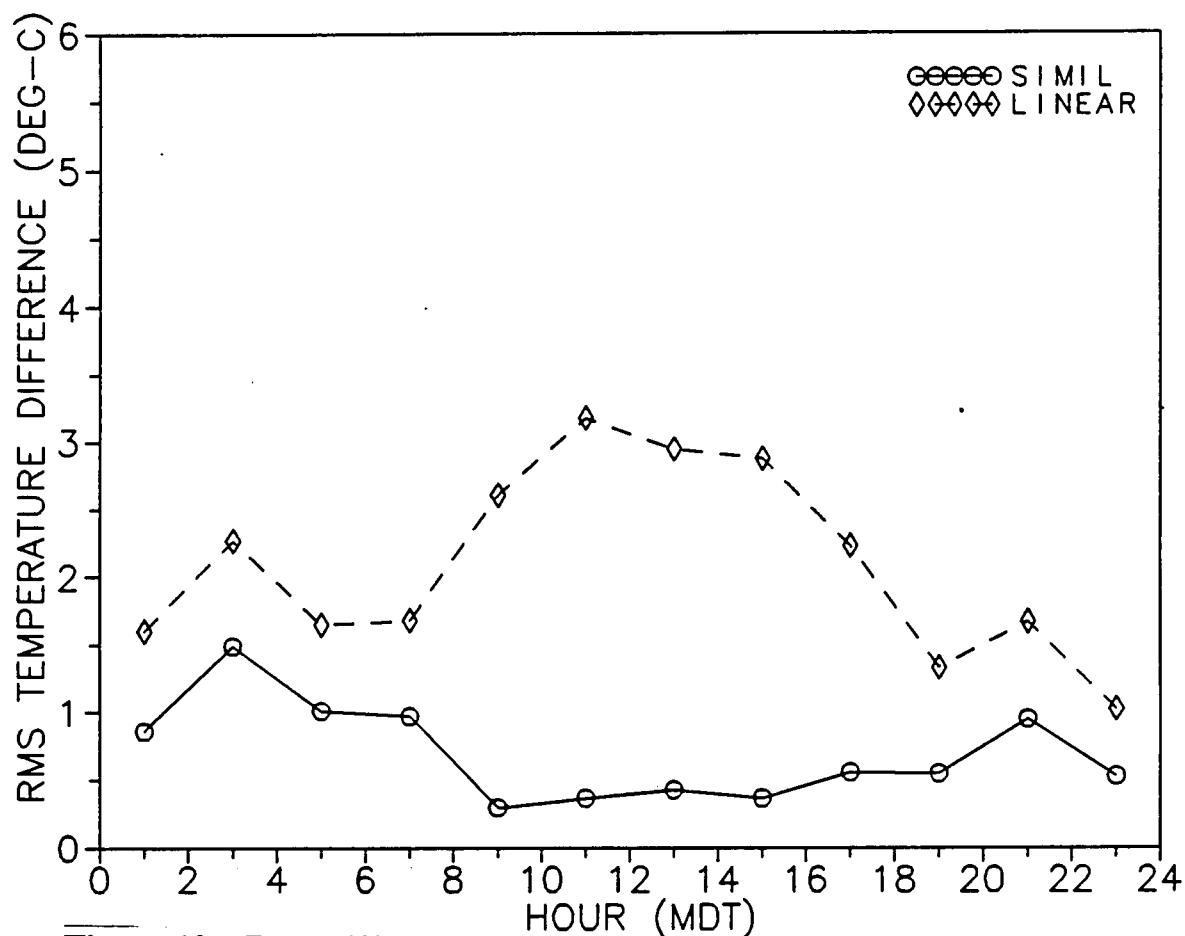


Figure 12. Rms differences between measured 30-m temperatures and values estimated from 2- and 8-m measurements using Monin-Obukhov similarity and a linear extrapolation.

4.2 Sodar Data Comparison

The statistical analyses described in the previous section were used to compare wind speed estimated by the similarity and p-profile models with conjunctive sodar data collected at the three test sites. Fifteen-minute averaged 2- and 10-m data collected on a 10-m mast were used by the two models to predict the wind speed at the six sodar measurement heights of 50, 100, 150, 200, 300, and 400 m at WSMR and 60, 110, 160, 210, 310, and 410 m at Ft. Bliss and Champaign. Statistics were computed using only data in which a solution was obtained from both models.

The WSMR results are shown in table 3 and figures 13 through 18. As expected, there was better agreement between the predicted and measured data during midday when the surface layer is usually fairly deep. The comparability of the model predictions decreased only slowly with height during those times. Between 1000 and 1200 MDT, for example, the rms differences between the similarity estimates and the measured data ranged from 1.7 to 2.0 m s⁻¹ between 50 and 400 m. The p-profile rms differences during this time were between 1.6 and 2.2 m s⁻¹. At night, there was a much more rapid decrease in comparability with altitude. This was especially true for the similarity model. Between 0400 and 0600 MDT, for example, the rms differences ranged from 2.6 to 24.7 m s⁻¹ for the similarity predictions and from 1.7 to 5.6 m s⁻¹ for the p-profile estimates. In comparison to the above results, the rms differences between in situ wind speed measurements on a 300-m tower and conjunctive Doppler sodar measurements were found to be 1.0 to 1.4 m s⁻¹ in a study by Chintawongvanich et al. [15]

The Ft. Bliss statistics have similar characteristics (figures 19 through 24 and table 4). The comparability of the p-profile estimates were considerably poorer than the WSMR p-profile estimates. Other difference is that there was better agreement between the Ft. Bliss late afternoon similarity estimates and the measured data. The rms differences between the similarity predictions and the WSMR measurements were the smallest between 0900 and 1300 MDT and became larger later in the afternoon. In contrast, the Ft. Bliss rms differences remained fairly constant throughout the afternoon and did not start to increase until 1900 MDT.

Statistics for the Champaign data are shown in table 5 and figures 25 through 30. The amount of data collected at night was limited so that only day statistics were computed above 160 m. In general, these statistics are comparable to the Ft. Bliss statistics except that the p-profile rms differences were somewhat smaller at Champaign than at Ft. Bliss.

Table 3. Statistics of differences between wind speeds measured by sodar at WSMR and values estimated from 2- and 10-m mast data using Monin-Obukhov similarity algorithms and p-profile fit

Jul 12 - Aug 31, 1991				
0000 - 0200 MDT				
	Mean	STDV (m/s)	rms	NPTS
50-m similarity measured	1.39	1.96	2.40	231
100-m similarity measured	3.94	3.07	4.99	248
150-m similarity measured	6.33	4.31	7.66	241
200-m similarity measured	8.70	5.52	10.31	241
300-m similarity measured	14.21	7.69	16.15	211
400-m similarity measured	19.84	10.48	22.44	177
50-m p-profile measured	.34	1.72	1.76	231
100-m p-profile measured	1.01	2.13	2.36	248
150-m p-profile measured	1.28	2.41	2.73	241
200-m p-profile measured	1.55	2.67	3.09	241
300-m p-profile measured	2.19	3.08	3.78	211
400-m p-profile measured	2.76	3.77	4.67	177
0200 - 0400 MDT				
	Mean	STDV (m/s)	rms	NPTS
50-m similarity measured	1.53	1.79	2.35	177
100-m similarity measured	4.13	3.29	5.28	194
150-m similarity measured	6.81	4.83	8.35	192
200-m similarity measured	9.39	6.19	11.24	180
300-m similarity measured	14.76	9.46	17.53	171
400-m similarity measured	20.81	12.78	24.42	160
50-m p-profile measured	.51	1.55	1.64	177
100-m p-profile measured	1.24	2.20	2.53	194
150-m p-profile measured	1.74	2.61	3.14	192
200-m p-profile measured	2.21	3.02	3.74	180
300-m p-profile measured	3.23	3.37	4.67	171
400-m p-profile measured	3.94	3.89	5.54	160

Table 3. Statistics of differences between wind speeds measured by sodar at WSMR and values estimated from 2- and 10-m mast data using Monin-Obukhov similarity algorithms and p-profile fit (continued)

Jul 12 - Aug 31, 1991				
0400 - 0600 MDT				
	Mean	STDV (m/s)	rms	NPTS
50-m similarity measured	1.69	1.91	2.55	133
100-m similarity measured	4.39	2.89	5.26	148
150-m similarity measured	7.34	4.32	8.51	150
200-m similarity measured	10.57	5.70	12.01	149
300-m similarity measured	15.98	7.87	17.82	137
400-m similarity measured	22.46	10.38	24.74	118
50-m p-profile measured	.45	1.62	1.68	133
100-m p-profile measured	1.03	1.95	2.20	148
150-m p-profile measured	1.62	2.39	2.89	150
200-m p-profile measured	2.29	2.87	3.68	149
300-m p-profile measured	3.06	3.51	4.66	137
400-m p-profile measured	4.14	3.79	5.61	118
0600 - 0800 MDT				
	Mean	STDV (m/s)	rms	NPTS
50-m similarity measured	.60	2.13	2.22	194
100-m similarity measured	2.00	3.73	4.23	219
150-m similarity measured	3.50	5.40	6.44	214
200-m similarity measured	4.78	7.36	8.78	220
300-m similarity measured	7.50	10.59	12.98	188
400-m similarity measured	10.64	14.46	17.95	161
50-m p-profile measured	.11	1.70	1.71	194
100-m p-profile measured	.52	2.21	2.27	219
150-m p-profile measured	.85	2.51	2.65	214
200-m p-profile measured	1.04	3.04	3.21	220
300-m p-profile measured	1.70	3.62	4.00	188
400-m p-profile measured	2.47	4.14	4.82	161

Table 3. Statistics of differences between wind speeds measured by sodar at WSMR and values estimated from 2- and 10-m mast data using Monin-Obukhov similarity algorithms and p-profile fit (continued)

Jul 12 - Aug 31, 1991				
0800 - 1000 MDT				
	Mean	STDV (m/s)	rms	NPTS
50-m similarity measured	-.47	1.36	1.44	329
100-m similarity measured	-.48	1.46	1.54	355
150-m similarity measured	-.59	1.58	1.69	356
200-m similarity measured	-.79	1.67	1.84	351
300-m similarity measured	-.88	1.91	2.10	331
400-m similarity measured	-.84	2.28	2.43	300
50-m p-profile measured	-.19	1.48	1.50	329
100-m p-profile measured	.00	1.68	1.68	355
150-m p-profile measured	.05	1.86	1.86	356
200-m p-profile measured	-.03	2.01	2.01	351
300-m p-profile measured	.08	2.31	2.31	331
400-m p-profile measured	.24	2.51	2.52	300
1000 - 1200 MDT				
	Mean	STDV (m/s)	rms	NPTS
50-m similarity measured	-.96	1.53	1.81	327
100-m similarity measured	-1.00	1.41	1.73	339
150-m similarity measured	-.93	1.62	1.87	337
200-m similarity measured	-1.04	1.58	1.90	322
300-m similarity measured	-.92	1.82	2.04	304
400-m similarity measured	-.84	1.71	1.90	290
50-m p-profile measured	-.69	1.60	1.74	327
100-m p-profile measured	-.52	1.52	1.60	339
150-m p-profile measured	-.31	1.80	1.82	337
200-m p-profile measured	-.33	1.76	1.79	322
300-m p-profile measured	-.01	2.20	2.20	304
400-m p-profile measured	.23	2.22	2.23	290

Table 3. Statistics of differences between wind speeds measured by sodar at WSMR and values estimated from 2- and 10-m mast data using Monin-Obukhov similarity algorithms and p-profile fit (continued)

Jul 12 - Aug 31, 1991				
1200 - 1400 MDT				
	Mean	STDV (m/s)	rms	NPTS
50-m similarity measured	-1.01	2.14	2.37	315
100-m similarity measured	-1.28	2.49	2.80	328
150-m similarity measured	-1.05	2.41	2.63	297
200-m similarity measured	-1.07	2.51	2.73	272
300-m similarity measured	-1.27	2.97	3.23	272
400-m similarity measured	-.67	2.78	2.86	231
50-m p-profile measured	-.70	2.24	2.35	315
100-m p-profile measured	-.72	2.74	2.83	328
150-m p-profile measured	-.31	2.75	2.77	297
200-m p-profile measured	-.21	2.93	2.94	272
300-m p-profile measured	-.18	3.54	3.55	272
400-m p-profile measured	.58	3.62	3.67	231
1400 - 1600 MDT				
	Mean	STDV (m/s)	rms	NPTS
50-m similarity measured	-.75	2.38	2.50	305
100-m similarity measured	-.52	3.01	3.06	314
150-m similarity measured	-.54	2.92	2.97	273
200-m similarity measured	-.36	3.79	3.80	271
300-m similarity measured	-.43	4.17	4.19	244
400-m similarity measured	-.40	4.56	4.58	216
50-m p-profile measured	-.37	2.43	2.46	305
100-m p-profile measured	.14	3.03	3.03	314
150-m p-profile measured	.44	3.05	3.08	273
200-m p-profile measured	.72	3.56	3.63	271
300-m p-profile measured	.72	3.74	3.81	244
400-m p-profile measured	.90	4.10	4.19	216

Table 3. Statistics of differences between wind speeds measured by sodar at WSMR and values estimated from 2- and 10-m mast data using Monin-Obukhov similarity algorithms and p-profile fit (continued)

Jul 12 - Aug 31, 1991				
1600 - 1800 MDT				
	Mean	STDV (m/s)	rms	NPTS
50-m similarity measured	-.20	2.14	2.15	322
100-m similarity measured	.05	2.88	2.88	328
150-m similarity measured	.24	3.61	3.62	312
200-m similarity measured	.91	4.44	4.53	302
300-m similarity measured	1.25	5.72	5.86	283
400-m similarity measured	1.67	6.99	7.19	249
50-m p-profile measured	.13	2.10	2.11	322
100-m p-profile measured	.56	2.43	2.49	328
150-m p-profile measured	.80	2.69	2.81	312
200-m p-profile measured	1.50	3.04	3.39	302
300-m p-profile measured	1.83	3.19	3.68	283
400-m p-profile measured	2.23	3.93	4.52	249
1800 - 2000 MDT				
	Mean	STDV (m/s)	rms	NPTS
50-m similarity measured	.59	2.24	2.32	250
100-m similarity measured	1.69	3.39	3.79	276
150-m similarity measured	2.91	4.74	5.56	281
200-m similarity measured	4.04	6.10	7.32	271
300-m similarity measured	6.06	8.58	10.50	244
400-m similarity measured	8.04	11.40	13.95	205
50-m p-profile measured	.44	2.06	2.10	250
100-m p-profile measured	1.01	2.44	2.64	276
150-m p-profile measured	1.57	2.75	3.17	281
200-m p-profile measured	2.11	3.21	3.84	271
300-m p-profile measured	2.78	3.53	4.49	244
400-m p-profile measured	3.14	4.18	5.23	205

Table 3. Statistics of differences between wind speeds measured by sodar at WSMR and values estimated from 2- and 10-m mast data using Monin-Obukhov similarity algorithms and p-profile fit (continued)

Jul 12 - Aug 31, 1991				
2000 - 2200 MDT				
	Mean	STDV (m/s)	rms	NPTS
50-m similarity measured	1.28	2.29	2.62	196
100-m similarity measured	3.76	3.74	5.30	214
150-m similarity measured	6.11	5.46	8.19	195
200-m similarity measured	8.12	7.23	10.88	200
300-m similarity measured	12.48	10.29	16.18	164
400-m similarity measured	18.28	13.86	22.94	141
50-m p-profile measured	.35	2.06	2.09	196
100-m p-profile measured	1.18	2.66	2.91	214
150-m p-profile measured	1.52	3.03	3.39	195
200-m p-profile measured	1.84	3.47	3.93	200
300-m p-profile measured	2.39	4.03	4.68	164
400-m p-profile measured	3.59	4.45	5.72	141
2200 - 2400 MDT				
	Mean	STDV (m/s)	rms	NPTS
50-m similarity measured	1.52	2.62	3.02	223
100-m similarity measured	3.78	3.75	5.32	233
150-m similarity measured	5.97	5.14	7.88	216
200-m similarity measured	8.51	6.40	10.65	209
300-m similarity measured	14.45	10.31	17.75	201
400-m similarity measured	19.33	12.86	23.22	162
50-m p-profile measured	.62	2.68	2.75	223
100-m p-profile measured	1.31	3.43	3.67	233
150-m p-profile measured	1.86	3.99	4.40	216
200-m p-profile measured	2.26	4.25	4.81	209
300-m p-profile measured	3.14	4.90	5.82	201
400-m p-profile measured	3.51	4.94	6.06	162

RMS DIFFERENCE BETWEEN
50M MEASURED AND PREDICTED PARAMETER
JUL 12 - AUG 31, 1991 - DIRT SITE

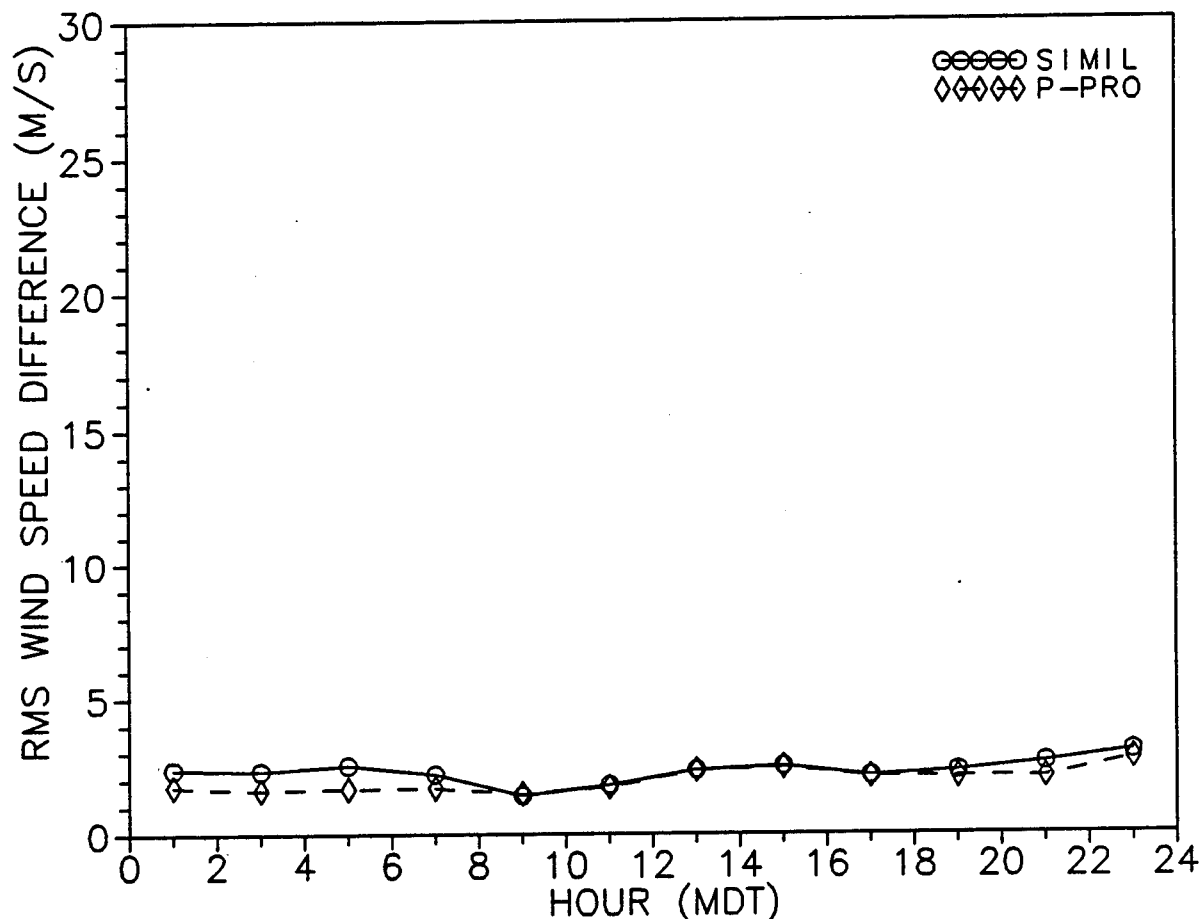


Figure 13. Rms differences between 50-m sodar wind speed measurements collected at WSMR and values estimated from 2- and 10-m mast data using Monin-Obukhov similarity and a p-profile fit.

RMS DIFFERENCE BETWEEN
100M MEASURED AND PREDICTED PARAMETER
JUL 12 - AUG 31, 1991 - DIRT SITE

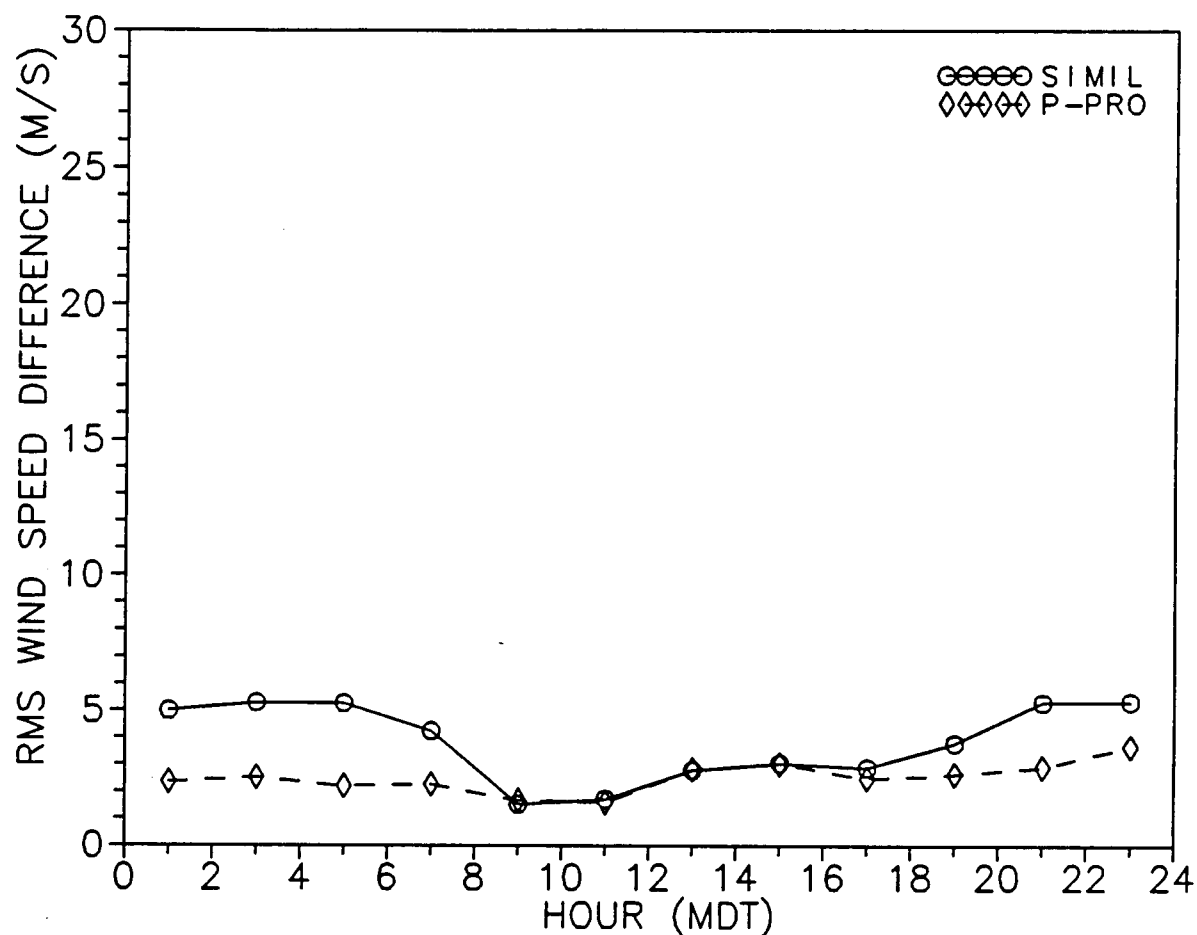


Figure 14. Rms differences between 100-m sodar wind speed measurements collected at WSMR and values estimated from 2- and 10-m mast data using Monin-Obukhov similarity and a p-profile fit.

RMS DIFFERENCE BETWEEN
150M MEASURED AND PREDICTED PARAMETER
JUL 12 - AUG 31, 1991 - DIRT SITE

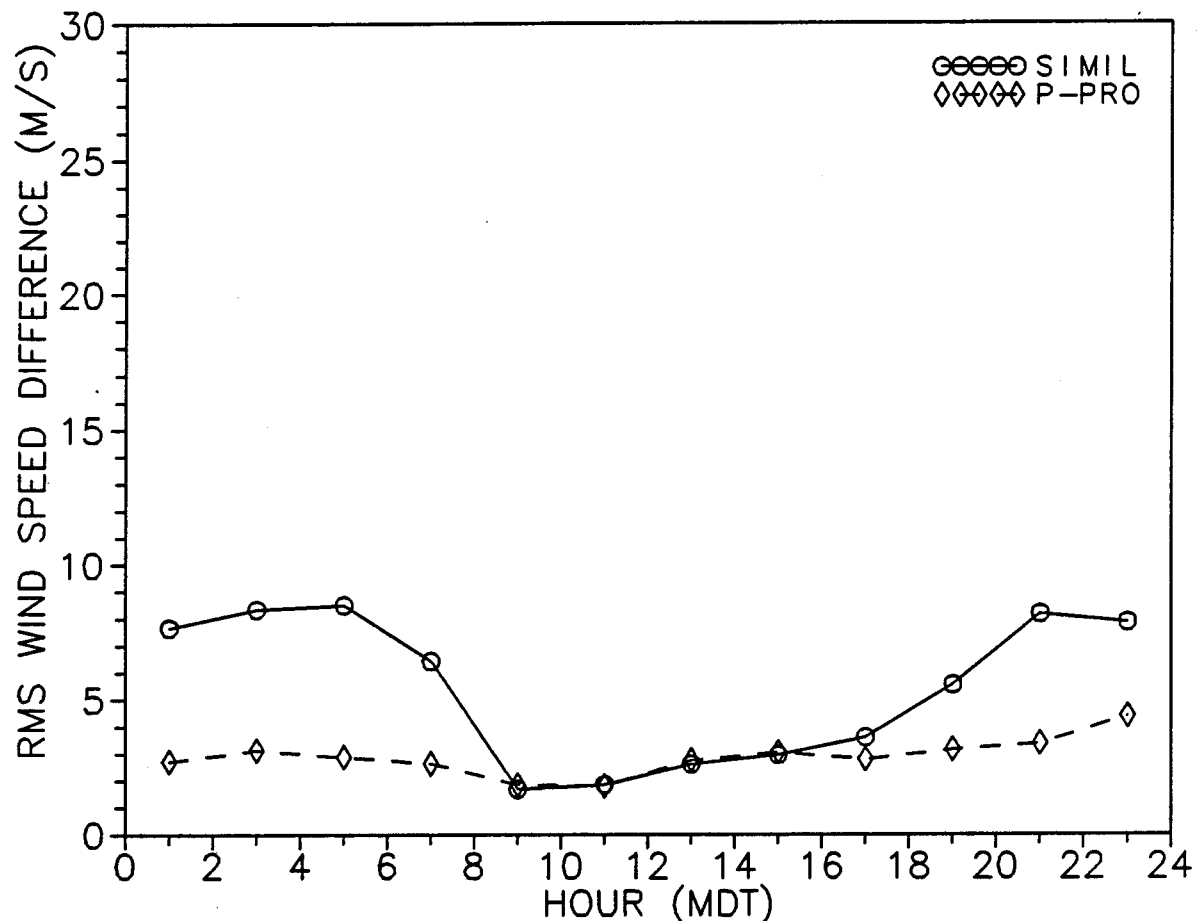


Figure 15. Rms differences between 150-m sodar wind speed measurements collected at WSMR and values estimated from 2- and 10-m mast data using Monin-Obukhov similarity and a p-profile fit.

RMS DIFFERENCE BETWEEN
200M MEASURED AND PREDICTED PARAMETER
JUL 12 - AUG 31, 1991 - DIRT SITE

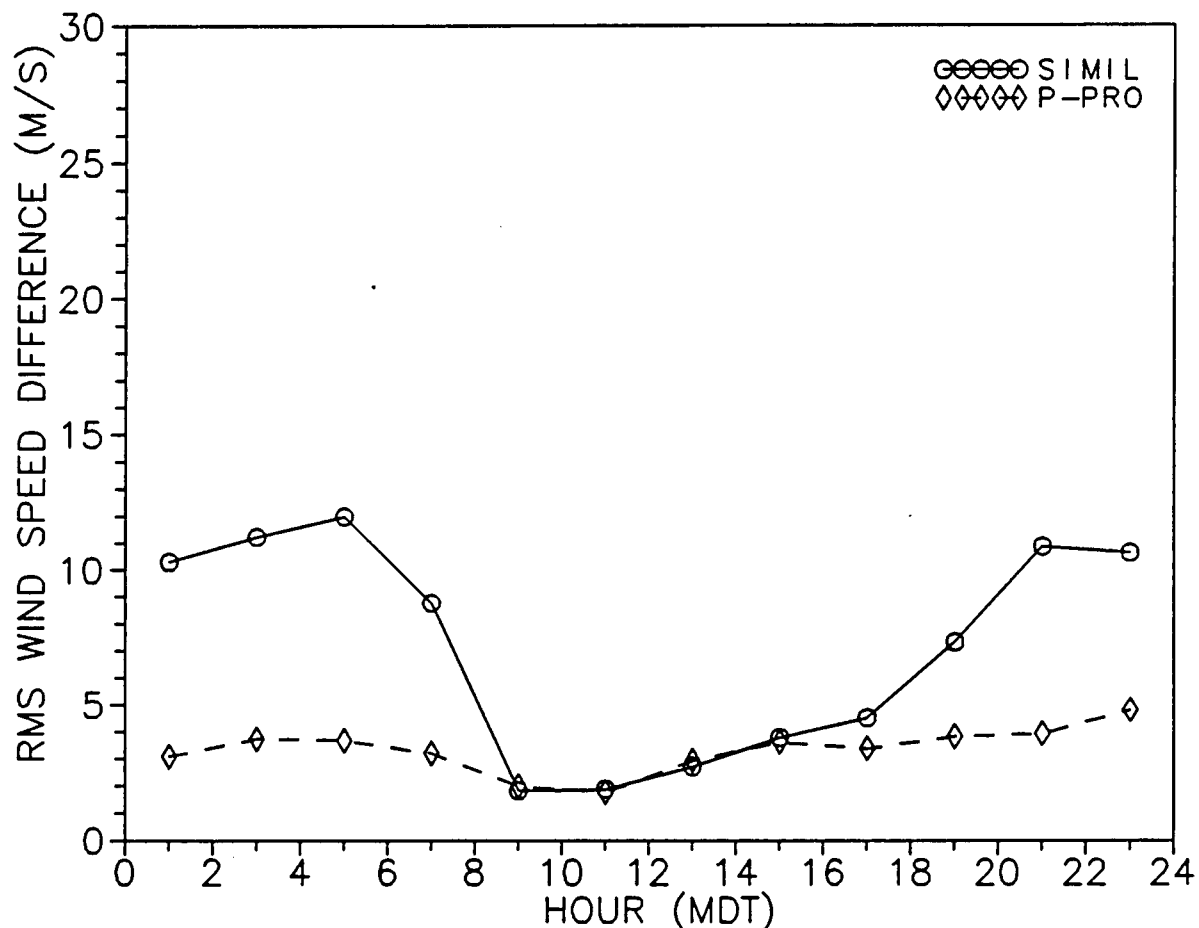


Figure 16. Rms differences between 200-m sodar wind speed measurements collected at WSMR and values estimated from 2- and 10-m mast data using Monin-Obukhov similarity and a p-profile fit.

RMS DIFFERENCE BETWEEN
300M MEASURED AND PREDICTED PARAMETER
JUL 12 - AUG 31, 1991 - DIRT SITE

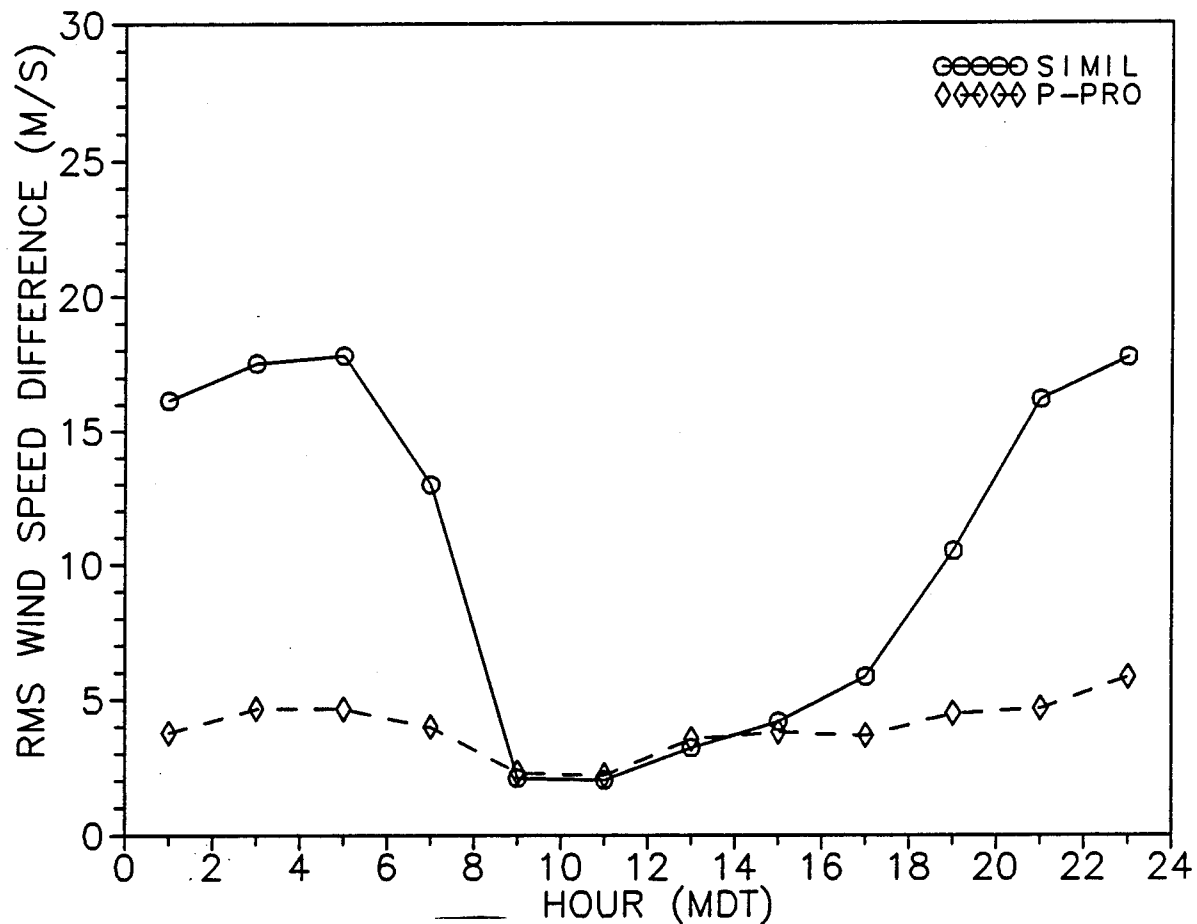


Figure 17. Rms differences between 300-m sodar wind speed measurements collected at WSMR and values estimated from 2- and 10-m mast data using Monin-Obukhov similarity and a p-profile fit.

RMS DIFFERENCE BETWEEN
400M MEASURED AND PREDICTED PARAMETER
JUL 12 - AUG 31, 1991 - DIRT SITE

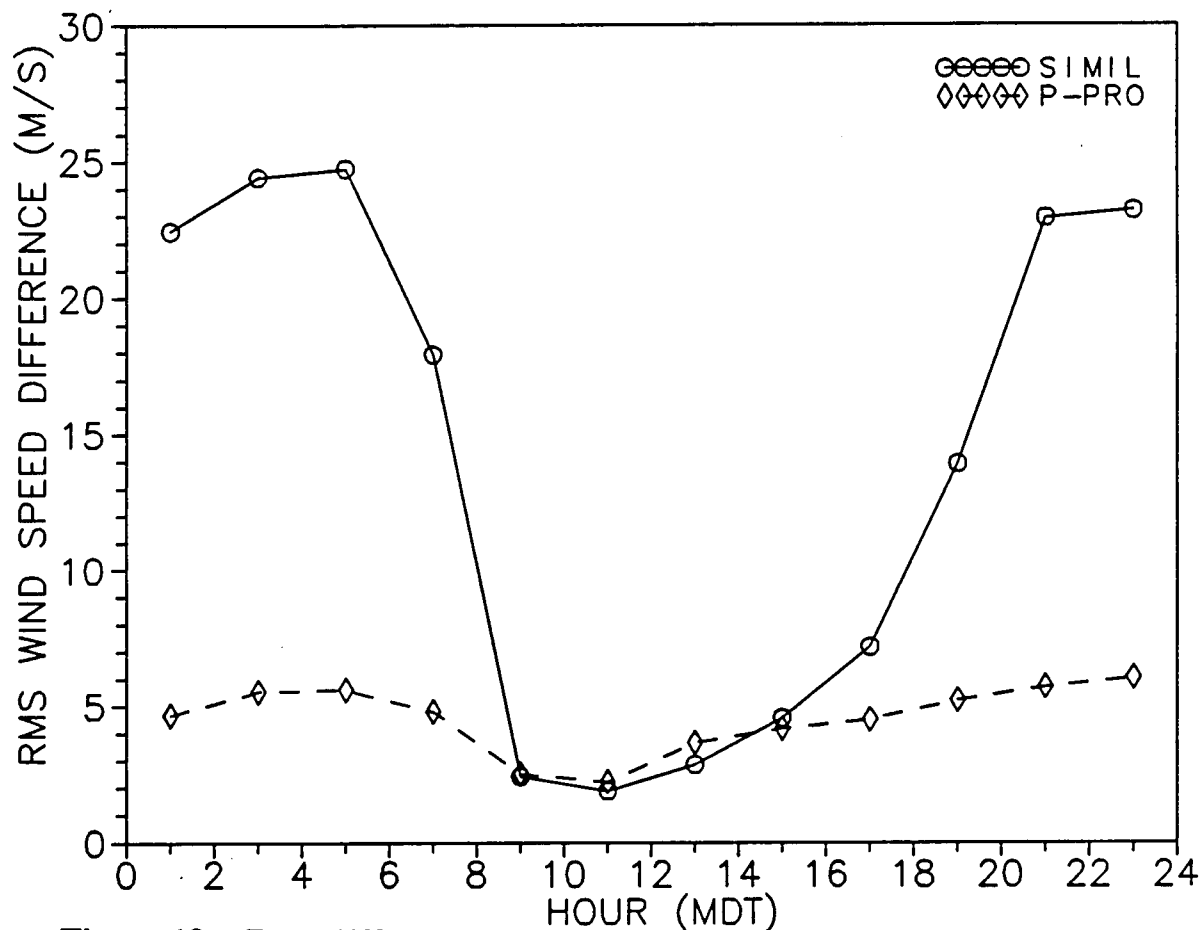


Figure 18. Rms differences between 400-m sodar wind speed measurements collected at WSMR and values estimated from 2- and 10-m mast data using Monin-Obukhov similarity and a p-profile fit.

Table 4. Statistics of differences between wind speeds measured by sodar at Ft. Bliss and values estimated from 2- and 10-m mast data using Monin-Obukhov similarity algorithm and p-profile fit

Jun 4 - Jun 25, 1990				
0000 - 0200 MDT				
	Mean	STDV (m/s)	rms	NPTS
60-m similarity measured	1.73	3.14	3.58	76
110-m similarity measured	5.99	5.25	7.97	77
160-m similarity measured	9.06	7.43	11.72	77
210-m similarity measured	11.78	9.65	15.23	69
310-m similarity measured	16.95	14.52	22.32	41
410-m similarity measured	19.39	15.32	24.71	33
60-m p-profile measured	.75	2.42	2.54	76
110-m p-profile measured	2.94	3.34	4.45	77
160-m p-profile measured	3.61	4.10	5.47	77
210-m p-profile measured	3.83	4.82	6.15	69
310-m p-profile measured	5.15	5.95	7.87	41
410-m p-profile measured	5.66	5.13	7.63	33
0200 - 0400 MDT				
	Mean	STDV (m/s)	rms	NPTS
60-m similarity measured	.80	2.42	2.55	78
110-m similarity measured	4.65	3.97	6.12	79
160-m similarity measured	7.86	6.15	9.98	79
210-m similarity measured	11.07	8.39	13.89	79
310-m similarity measured	17.57	12.52	21.58	56
410-m similarity measured	20.23	12.32	23.68	39
60-m p-profile measured	-.04	1.96	1.96	78
110-m p-profile measured	2.03	2.42	3.16	79
160-m p-profile measured	3.08	3.22	4.46	79
210-m p-profile measured	3.92	4.06	5.65	79
310-m p-profile measured	5.49	5.37	7.68	56
410-m p-profile measured	5.71	4.69	7.39	39

Table 4. Statistics of differences between wind speeds measured by sodar at Ft. Bliss and values estimated from 2- and 10-m mast data using Monin-Obukhov similarity algorithm and p-profile fit (continued)

Jun 4 - Jun 25, 1990				
0400 - 0600 MDT				
	Mean	STDV (m/s)	rms	NPTS
60-m similarity measured	.72	2.05	2.18	74
110-m similarity measured	4.48	3.82	5.89	74
160-m similarity measured	7.63	6.15	9.80	74
210-m similarity measured	10.49	8.13	13.27	71
310-m similarity measured	15.30	10.97	18.83	54
410-m similarity measured	17.39	13.61	22.08	37
60-m p-profile measured	.04	1.42	1.42	74
110-m p-profile measured	2.19	1.86	2.87	74
160-m p-profile measured	3.37	2.79	4.37	74
210-m p-profile measured	4.30	3.81	5.74	71
310-m p-profile measured	6.31	5.18	8.16	54
410-m p-profile measured	6.68	5.52	8.67	37
0600 - 0800 MDT				
	Mean	STDV (m/s)	rms	NPTS
60-m similarity measured	-.40	1.56	1.61	89
110-m similarity measured	.99	2.44	2.63	89
160-m similarity measured	1.94	3.90	4.36	88
210-m similarity measured	2.76	5.41	6.07	85
310-m similarity measured	3.33	6.40	7.22	59
410-m similarity measured	2.79	7.74	8.23	43
60-m p-profile measured	.09	1.67	1.68	89
110-m p-profile measured	1.47	2.08	2.54	89
160-m p-profile measured	2.14	2.89	3.60	88
210-m p-profile measured	2.62	3.67	4.51	85
310-m p-profile measured	2.78	3.38	4.38	59
410-m p-profile measured	2.84	3.78	4.72	43

Table 4. Statistics of differences between wind speeds measured by sodar at Ft. Bliss and values estimated from 2- and 10-m mast data using Monin-Obukhov similarity algorithm and p-profile fit (continued)

Jun 4 - Jun 25, 1990

0800 - 1000 MDT

	Mean	STDV (m/s)	rms	NPTS
60-m similarity measured	.12	1.05	1.06	102
110-m similarity measured	.40	1.13	1.20	103
160-m similarity measured	.44	1.24	1.31	104
210-m similarity measured	.47	1.44	1.52	97
310-m similarity measured	.66	1.97	2.07	74
410-m similarity measured	.56	2.72	2.77	56
60-m p-profile measured	1.31	1.53	2.02	102
110-m p-profile measured	2.38	2.05	3.14	103
160-m p-profile measured	3.04	2.50	3.94	104
210-m p-profile measured	3.59	2.99	4.67	97
310-m p-profile measured	4.47	3.98	5.99	74
410-m p-profile measured	4.93	5.28	7.23	56

1000 - 1200 MDT

	Mean	STDV (m/s)	rms	NPTS
60-m similarity measured	-.08	1.40	1.40	103
110-m similarity measured	.21	1.45	1.46	103
160-m similarity measured	.31	1.62	1.65	103
210-m similarity measured	.30	1.84	1.87	95
310-m similarity measured	.42	2.14	2.18	62
410-m similarity measured	.51	2.44	2.50	46
60-m p-profile measured	.95	1.68	1.93	103
110-m p-profile measured	1.87	2.01	2.74	103
160-m p-profile measured	2.45	2.38	3.41	103
210-m p-profile measured	2.84	2.74	3.95	95
310-m p-profile measured	3.75	3.35	5.03	62
410-m p-profile measured	4.38	3.86	5.84	46

Table 4. Statistics of differences between wind speeds measured by sodar at Ft. Bliss and values estimated from 2- and 10-m mast data using Monin-Obukhov similarity algorithm and p-profile fit (continued)

Jun 4 - Jun 25, 1990				
1200 - 1400 MDT				
	Mean	STDV (m/s)	rms	NPTS
60-m similarity measured	-.01	1.66	1.66	102
110-m similarity measured	.26	1.69	1.71	103
160-m similarity measured	.25	1.89	1.90	101
210-m similarity measured	.27	2.15	2.17	78
310-m similarity measured	.03	1.92	1.92	55
410-m similarity measured	-.45	2.15	2.20	41
60-m p-profile measured	1.12	1.98	2.28	102
110-m p-profile measured	2.08	2.31	3.11	103
160-m p-profile measured	2.60	2.73	3.77	101
210-m p-profile measured	3.19	3.26	4.56	78
310-m p-profile measured	3.64	3.30	4.91	55
410-m p-profile measured	3.71	3.72	5.26	41
1400-1600 MDT				
	Mean	STDV (m/s)	rms	NPTS
60-m similarity measured	-.23	1.41	1.42	103
110-m similarity measured	.03	1.40	1.40	103
160-m similarity measured	.00	1.49	1.49	100
210-m similarity measured	-.07	1.77	1.77	80
310-m similarity measured	.07	1.96	1.96	54
410-m similarity measured	-.02	2.52	2.52	44
60-m p-profile measured	.90	1.76	1.98	103
110-m p-profile measured	1.86	2.07	2.78	103
160-m p-profile measured	2.32	2.33	3.29	100
210-m p-profile measured	2.82	2.75	3.93	80
310-m p-profile measured	3.75	3.21	4.94	54
410-m p-profile measured	4.34	3.77	5.75	44

Table 4. Statistics of differences between wind speeds measured by sodar at Ft. Bliss and values estimated from 2- and 10-m mast data using Monin-Obukhov similarity algorithm and p-profile fit (continued)

Jun 4 - Jun 25, 1990				
1600 - 1800 MDT				
	Mean	STDV (m/s)	rms	NPTS
60-m similarity measured	-.06	1.39	1.39	101
110-m similarity measured	.25	1.43	1.45	101
160-m similarity measured	.27	1.57	1.59	95
210-m similarity measured	.21	1.83	1.84	76
310-m similarity measured	-.06	1.92	1.93	55
410-m similarity measured	-.62	3.09	3.15	43
60-m p-profile measured	1.12	1.71	2.04	101
110-m p-profile measured	2.18	2.04	2.98	101
160-m p-profile measured	2.72	2.32	3.58	95
210-m p-profile measured	3.06	2.71	4.08	76
310-m p-profile measured	3.42	3.03	4.57	55
410-m p-profile measured	2.99	4.13	5.10	43
1800 - 2000 MDT				
	Mean	STDV (m/s)	rms	NPTS
60-m similarity measured	.29	1.65	1.68	100
110-m similarity measured	1.07	2.00	2.27	92
160-m similarity measured	1.33	2.33	2.68	80
210-m similarity measured	1.17	2.50	2.76	48
310-m similarity measured	-.30	2.98	3.00	25
410-m similarity measured	-.71	5.19	5.23	19
60-m p-profile measured	1.24	1.76	2.15	100
110-m p-profile measured	2.54	2.07	3.27	92
160-m p-profile measured	3.25	2.32	3.99	80
210-m p-profile measured	4.07	2.59	4.82	48
310-m p-profile measured	3.39	3.53	4.90	25
410-m p-profile measured	3.49	5.36	6.40	19

Table 4. Statistics of differences between wind speeds measured by sodar at Ft. Bliss and values estimated from 2- and 10-m mast data using Monin-Obukhov similarity algorithm and p-profile fit (continued)

Jun 4, 1990 - Jun 25, 1990				
2000 - 2200 MDT				
	Mean	STDV (m/s)	rms	NPTS
60-m similarity measured	1.85	2.81	3.36	81
110-m similarity measured	5.37	4.47	6.98	73
160-m similarity measured	8.50	6.64	10.79	71
210-m similarity measured	11.17	8.46	14.01	56
310-m similarity measured	13.88	10.79	17.58	24
410-m similarity measured	19.41	15.06	24.57	19
60-m p-profile measured	.67	2.05	2.15	81
110-m p-profile measured	2.35	2.62	3.52	73
160-m p-profile measured	3.33	3.54	4.86	71
210-m p-profile measured	4.09	4.25	5.90	56
310-m p-profile measured	5.87	5.18	7.83	24
410-m p-profile measured	8.34	6.43	10.53	19
2200 - 2400 MDT				
	Mean	STDV (m/s)	rms	NPTS
60-m similarity measured	2.45	2.90	3.80	78
110-m similarity measured	6.62	5.45	8.58	79
160-m similarity measured	9.92	8.16	12.84	74
210-m similarity measured	11.03	9.26	14.40	55
310-m similarity measured	14.68	13.32	19.83	29
410-m similarity measured	20.59	17.31	26.89	20
60-m p-profile measured	1.39	2.01	2.45	78
110-m p-profile measured	3.54	2.92	4.59	79
160-m p-profile measured	4.44	3.77	5.82	74
210-m p-profile measured	4.17	4.13	5.87	55
310-m p-profile measured	5.12	5.21	7.30	29
410-m p-profile measured	7.50	5.75	9.45	20

RMS DIFFERENCE BETWEEN
60M MEASURED AND PREDICTED PARAMETER
JUN 04 - JUN 25, 1990 - FT. BLISS

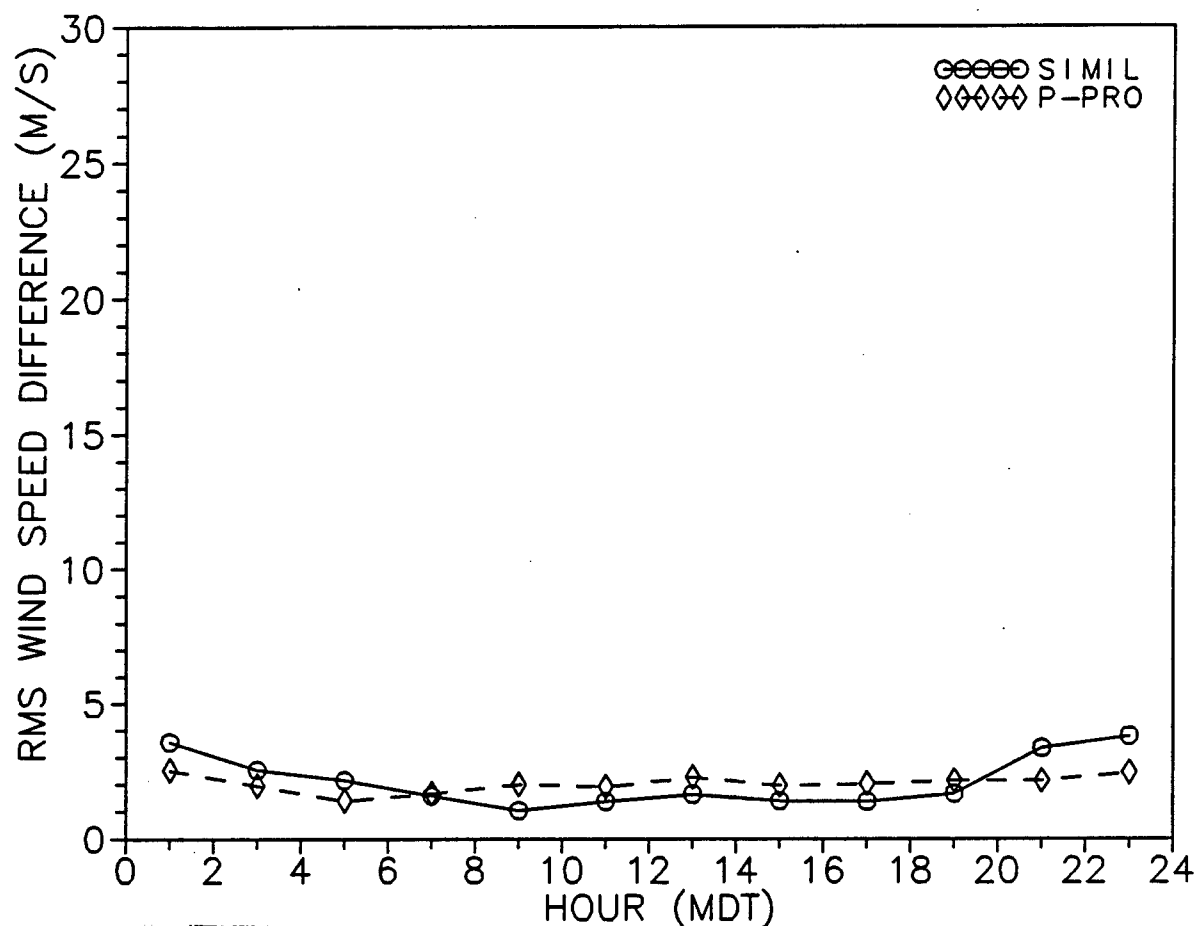


Figure 19. Rms differences between 60-m sodar wind speed measurements collected at Ft. Bliss and values estimated from 2- and 10-m mast data using Monin-Obukhov similarity and a p-profile fit.

RMS DIFFERENCE BETWEEN
110M MEASURED AND PREDICTED PARAMETER
JUN 04 - JUN 25, 1990 - FT. BLISS

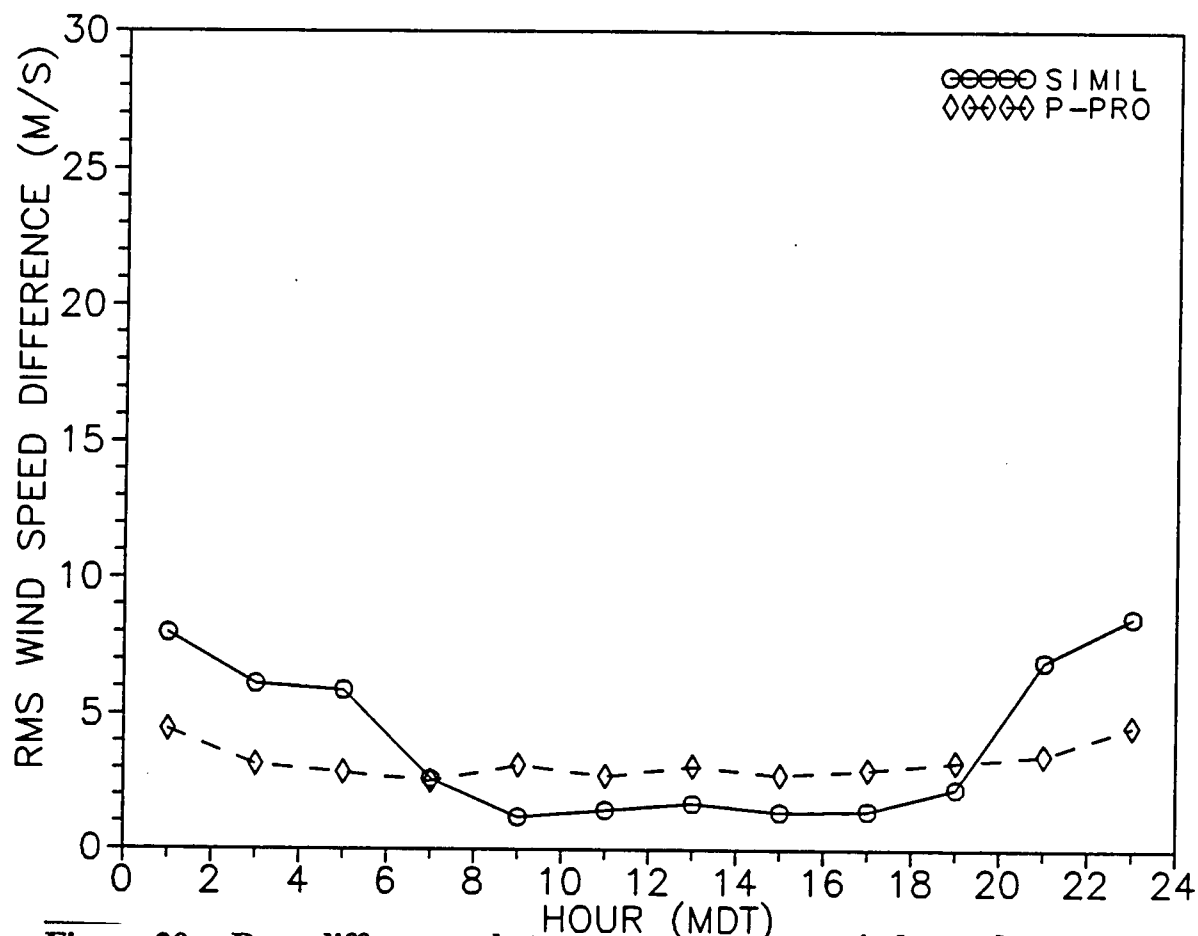


Figure 20. Rms differences between 110-m sodar wind speed measurements collect at Ft. Bliss and values estimated from 2- and 10-m mast data using Monin-Obukhov similarity and a p-profile fit.

RMS DIFFERENCE BETWEEN
160M MEASURED AND PREDICTED PARAMETER
JUN 04 - JUN 25, 1990 - FT. BLISS

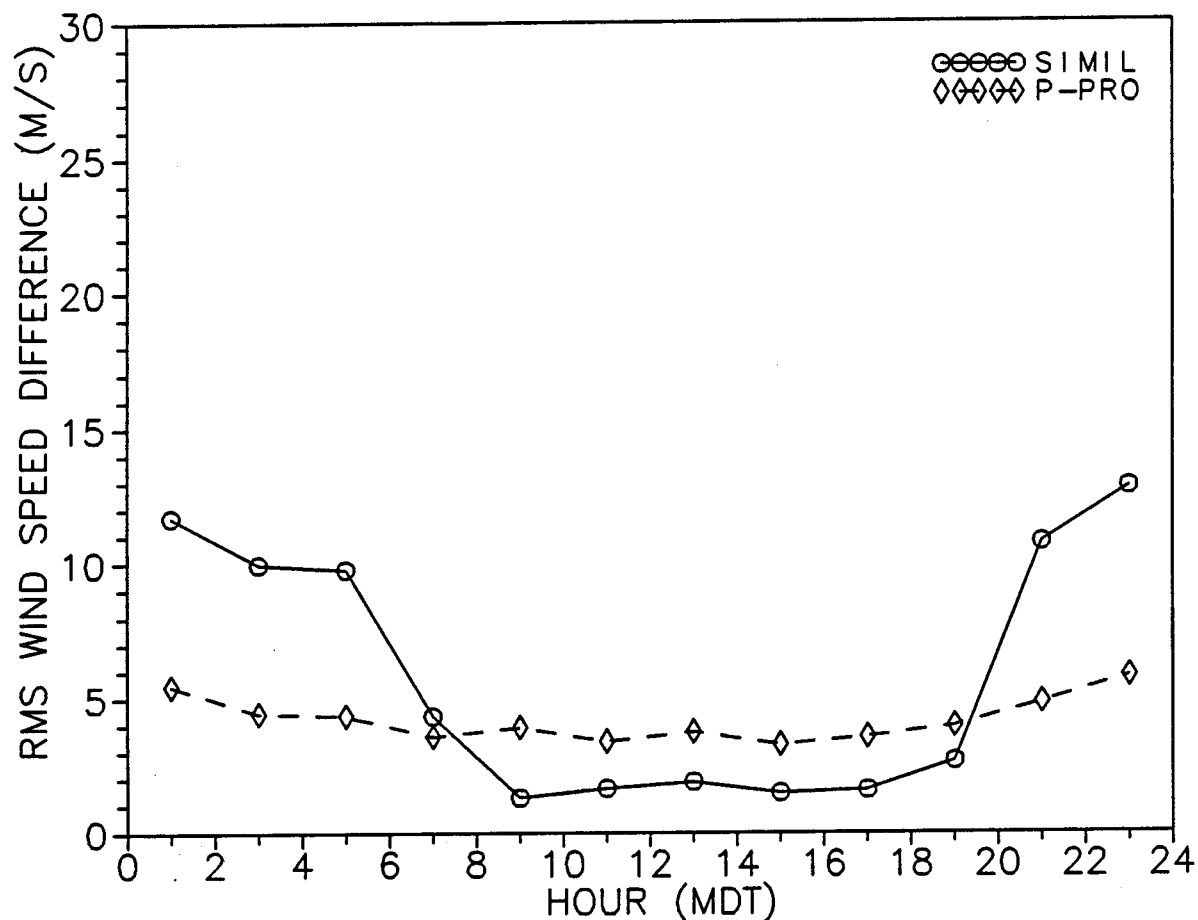


Figure 21. Rms differences between 160-m sodar wind speed measurements collected at Ft. Bliss and values estimated from 2- and 10-m mast data using Monin-Obukhov similarity and a p-profile fit.

RMS DIFFERENCE BETWEEN
210M MEASURED AND PREDICTED PARAMETER
JUN 04 - JUN 25, 1990 - FT. BLISS

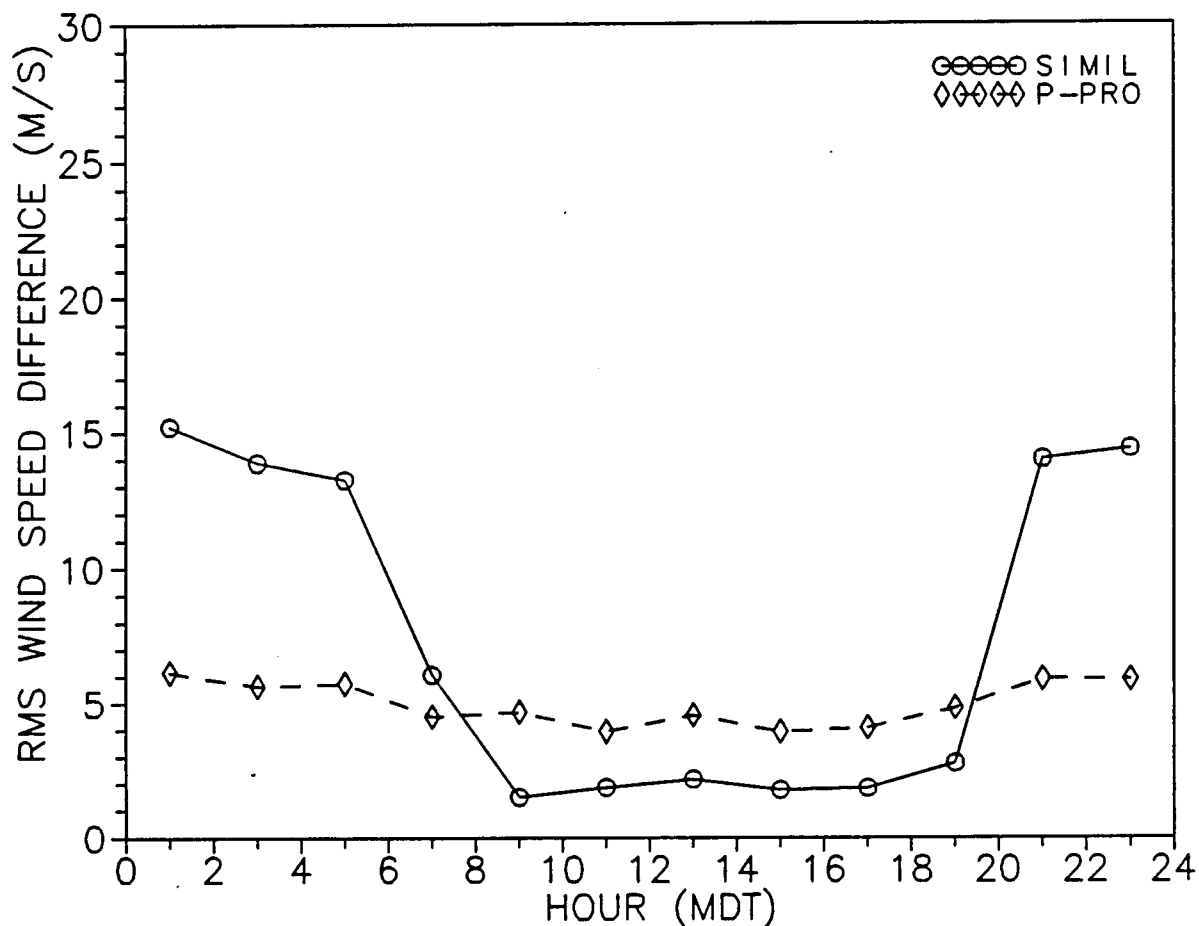


Figure 22. Rms differences between 210-m sodar wind speed measurements collected at Ft. Bliss and values estimated from 2- and 10-m mast data using Monin-Obukhov similarity and a p-profile fit.

RMS DIFFERENCE BETWEEN
310M MEASURED AND PREDICTED PARAMETER
JUN 04 - JUN 25, 1990 - FT. BLISS

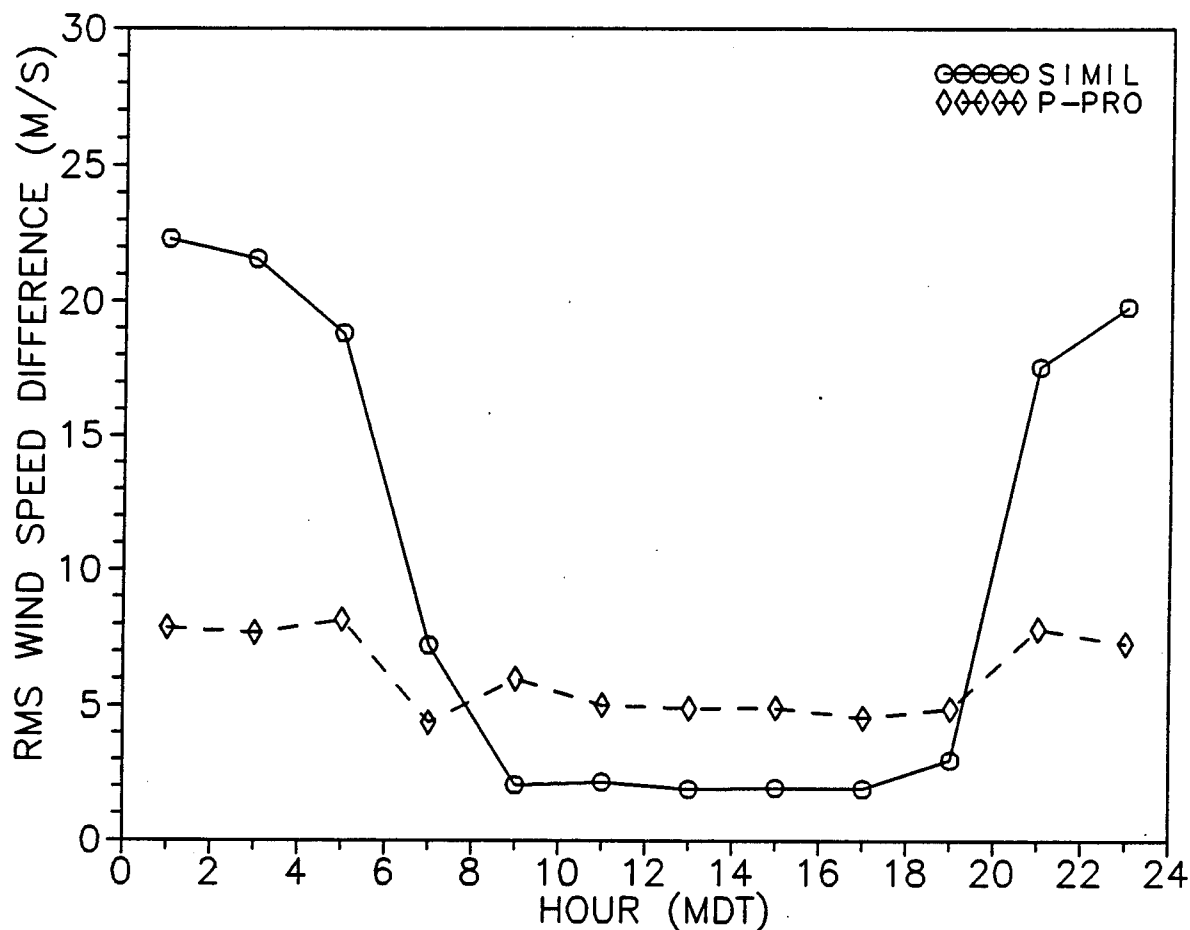


Figure 23. Rms differences between 310-m sodar wind speed measurements collected at Ft. Bliss and values estimated from 2- and 10-m mast data using Monin-Obukhov similarity and a p-profile fit.

RMS DIFFERENCE BETWEEN
410M MEASURED AND PREDICTED PARAMETER
JUN 04 - JUN 25, 1990 - FT. BLISS

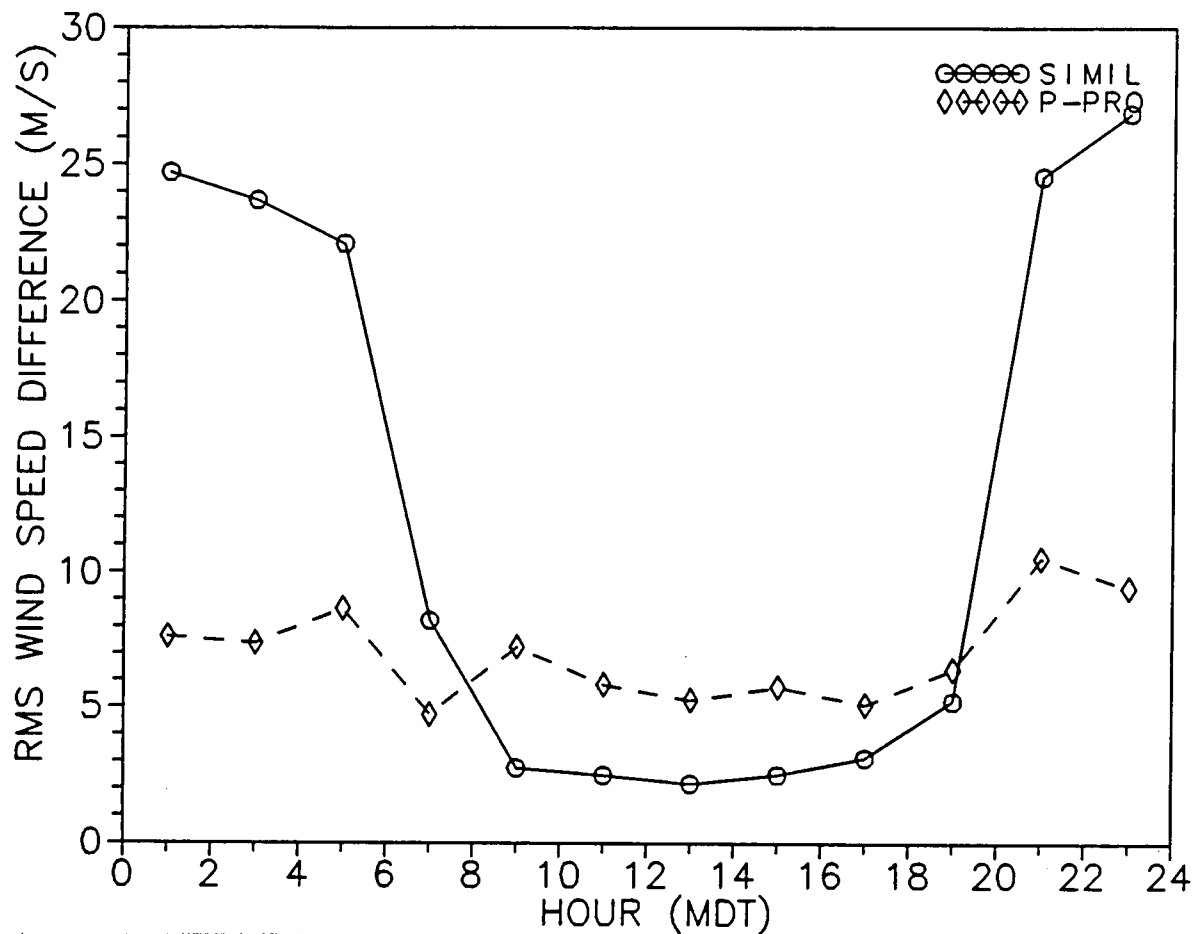


Figure 24. Rms differences between 410-m sodar wind speed measurements collected at Ft. Bliss and values estimated from 2- and 10-m mast data using Monin-Obukhov similarity and a p-profile fit.

Table 5. Statistics of differences between wind speeds measured by sodar at Champaign and values estimated from 2- and 10-m mast data using Monin-Obukhov similarity algorithm and p-profile fit

Jul 23 - Aug 2, 1990				
0000 - 0200 MDT				
	Mean	STDV (m/s)	rms	NPTS
60-m similarity measured	3.18	3.86	5.00	16
110-m similarity measured	8.94	5.37	10.43	14
160-m similarity measured	13.45	7.14	15.23	11
210-m similarity measured	-99.00	-99.00	-99.00	9
310-m similarity measured	-99.00	-99.00	-99.00	1
410-m similarity measured	-99.00	-99.00	-99.00	0
60-m p-profile measured	.53	3.72	3.75	16
110-m p-profile measured	2.57	4.91	5.54	14
160-m p-profile measured	3.03	6.70	7.36	11
210-m p-profile measured	-99.00	-99.00	-99.00	9
310-m p-profile measured	-99.00	-99.00	-99.00	1
410-m p-profile measured	-99.00	-99.00	-99.00	0
0200 - 0400 MDT				
	Mean	STDV (m/s)	rms	NPTS
60-m similarity measured	.90	2.89	3.03	21
110-m similarity measured	4.70	3.62	5.94	20
160-m similarity measured	7.76	4.67	9.06	19
210-m similarity measured	-99.00	-99.00	-99.00	6
310-m similarity measured	-99.00	-99.00	-99.00	6
410-m similarity measured	-99.00	-99.00	-99.00	4
60-m p-profile measured	-1.44	2.77	3.12	21
110-m p-profile measured	-.74	3.48	3.56	20
160-m p-profile measured	-1.03	4.38	4.50	19
210-m p-profile measured	-99.00	-99.00	-99.00	6
310-m p-profile measured	-99.00	-99.00	-99.00	6
410-m p-profile measured	-99.00	-99.00	-99.00	4

Table 5. Statistics of differences between wind speeds measured by sodar at Champaign and values estimated from 2- and 10-m mast data using Monin-Obukhov similarity algorithm and p-profile fit (continued)

Jul 23 - Aug 2, 1990				
0400 - 0600 MDT				
	Mean	STDV (m/s)	rms	NPTS
60-m similarity measured	2.42	3.35	4.14	16
110-m similarity measured	5.81	4.64	7.43	12
160-m similarity measured	-99.00	-99.00	-99.00	8
210-m similarity measured	-99.00	-99.00	-99.00	4
310-m similarity measured	-99.00	-99.00	-99.00	3
410-m similarity measured	-99.00	-99.00	-99.00	2
60-m p-profile measured	.51	3.23	3.27	16
110-m p-profile measured	1.08	4.10	4.24	12
160-m p-profile measured	-99.00	-99.00	-99.00	8
210-m p-profile measured	-99.00	-99.00	-99.00	4
310-m p-profile measured	-99.00	-99.00	-99.00	3
410-m p-profile measured	-99.00	-99.00	-99.00	2
0600 - 0800 MDT				
	Mean	STDV (m/s)	rms	NPTS
60-m similarity measured	-2.23	4.66	5.17	47
110-m similarity measured	.02	4.68	4.68	38
160-m similarity measured	.13	6.20	6.20	29
210-m similarity measured	.53	6.58	6.60	12
310-m similarity measured	-99.00	-99.00	-99.00	7
410-m similarity measured	-99.00	-99.00	-99.00	6
60-m p-profile measured	-2.21	4.36	4.89	47
110-m p-profile measured	-.47	2.83	2.87	38
160-m p-profile measured	-.69	3.35	3.42	29
210-m p-profile measured	-1.25	3.71	3.91	12
310-m p-profile measured	-99.00	-99.00	-99.00	7
410-m p-profile measured	-99.00	-99.00	-99.00	6

Table 5. Statistics of differences between wind speeds measured by sodar at Champaign and values estimated from 2- and 10-m mast data using Monin-Obukhov similarity algorithm and p-profile fit (continued)

Jul 23 - Aug 2, 1990				
0800 - 1000 MDT				
	Mean	STDV (m/s)	rms	NPTS
60-m similarity measured	-.42	2.21	2.25	72
110-m similarity measured	-.53	2.85	2.90	69
160-m similarity measured	-.69	2.28	2.39	67
210-m similarity measured	-.74	1.79	1.94	55
310-m similarity measured	-1.58	3.15	3.52	31
410-m similarity measured	-2.71	4.57	5.31	23
60-m p-profile measured	.21	2.28	2.29	72
110-m p-profile measured	.49	3.04	3.08	69
160-m p-profile measured	.63	2.56	2.63	67
210-m p-profile measured	.91	2.27	2.45	55
310-m p-profile measured	.56	3.78	3.82	31
410-m p-profile measured	-.07	5.18	5.18	23
1000 - 1200 MDT				
	Mean	STDV (m/s)	rms	NPTS
60-m similarity measured	.04	1.28	1.28	71
110-m similarity measured	.31	1.27	1.31	65
160-m similarity measured	.29	1.34	1.37	62
210-m similarity measured	.25	1.36	1.39	59
310-m similarity measured	.27	1.54	1.56	47
410-m similarity measured	.38	1.84	1.88	40
60-m p-profile measured	.78	1.53	1.71	71
110-m p-profile measured	1.47	1.78	2.31	65
160-m p-profile measured	1.79	2.02	2.70	62
210-m p-profile measured	1.99	2.19	2.95	59
310-m p-profile measured	2.40	2.53	3.49	47
410-m p-profile measured	2.77	2.95	4.05	40

Table 5. Statistics of differences between wind speeds measured by sodar at Champaign and values estimated from 2- and 10-m mast data using Monin-Obukhov similarity algorithm and p-profile fit (continued)

Jul 23- Aug 2, 1990				
1200 - 1400 MDT				
	Mean	STDV (m/s)	rms	NPTS
60-m similarity measured	.28	1.48	1.51	70
110-m similarity measured	.39	1.54	1.59	70
160-m similarity measured	.27	1.62	1.64	70
210-m similarity measured	.16	1.75	1.75	66
310-m similarity measured	.38	1.97	2.01	53
410-m similarity measured	.07	1.94	1.94	38
60-m p-profile measured	.97	1.72	1.97	70
110-m p-profile measured	1.49	1.97	2.47	70
160-m p-profile measured	1.67	2.20	2.76	70
210-m p-profile measured	1.81	2.47	3.06	66
310-m p-profile measured	2.39	2.97	3.81	53
410-m p-profile measured	2.40	3.06	3.89	38
1400 - 1600 MDT				
	Mean	STDV (m/s)	rms	NPTS
60-m similarity measured	-.33	2.32	2.35	71
110-m similarity measured	.29	.97	1.01	67
160-m similarity measured	.26	.99	1.02	67
210-m similarity measured	.20	1.03	1.05	64
310-m similarity measured	.29	1.21	1.25	55
410-m similarity measured	.05	1.52	1.52	42
60-m p-profile measured	.41	2.50	2.53	71
110-m p-profile measured	1.54	1.32	2.03	67
160-m p-profile measured	1.87	1.47	2.38	67
210-m p-profile measured	2.10	1.65	2.67	64
310-m p-profile measured	2.74	2.06	3.43	55
410-m p-profile measured	2.87	2.59	3.87	42

Table 5. Statistics of differences between wind speeds measured by sodar at Champaign and values estimated from 2- and 10-m mast data using Monin-Obukhov similarity algorithm and p-profile fit (continued)

Jul 23 - Aug 2, 1990				
1600 - 1800 MDT				
	Mean	STDV (m/s)	rms	NPTS
60-m similarity measured	-.79	3.00	3.10	72
110-m similarity measured	-.30	1.32	1.35	70
160-m similarity measured	-.38	1.39	1.44	68
210-m similarity measured	-.38	1.47	1.52	56
310-m similarity measured	-.16	1.30	1.31	36
410-m similarity measured	-.65	1.69	1.81	30
60-m p-profile measured	-.09	3.09	3.10	72
110-m p-profile measured	.85	1.63	1.84	70
160-m p-profile measured	1.13	1.81	2.13	68
210-m p-profile measured	1.58	1.97	2.52	56
310-m p-profile measured	2.21	1.92	2.92	36
410-m p-profile measured	2.28	2.59	3.45	30
1800 - 2000 MDT				
	Mean	STDV (m/s)	rms	NPTS
60-m similarity measured	.51	1.65	1.73	42
110-m similarity measured	1.87	3.31	3.80	42
160-m similarity measured	2.88	4.82	5.62	35
210-m similarity measured	4.54	6.74	8.12	21
310-m similarity measured	-99.00	-99.00	-99.00	9
410-m similarity measured	-99.00	-99.00	-99.00	9
60-m p-profile measured	.12	1.12	1.13	42
110-m p-profile measured	.73	1.62	1.78	42
160-m p-profile measured	.77	1.94	2.08	35
210-m p-profile measured	1.13	2.75	2.98	21
310-m p-profile measured	-99.00	-99.00	-99.00	9
410-m p-profile measured	-99.00	-99.00	-99.00	9

Table 5. Statistics of differences between wind speeds measured by sodar at Champaign and values estimated from 2- and 10-m mast data using Monin-Obukhov similarity algorithm and p-profile fit (continued)

Jul 23, 1990 - Aug 2, 1990				
2000 - 2200 MDT				
	Mean	STDV (m/s)	rms	NPTS
60-m similarity measured	2.93	1.90	3.49	13
110-m similarity measured	7.06	3.98	8.11	11
160-m similarity measured	-99.00	-99.00	-99.00	9
210-m similarity measured	-99.00	-99.00	-99.00	5
310-m similarity measured	-99.00	-99.00	-99.00	2
410-m similarity measured	-99.00	-99.00	-99.00	1
60-m p-profile measured	1.02	1.99	2.24	13
110-m p-profile measured	2.95	4.10	5.05	11
160-m p-profile measured	-99.00	-99.00	-99.00	9
210-m p-profile measured	-99.00	-99.00	-99.00	5
310-m p-profile measured	-99.00	-99.00	-99.00	2
410-m p-profile measured	-99.00	-99.00	-99.00	1
2200 - 2400 MDT				
	Mean	STDV (m/s)	rms	NPTS
60-m similarity measured	3.40	2.10	4.00	15
110-m similarity measured	9.06	3.32	9.65	12
160-m similarity measured	12.39	2.96	12.74	10
210-m similarity measured	-99.00	-99.00	-99.00	9
310-m similarity measured	-99.00	-99.00	-99.00	8
410-m similarity measured	-99.00	-99.00	-99.00	3
60-m p-profile measured	.69	2.14	2.25	15
110-m p-profile measured	2.41	2.65	3.58	12
160-m p-profile measured	2.10	2.75	3.46	10
210-m p-profile measured	-99.00	-99.00	-99.00	9
310-m p-profile measured	-99.00	-99.00	-99.00	8
410-m p-profile measured	-99.00	-99.00	-99.00	3

RMS DIFFERENCE BETWEEN
60M MEASURED AND PREDICTED PARAMETER
JUL 23 - AUG 02, 1990 - CHAMPAIGN, ILLINOIS

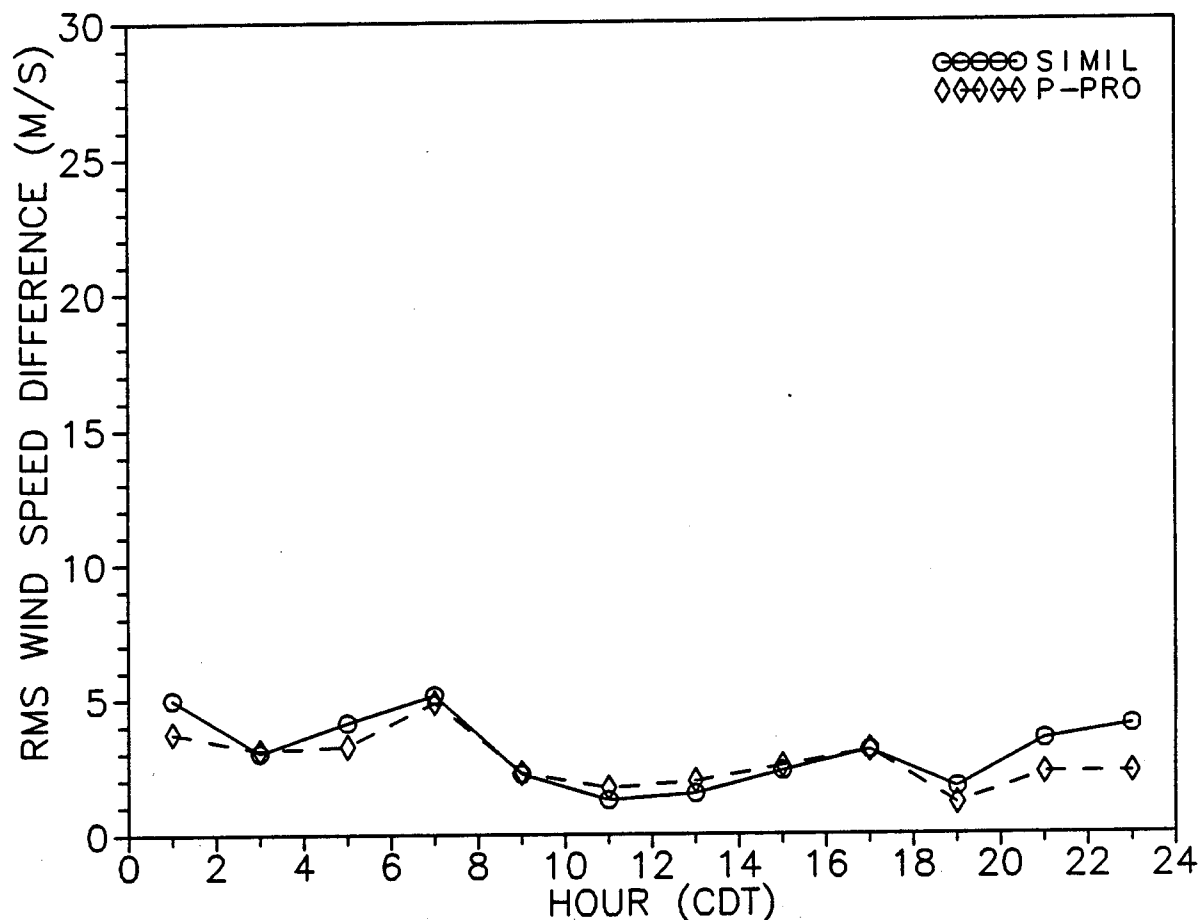


Figure 25. Rms differences between 60-m sodar wind speed measurements collected at Champaign and values estimated from 2- and 10-m mast data using Monin-Obukhov similarity and a p-profile fit.

RMS DIFFERENCE BETWEEN
110M MEASURED AND PREDICTED PARAMETER
JUL 23 - AUG 02, 1990 - CHAMPAIGN, ILLINOIS

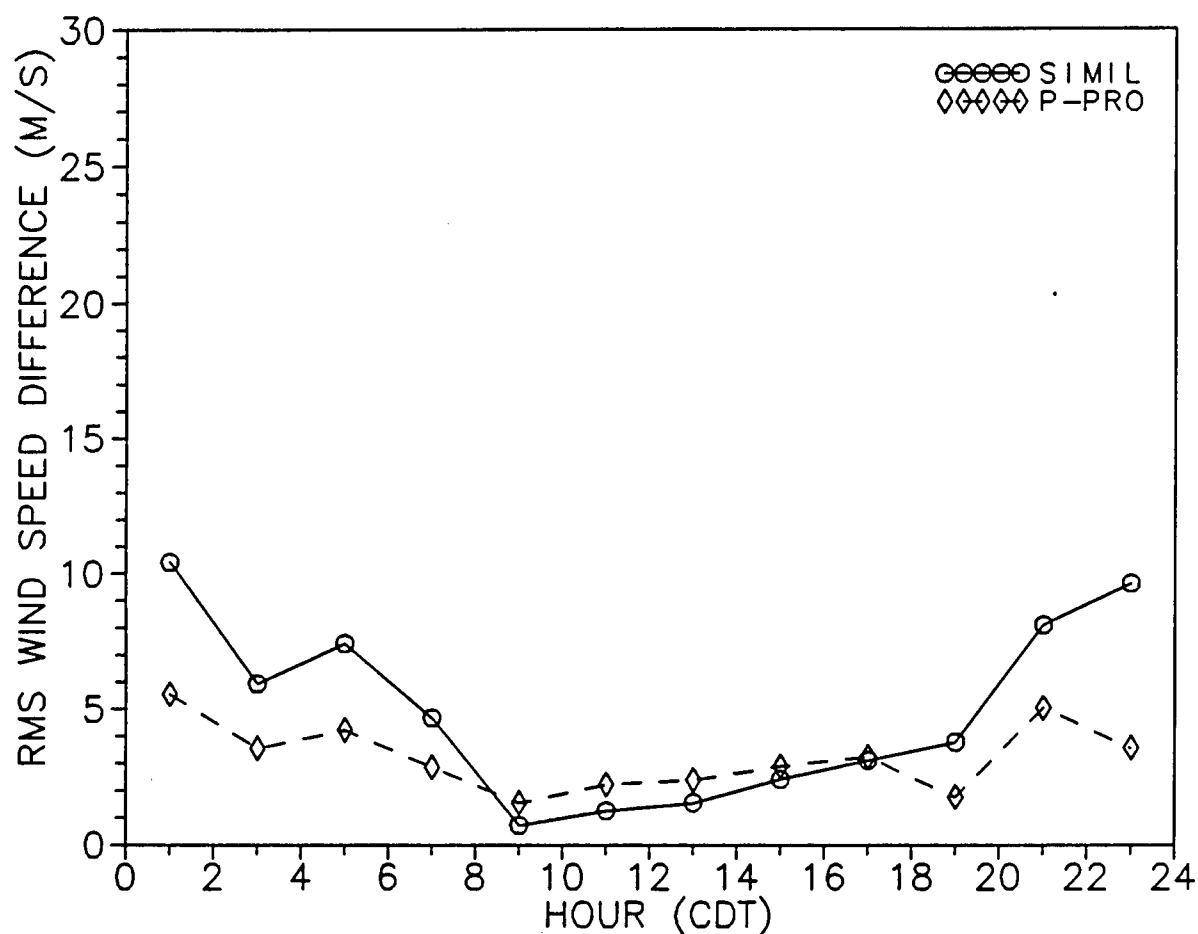


Figure 26. Rms differences between 110-m sodar wind speed measurements collected at Champaign and values estimated from 2- and 10-m mast data using Monin-Obukhov similarity and a p-profile fit.

RMS DIFFERENCE BETWEEN
160M MEASURED AND PREDICTED PARAMETER
JUL 23 - AUG 02, 1990 - CHAMPAIGN, ILLINOIS

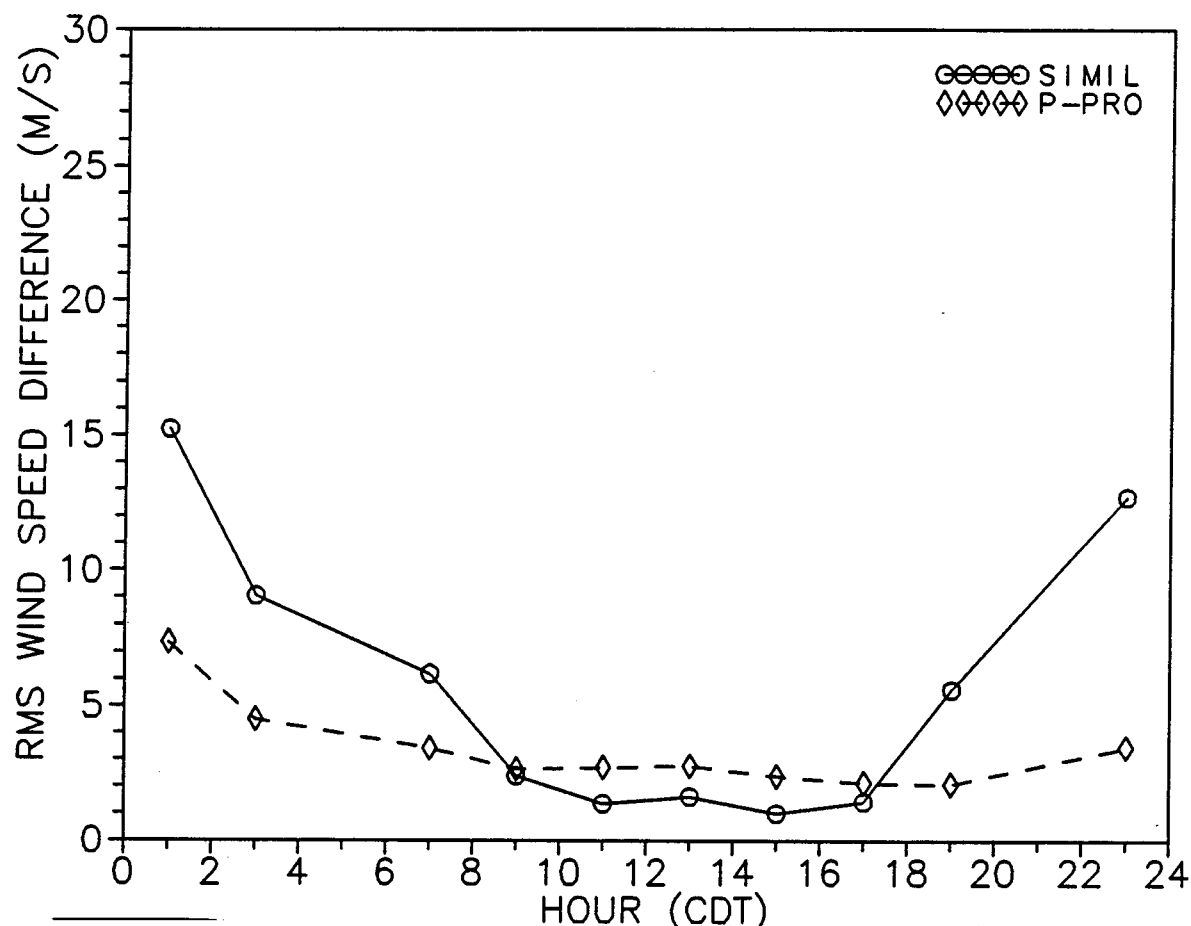


Figure 27. Rms differences between 160-m sodar wind speed measurements collected at Champaign and values estimated from 2- and 10-m mast data using Monin-Obukhov similarity and a p-profile fit.

RMS DIFFERENCE BETWEEN
210M MEASURED AND PREDICTED PARAMETER
JUL 23 - AUG 02, 1990 - CHAMPAIGN, ILLINOIS

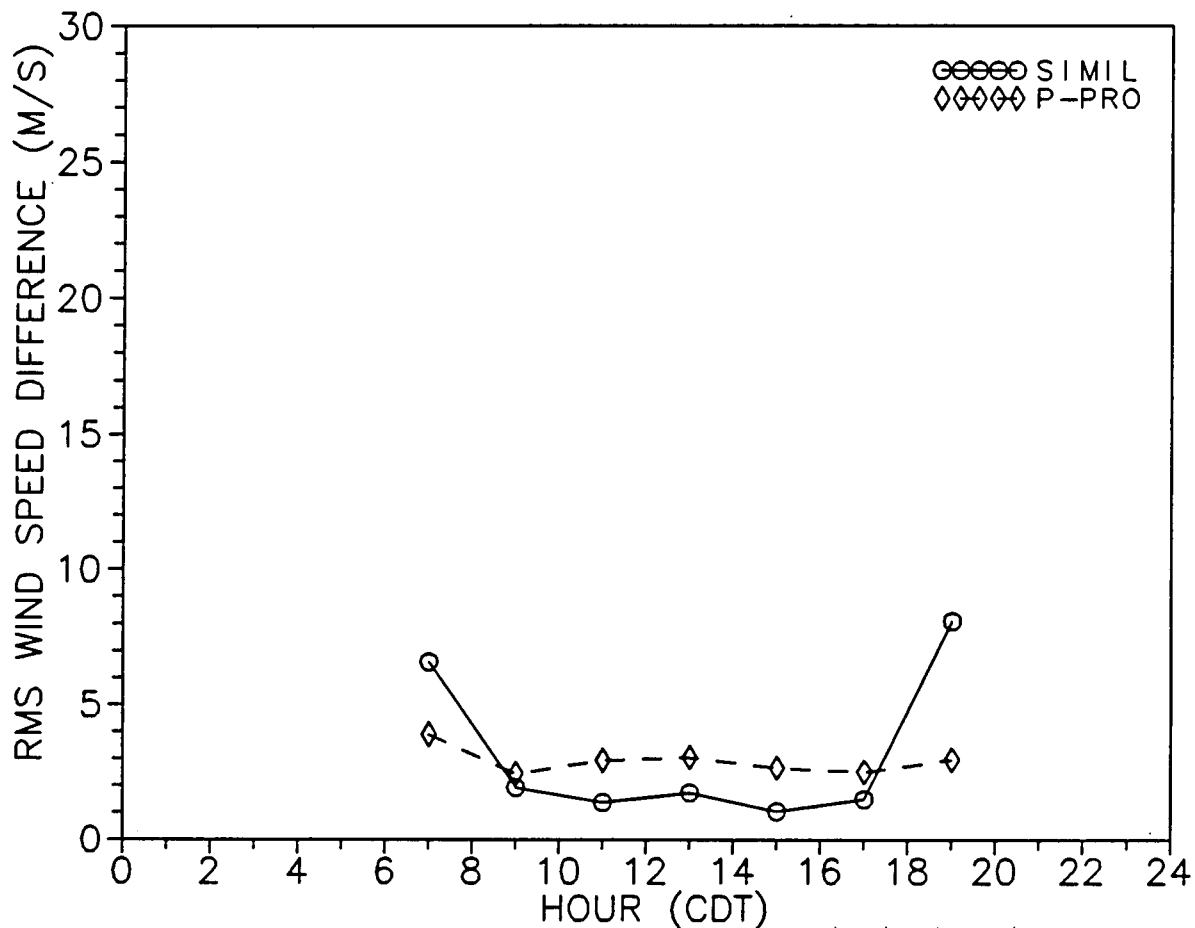


Figure 28. Rms differences between 210-m sodar wind speed measurements collected at Champaign and values estimated from 2- and 10-m mast data using Monin-Obukhov similarity and a p-profile fit.

RMS DIFFERENCE BETWEEN
310M MEASURED AND PREDICTED PARAMETER
JUL 23 - AUG 02, 1990 - CHAMPAIGN, ILLINOIS

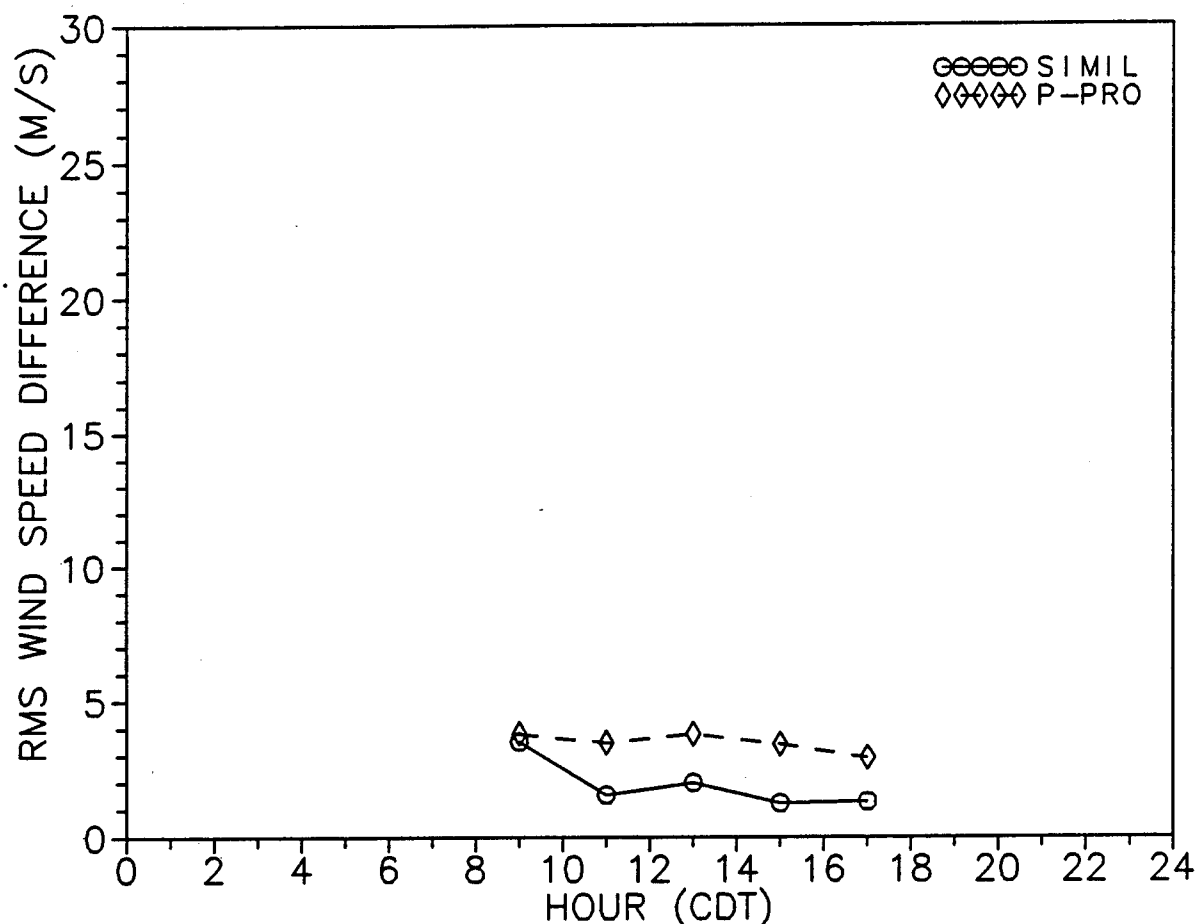


Figure 29. Rms differences between 310-m sodar wind speed measurements collected at Champaign and values estimated from 2- and 10-m mast data using Monin-Obukhov similarity and a p-profile fit.

RMS DIFFERENCE BETWEEN
410M MEASURED AND PREDICTED PARAMETER
JUL 23 - AUG 02, 1990 - CHAMPAIGN, ILLINOIS

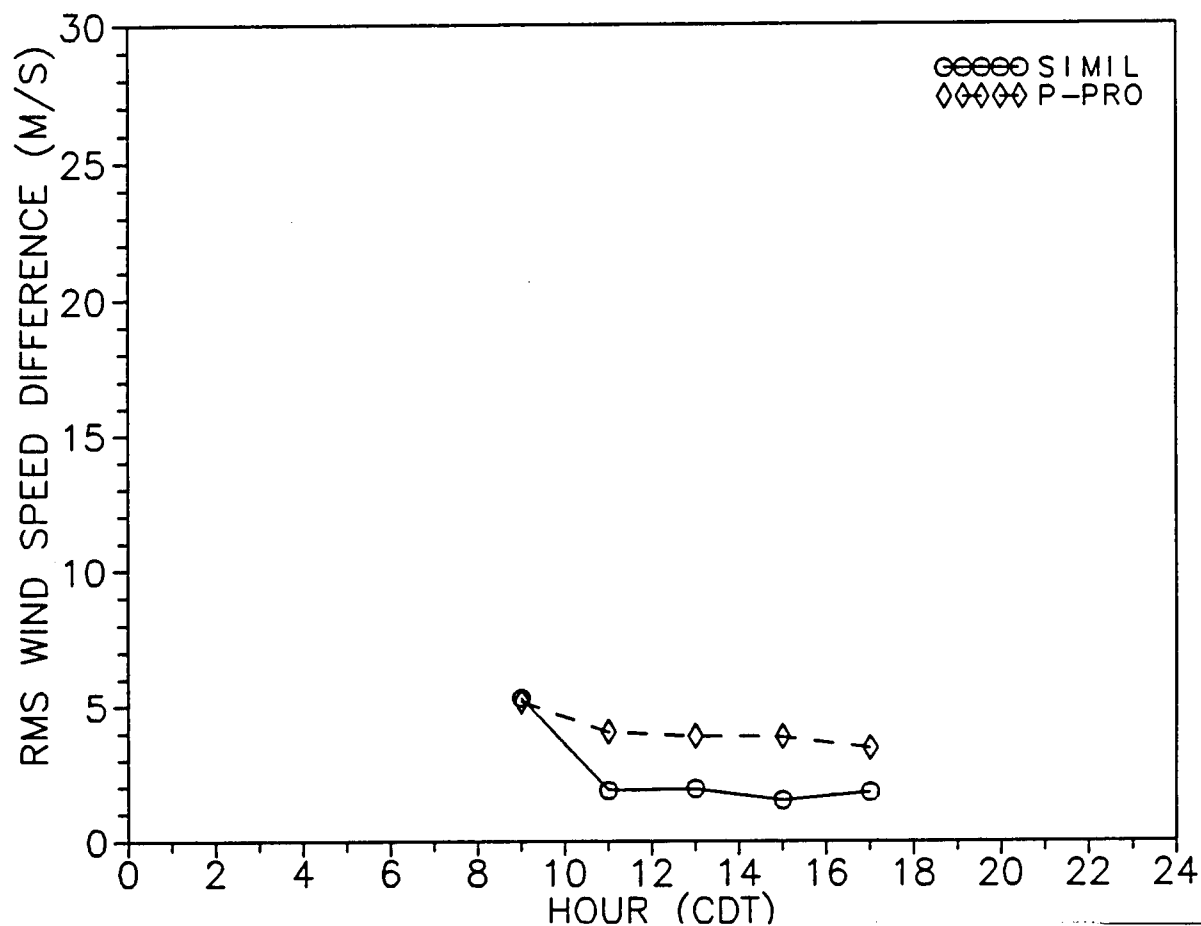


Figure 30. Rms differences between 410-m sodar wind speed measurements collected at Champaign and values estimated from 2- and 10-m mast data using Monin-Obukhov similarity and a p-profile fit.

4.3 Radiosonde Data Comparison

The similarity, p-profile, and inversion models were used to estimate wind speed or temperature at several radiosonde measurement heights for statistical comparison with the radiosonde data. Fifteen-minute averaged in situ measurements collected on the 10-m mast were utilized for the model inputs. Two- and 10-m data closest in time to the balloon release were fed into the similarity and p-profile models, and 24 h of 10-m temperature data collected on the day of the launch were required by the inversion algorithm. The minimum radiosonde measurement heights used in the analyses were 50 m for temperature, 200 m for wind data collected by the radio theodolite, and 600 m for wind data collected by the Omega Navaid system. The maximum height was 3000 m. Because of the comparably small number of radiosonde flights, statistics were computed for only two time-of-day intervals. One interval, 0900 MDT inclusive to 1900 MDT, represents the unstable day boundary layer, and the other, composed of the rest of the times, represents the stable night atmosphere. Only data for which a solution was obtained by all three models were used in the computations.

The wind speed statistics for WSMR are listed in tables 6 through 9. The last column contains the number of radiosonde measurements used in the computation. The rms differences between the measured and predicted data are also plotted in figures 31 and 32 for the day and night cases, respectively. Comparability between the measured and predicted data was fairly good during the day for the first few hundred meters above the surface. The rms differences were 1.0 through 1.1 m s^{-1} for the similarity predictions and 1.1 through 1.4 m s^{-1} for the p-profile estimates up to 500 m. Above 500 m, these statistics steadily increased with altitude. By comparison, the rms vector wind differences between simultaneously tracked rawinsondes were found to be 1.0 to 2.0 m s^{-1} in a study by Olsen et al. [16]. Agreement between the predicted and measured data was poor at all heights at night.

The WSMR temperature statistics are shown in tables 10 through 13 and figures 33 and 34. The comparability of the day temperatures predicted by the similarity model was fairly good near the surface. Rms differences were .5 to .6 $^{\circ}\text{C}$ up to 200 m increasing to 1.3 $^{\circ}\text{C}$ at 500 m. These are comparable to

the .5 °C rms differences between simultaneous radiosonde measurements found by Olsen et al. [16]. The rms differences between the day inversion model predictions and the radiosonde measurements were 3.0 °C at the lowest heights, but ranged between 1.3 and 2.0 °C above 800 m. The rms differences were smaller than the similarity rms differences above 700 m. At night, the comparabilities of the similarity predictions were considerably worse than the day predictions except at 50 m. Similarity rms differences were .7 °C at 50 m and 3.1 °C at 500 m. The night inversion rms differences, which ranged between 1.0 and 2.1 °C, were smaller than the similarity rms differences above 200 m.

Results of these same analyses using the Ft. Bliss data are shown in tables 14 through 21 and figures 35 through 38. Agreement between the day similarity predictions and the radiosonde data was somewhat poorer than it was at WSMR. For the first 500 m, similarity rms differences were 1.6 to 1.8 m s⁻¹. The p-profile rms differences at the same altitudes were 4.0 to 5.7 m s⁻¹, which is much larger than both the similarity differences and the WSMR p-profile differences. Predictions from both models were poor at night. The temperature statistics were more comparable with WSMR. During the day, the similarity rms temperature differences were .6 to .9 °C up to 500 m. The night similarity rms difference was 1.3 °C at 50 m and rapidly became larger at greater heights. The inversion rms differences ranged between 1.2 and 4.1 °C and were smaller than the day similarity differences above 1200 m and the night similarity differences above 50 m.

Results of the Champaign data analyses are shown in tables 22 through 29 and figures 39 through 42. The similarity rms differences of .9 to 1.2 m s⁻¹ within the first 500 m were comparable to the WSMR differences. The p-profile rms differences were considerably larger and are more comparable with the Ft. Bliss statistics. Both models gave poor predictions at night. The day temperature rms differences for the similarity model ranged between .9 and 1.8 °C up to 500 m, which were a few tenths of a degree larger than the Ft. Bliss and WSMR differences. Except at 50 m, the night similarity rms differences were much greater than the day differences. The inversion rms differences were smaller than the similarity rms differences above 700 m during the day and above 50 m at night.

Another way to show the comparability between model predictions and the radiosonde data as a function of time of day is presented in figures 43 through 46. The absolute values of the differences between the modeled and measured data at 600 m were plotted using data collected at all three locations. Differences of 10 m s^{-1} or greater were placed at 10 m s^{-1} on the graphs. The main characteristics shown are (1) the similarity predictions were much better between 0900 and 1900 MDT than at other times, (2) many of the day p-profile estimates were much poorer than the worst day similarity estimates, and (3) the inversion algorithm predictions were better at night than during the day.

Examples of how well model predictions compare with radiosonde data at different times of the day are shown in figures 47 through 52 where predictions and measurements for three sample flights launched at WSMR are plotted. The first sample flight, plotted in figures 47 and 48, was launched during midday when the surface layer is expected to be fairly deep. There was good agreement between the radiosonde measurements and the similarity and p-profile predictions up to 1200 m. The small gap between the similarity and radiosonde temperature profiles was probably due to a systematic bias between the radiosonde and tower sensors. Temperature predictions from the inversion model were closer to the data than the similarity predictions above 1200 m. The second sample sounding, shown in figures 49 and 50, was flown during late afternoon. In this case, the p-profile and similarity models provided good estimates to about 400 m, and the inversion model temperature predictions were closer to the measurements above 1000 m. For the night case, plotted in figures 51 and 52, only the inversion model provided reasonable predictions.

Table 6. Statistics of differences between day radiosonde wind data collected at WSMR and data estimated from 2- and 10-m measurements using Monin-Obukhov similarity

Data differences (day) similarity - radiosonde Jul 11 - Aug 26, 1991				
Alt (m)	Wind Speed (m/s)			No.
	Mean	STDV	rms	
200	.01	.01	.0	14
300	-.1	1.1	1.1	14
400	-.3	1.0	1.0	14
500	-.6	.8	1.0	14
600	-.4	1.3	1.4	17
700	-.4	1.6	1.6	17
800	-.5	1.8	1.8	17
900	-.5	1.8	1.9	17
1000	-.6	1.8	1.9	17
1200	-.8	2.3	2.5	17
1400	-.8	2.9	3.1	17
1600	-.5	3.1	3.1	17
1800	-.8	3.9	4.0	17
2000	-1.5	4.6	4.8	17
2200	-2.2	5.2	5.7	17
2400	-2.5	5.6	6.1	17
2600	-2.3	5.4	5.8	17
2800	-1.9	4.8	5.2	17
3000	-1.4	4.1	4.4	17

Table 7. Statistics of differences between day radiosonde wind data collected at WSMR and data estimated from 2- and 10-m measurements using p-profile fit

Data differences (day) p-profile - radiosonde Jul 11 - Aug 26, 1991				
Alt (m)	Wind Speed (m/s)			No.
	Mean	STDV	rms	
200	.7	1.0	1.2	14
300	.8	1.1	1.4	14
400	.8	1.1	1.4	14
500	.5	1.0	1.1	14
600	1.2	2.2	2.5	17
700	1.3	2.4	2.7	17
800	1.3	2.7	3.0	17
900	1.4	2.8	3.1	17
1000	1.4	2.9	3.2	17
1200	1.3	3.4	3.6	17
1400	1.4	3.9	4.1	17
1600	1.9	3.9	4.3	17
1800	1.7	4.7	5.0	17
2000	1.1	5.4	5.5	17
2200	.5	6.1	6.1	17
2400	.3	6.6	6.6	17
2600	.6	6.5	6.5	17
2800	1.0	6.1	6.2	17
3000	1.5	5.7	5.9	17

Table 8. Statistics of differences between night radiosonde wind data collected at WSMR and data estimated from 2- and 10-m measurements using Monin-Obukhov similarity

Data differences (night) similarity - radiosonde Jul 11 - Aug 20, 1991				
Alt (m)	Wind Speed (m/s)			No.
	Mean	STDV	rms	
200	3.8	4.2	5.6	6
300	5.9	5.8	8.3	6
400	8.6	7.2	11.2	6
500	11.6	8.3	14.3	6
600	12.0	11.0	16.3	7
700	14.6	12.5	19.2	7
800	16.9	14.0	21.9	7
900	19.3	15.4	24.7	7
1000	21.6	16.8	27.4	7
1200	26.9	19.9	33.4	7
1400	31.4	23.2	39.0	7
1600	35.4	26.6	44.3	7
1800	38.9	30.2	49.2	7
2000	42.4	33.5	54.0	7
2200	52.6	36.3	64.0	6
2400	57.3	40.3	70.1	6
2600	62.0	44.1	76.1	6
2800	66.5	47.8	81.9	6
3000	70.7	51.6	87.5	6

Table 9. Statistics of differences between night radiosonde wind data collected at WSMR and data estimated from 2- and 10-m measurements using p-profile fit

Data differences (night) p-profile - radiosonde Jul 11 - Aug 20, 1991				
Alt (m)	Wind Speed (m/s)			No.
	Mean	STDV	rms	
200	.9	2.5	2.7	6
300	1.2	3.2	3.4	6
400	1.8	3.6	4.0	6
500	2.8	4.0	4.9	6
600	2.9	4.5	5.3	7
700	3.7	4.7	6.0	7
800	4.1	4.6	6.2	7
900	4.7	4.6	6.6	7
1000	5.2	4.8	7.1	7
1200	6.7	5.3	8.6	7
1400	7.4	5.1	9.0	7
1600	7.7	4.9	9.1	7
1800	7.4	4.1	8.5	7
2000	7.1	4.1	8.2	7
2200	6.1	3.9	7.2	6
2400	6.3	3.9	7.4	6
2600	6.5	3.9	7.6	6
2800	6.5	3.9	7.6	6
3000	6.2	3.6	7.1	6

RMS DIFFERENCE BETWEEN MODEL
PREDICTIONS AND RADIOSONDE DATA
JUL 11 - AUG 26, 1991 (DAY)

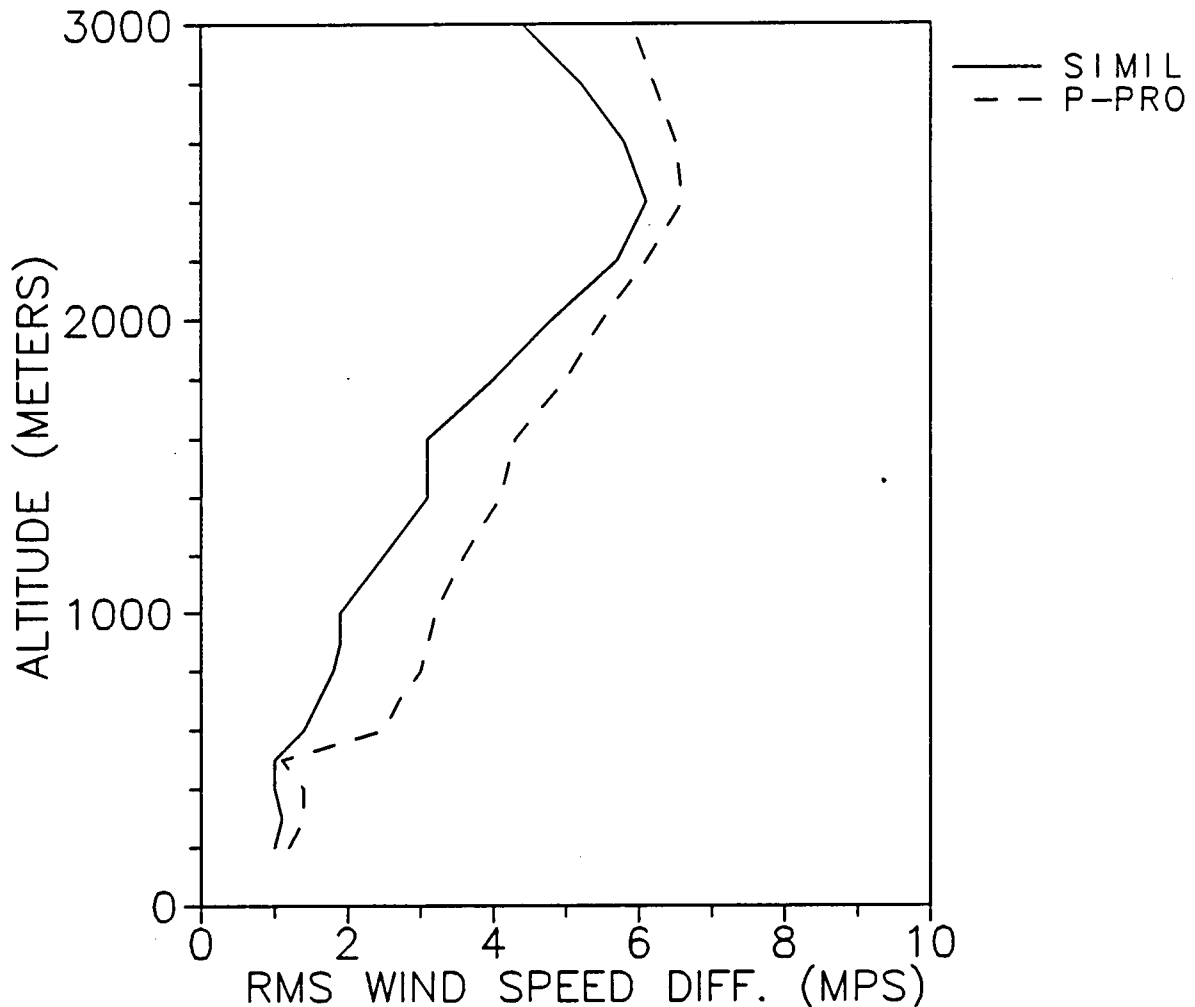


Figure 31. Rms differences between day radiosonde wind speed measurements collected at WSMR and data estimated from tower measurements using Monin-Obukhov similarity and p-profile fit.

RMS DIFFERENCE BETWEEN MODEL
PREDICTIONS AND RADIOSONDE DATA
JUL 11 - AUG 20, 1991 (NIGHT)

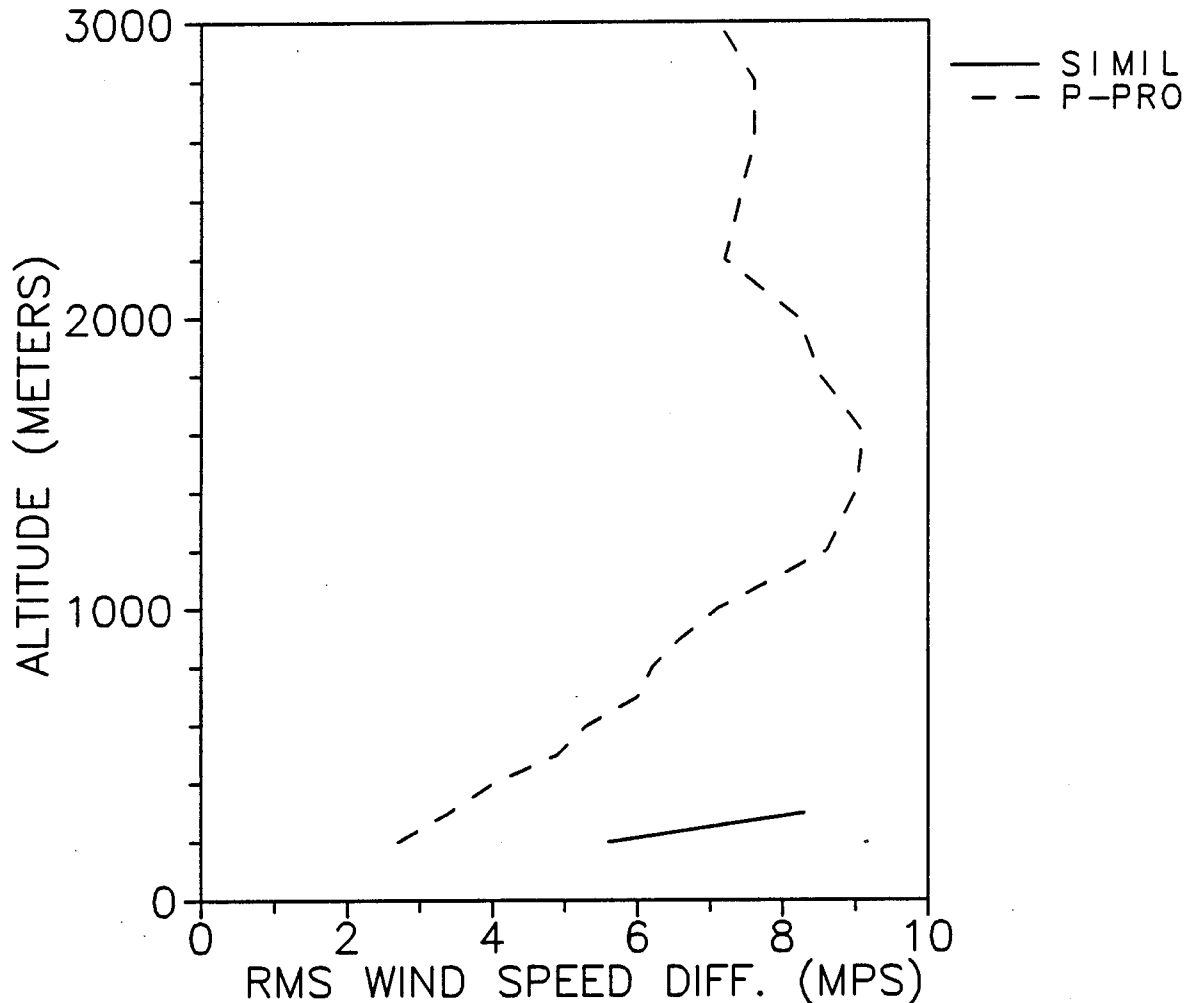


Figure 32. Rms differences between night radiosonde wind speed measurements collected at WSMR and data estimated from tower measurements using Monin-Obukhov similarity and p-profile fit.

Table 10. Statistics of differences between day radiosonde temperature data collected at WSMR and data estimated from 2- and 10-m measurements using Monin-Obukhov similarity

Data differences (day) similarity - radiosonde Jul 11 - Aug 26, 1991				
Alt (m)	Temp (°C)			No.
	Mean	STDV	rms	
50	-.4	.4	.6	18
100	-.3	.5	.6	18
150	-.4	.4	.6	18
200	-.4	.4	.6	18
300	-.7	.6	.9	18
400	-.9	.7	1.1	18
500	-1.0	.7	1.3	18
600	-1.3	.8	1.5	18
700	-1.6	1.0	1.9	18
800	-1.7	1.1	2.1	18
900	-2.0	1.2	2.3	18
1000	-2.2	1.4	2.6	18
1200	-2.7	1.7	3.2	18
1400	-3.1	1.9	3.7	18
1600	-3.6	2.2	4.3	18
1800	-4.0	2.4	4.7	18
2000	-4.7	2.4	5.3	18
2200	-5.2	2.4	5.7	18
2400	-5.6	2.7	6.2	18

Table 11. Statistics of differences between day radiosonde temperature data collected at WSMR and data estimated from 10-m measurements using inversion algorithm

Data differences (day) inversion algorithm - radiosonde Jul 11 - Aug 26, 1991				
Alt (m)	Temp (°C)			No.
	Mean	STDV	rms	
50	-2.7	1.5	3.1	18
100	-2.4	1.9	3.1	18
150	-2.2	2.1	3.0	18
200	-1.9	2.2	2.9	18
300	-1.5	2.0	2.5	18
400	-1.3	1.8	2.2	18
500	-1.1	1.7	2.0	18
600	-1.0	1.6	1.9	18
700	-1.0	1.5	1.8	18
800	-.9	1.4	1.6	18
900	-.8	1.3	1.5	18
1000	-.7	1.3	1.5	18
1200	-.5	1.2	1.3	18
1400	-.4	1.3	1.3	18
1600	-.3	1.3	1.4	18
1800	-.1	1.4	1.4	18
2000	-.1	1.4	1.4	18
2200	.0	1.4	1.4	18
2400	.2	1.5	1.5	18

Table 12. Statistics of differences between night radiosonde temperature data collected at WSMR and data estimated from 2- and 10-m measurements using Monin-Obukhov similarity

Data differences (night) similarity - radiosonde Jul 11 - Aug 20, 1991				
Alt (m)	Temp (°C)			No.
	Mean	STDV	rms	
50	.4	.6	.7	7
100	.0	1.1	1.1	7
150	-.3	1.5	1.6	7
200	-.6	1.8	1.9	7
300	-.6	2.2	2.3	7
400	-.5	2.4	2.4	7
500	-.5	2.8	2.8	7
600	-.4	3.2	3.2	7
700	-.3	3.4	3.4	7
800	-.1	3.7	3.7	7
900	.0	4.1	4.1	7
1000	.3	4.6	4.6	7
1200	.8	5.3	5.4	7
1400	1.5	6.2	6.4	7
1600	2.2	6.9	7.2	7
1800	2.9	7.6	8.1	7
2000	3.2	8.5	9.1	7
2200	4.8	9.4	10.6	6
2400	5.2	10.4	11.6	6

Table 13. Statistics of differences between night radiosonde temperature data collected at WSMR and data estimated from 10-m measurements using inversion algorithm

Data differences (night) inversion algorithm - radiosonde
Jul 11 - Aug 20, 1991

Alt (m)	Temp (°C)			No.
	Mean	STDV	rms	
50	1.3	1.3	1.8	7
100	.9	1.7	1.9	7
150	.4	1.9	2.0	7
200	.0	1.9	1.9	7
300	-.3	1.9	1.9	7
400	-.5	1.8	1.9	7
500	-.6	1.6	1.7	7
600	-.7	1.5	1.6	7
700	-.7	1.4	1.6	7
800	-.7	1.4	1.6	7
900	-.7	1.3	1.5	7
1000	-.6	1.3	1.4	7
1200	-.3	1.2	1.3	7
1400	.0	1.1	1.1	7
1600	.5	1.2	1.3	7
1800	.8	1.3	1.5	7
2000	.9	1.3	1.6	7
2200	.8	1.4	1.6	6
2400	.7	1.5	1.7	6

RMS DIFFERENCE BETWEEN MODEL
PREDICTIONS AND RADIOSONDE DATA
JUL 11 - AUG 26, 1991 (DAY)

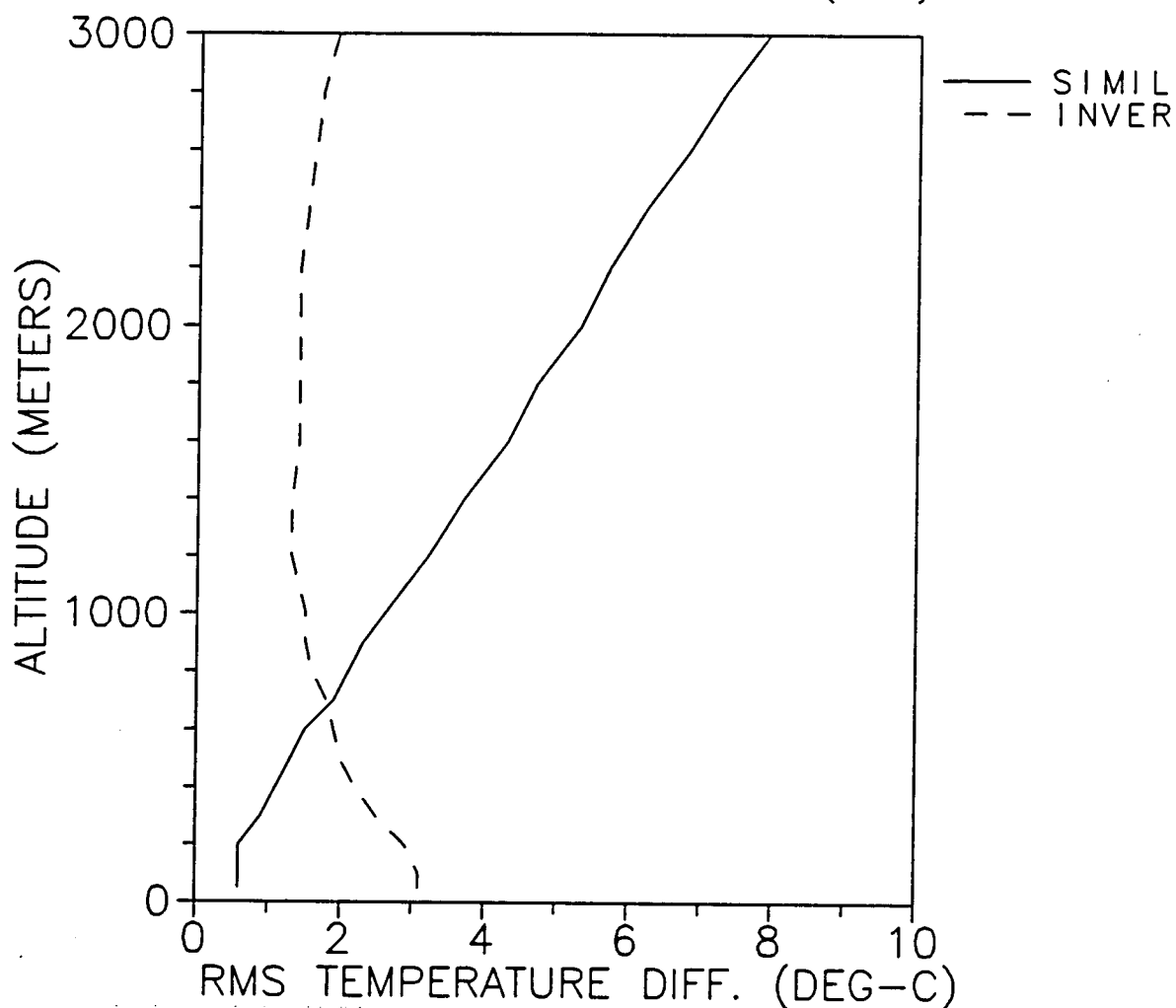


Figure 33. Rms differences between day radiosonde temperature measurements collected at WSMR and data estimated from tower measurements using Monin-Obukhov similarity and inversion algorithms.

RMS DIFFERENCE BETWEEN MODEL
PREDICTIONS AND RADIOSONDE DATA
JUL 11 - AUG 20, 1991 (NIGHT)

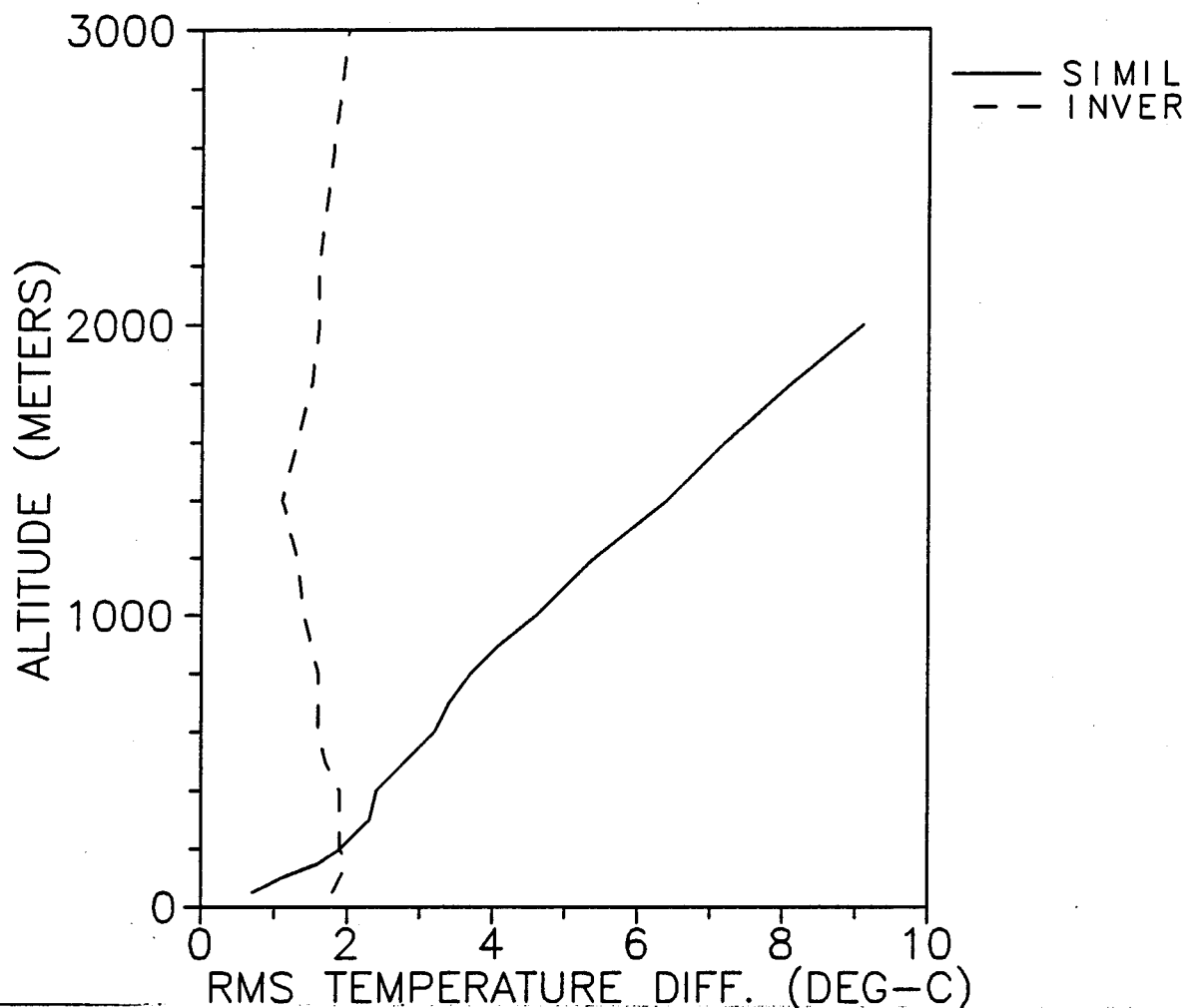


Figure 34. Rms differences between night radiosonde temperature measurements collected at WSMR and data estimated from tower measurements using Monin-Obukhov similarity and inversion algorithms.

Table 14. Statistics of differences between day radiosonde wind data collected at Ft. Bliss and data estimated from 2- and 10-m measurements using Monin-Obukhov similarity

Data differences (day) similarity - radiosonde Jun 4 - Jun 22, 1990				
Alt (m)	Wind Speed (m/s)			No.
	Mean	STDV	rms	
200	.6	1.5	1.6	27
300	.3	1.5	1.5	27
400	.2	1.7	1.7	27
500	.2	1.8	1.8	27
600	.2	1.7	1.7	27
700	.2	1.8	1.8	27
800	.2	2.2	2.3	27
900	.2	2.5	2.5	27
1000	.1	2.9	2.9	27
1200	.0	3.2	3.2	27
1400	.1	3.8	3.8	27
1600	.5	4.0	4.0	27
1800	1.0	4.0	4.1	27
2000	.9	4.0	4.1	27
2200	1.3	4.2	4.4	27
2400	1.4	3.8	4.1	27
2600	.9	3.6	3.7	27
2800	1.2	3.8	4.0	27
3000	1.3	3.9	4.1	27

Table 15. Statistics of differences between day radiosonde wind data collected at Ft. bliss and data estimated from 2- and 10-m measurements using p-profile fit

Data differences (day) p-profile - radiosonde Jun 4 - Jun 22, 1990				
Alt (m)	Wind Speed (m/s)			No.
	Mean	STDV	rms	
200	3.3	2.3	4.0	27
300	3.6	2.7	4.5	27
400	4.0	3.1	5.1	27
500	4.5	3.5	5.7	27
600	5.0	3.8	6.2	27
700	5.3	4.2	6.8	27
800	5.6	4.8	7.4	27
900	5.9	5.2	7.9	27
1000	6.1	5.6	8.2	27
1200	6.5	6.2	8.9	27
1400	7.0	7.1	9.9	27
1600	7.7	7.6	10.8	27
1800	8.5	7.7	11.5	27
2000	8.8	7.9	11.8	27
2200	9.5	8.4	12.7	27
2400	9.8	8.1	12.7	27
2600	9.7	7.9	12.5	27
2800	10.2	8.2	13.1	27
3000	10.5	8.1	13.3	27

Table 16. Statistics of differences between night radiosonde wind data collected at Ft. Bliss and data estimated from 2- and 10-m measurements using Monin-Obukhov similarity

Data differences (night) similarity - radiosonde Jun 4 - Jun 22, 1990				
Alt (m)	Wind Speed (m/s)			No.
	Mean	STDV	rms	
200	3.1	5.0	5.9	11
300	4.5	9.0	10.0	11
400	6.2	13.2	14.6	11
500	7.9	17.5	19.1	11
600	9.4	21.4	23.4	11
700	11.2	25.3	27.7	11
800	13.2	29.0	31.8	11
900	15.2	32.6	36.0	11
1000	17.1	36.2	40.1	11
1200	20.6	43.8	48.4	11
1400	24.2	51.2	56.6	11
1600	27.9	58.3	64.6	11
1800	31.6	65.5	72.8	11
2000	35.3	72.6	80.7	11
2200	39.3	79.7	88.8	11
2400	43.8	86.9	97.3	11
2600	47.9	93.5	105.1	11
2800	51.2	100.8	113.0	11
3000	54.2	108.3	121.1	11

Table 17. Statistics of differences between night radiosonde wind data collected at Ft. Bliss and data estimated from 2- and 10-m measurements using p-profile fit

Data differences (night) p-profile - radiosonde Jun 4 - Jun 22, 1990				
Alt (m)	Wind Speed (m/s)			No.
	Mean	STDV	rms	
200	4.1	2.8	5.0	11
300	4.9	3.8	6.2	11
400	5.9	5.1	7.7	11
500	6.6	6.2	9.1	11
600	7.2	7.2	10.2	11
700	7.9	7.9	11.2	11
800	8.8	8.3	12.1	11
900	9.7	8.6	12.9	11
1000	10.4	8.7	13.6	11
1200	11.4	9.6	14.9	11
1400	12.4	10.6	16.3	11
1600	13.4	11.5	17.7	11
1800	14.5	12.2	18.9	11
2000	15.3	12.3	19.7	11
2200	16.5	12.3	20.6	11
2400	18.2	12.6	22.2	11
2600	19.4	12.8	23.2	11
2800	19.8	13.1	23.7	11
3000	19.9	13.5	24.1	11

RMS DIFFERENCE BETWEEN MODEL
PREDICTIONS AND RADIOSONDE DATA
JUN 04 - JUN 22, 1990 (DAY)

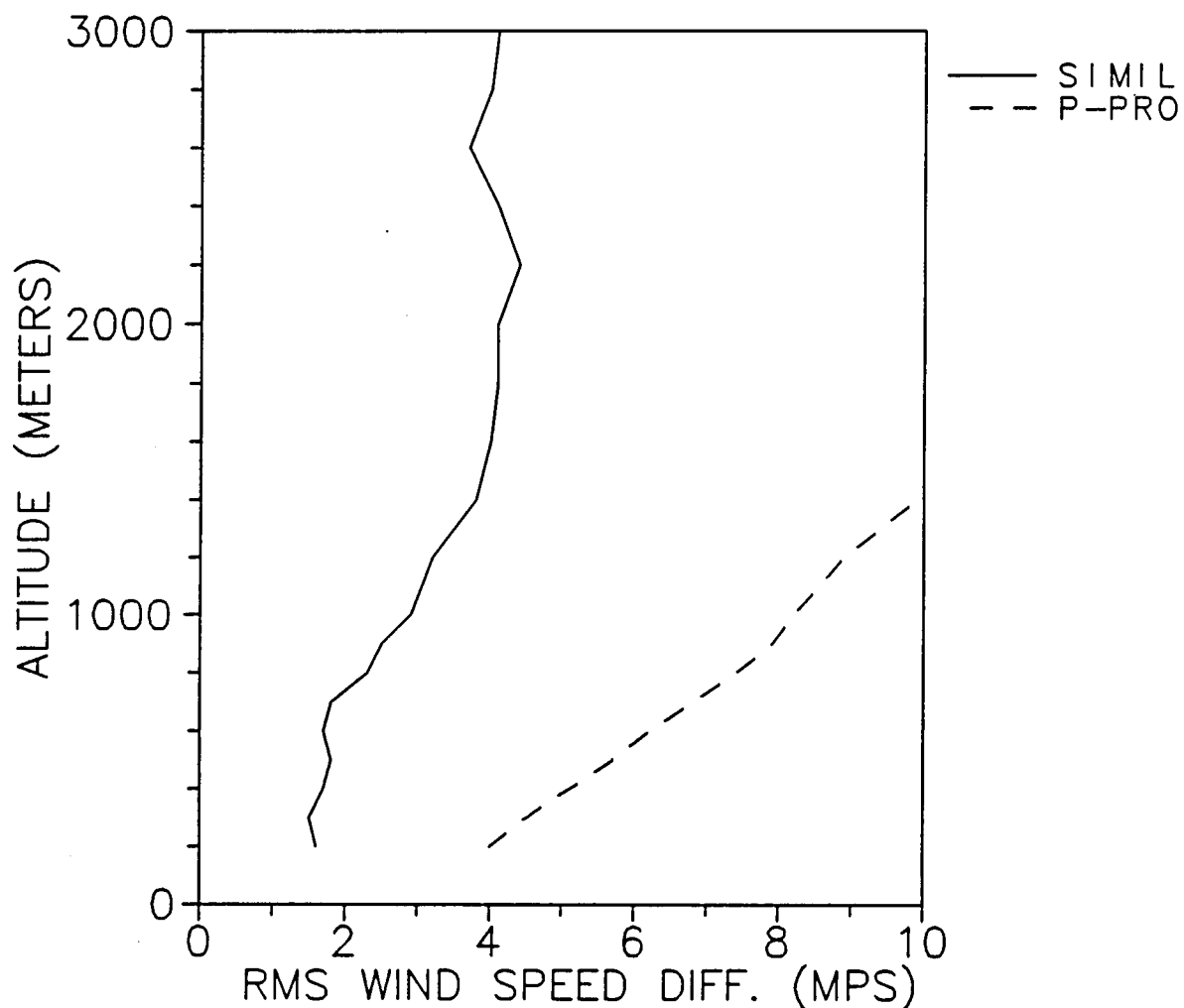


Figure 35. Rms differences between day radiosonde wind speed measurements collected at Ft. Bliss and data estimated from tower measurements using Monin-Obukhov similarity and p-profile fit.

RMS DIFFERENCE BETWEEN MODEL
PREDICTIONS AND RADIOSONDE DATA
JUN 04 - JUN 22, 1990 (NIGHT)

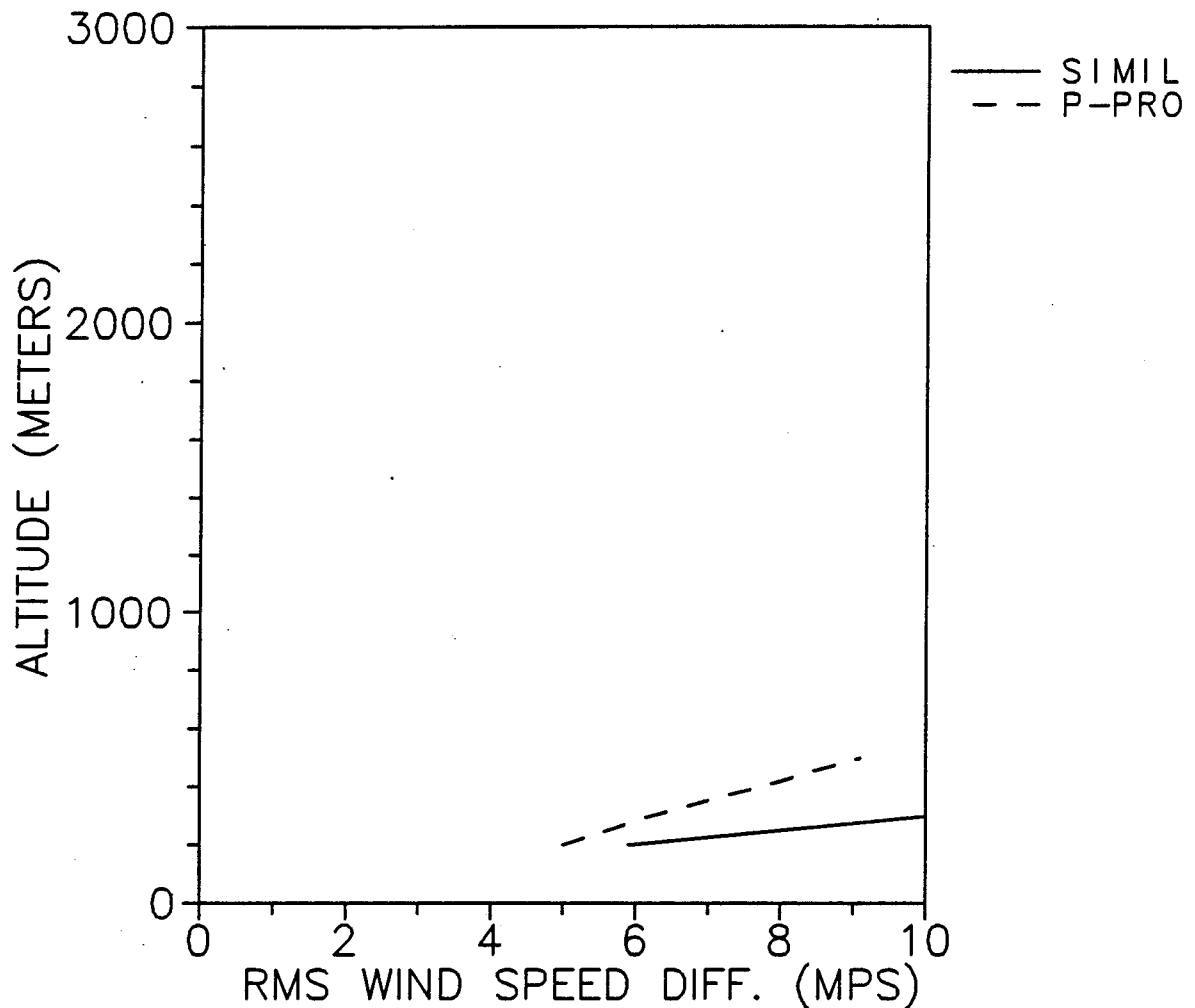


Figure 36. Rms differences between night radiosonde wind speed measurements collected at Ft. Bliss and data estimated from tower measurements using Monin-Obukhov similarity and p-profile fit.

Table 18. Statistics of differences between day radiosonde temperature data collected at Ft. Bliss and data estimated from 2- and 10-m measurements using Monin-Obukhov similarity

Data differences (day) similarity - radiosonde				
Jun 4 - Jun 22, 1990				
Alt (m)	Temp (°C)			No.
	Mean	STDV	rms	
50	-.6	.7	.9	27
100	-.4	.6	.7	27
150	-.3	.5	.6	27
200	-.3	.5	.6	27
300	-.4	.5	.7	27
400	-.5	.5	.7	27
500	-.6	.5	.8	27
600	-.7	.5	.9	27
700	-.8	.7	1.1	27
800	-1.0	.7	1.2	27
900	-1.0	.8	1.3	27
1000	-1.1	.8	1.4	27
1200	-1.5	1.2	1.9	27
1400	-1.9	1.6	2.5	27
1600	-2.3	1.8	2.9	27
1800	-2.5	2.1	3.3	27
2000	-2.8	2.2	3.6	27
2200	-3.0	2.4	3.9	27
2400	-3.3	2.5	4.1	27

Table 19. Statistics of differences between day radiosonde temperature data collected at Ft. Bliss and data estimated from 10-m measurements using inversion algorithm

Data differences (day) inversion algorithm - radiosonde Jun 4 - Jun 22, 1990				
Alt (m)	Temp (°C)			No.
	Mean	STDV	rms	
50	-3.7	1.3	4.0	27
100	-3.6	1.9	4.1	27
150	-3.3	2.2	4.0	27
200	-3.0	2.5	3.9	27
300	-2.4	2.5	3.5	27
400	-2.0	2.5	3.2	27
500	-1.7	2.4	2.9	27
600	-1.5	2.3	2.7	27
700	-1.3	2.2	2.5	27
800	-1.1	2.1	2.4	27
900	-.9	2.1	2.3	27
1000	-.7	2.1	2.2	27
1200	-.5	1.8	1.9	27
1400	-.3	1.6	1.6	27
1600	-.1	1.5	1.5	27
1800	.3	1.4	1.4	27
2000	.6	1.4	1.6	27
2200	.9	1.5	1.7	27
2400	1.3	1.4	1.9	27

Table 20. Statistics of differences between night radiosonde temperature data collected at Ft. Bliss and data estimated from 2- and 10-m measurements using Monin-Obukhov similarity

Data differences (night) similarity - radiosonde Jun 4 - Jun 22, 1990				
Alt (m)	Temp (°C)			No.
	Mean	STDV	rms	
50	.2	1.2	1.3	11
100	.5	2.2	2.2	11
150	.9	3.3	3.5	11
200	1.2	4.6	4.7	11
300	1.7	7.1	7.3	11
400	2.3	9.8	10.0	11
500	3.0	12.3	12.7	11
600	3.6	14.9	15.4	11
700	4.4	17.5	18.0	11
800	5.2	20.0	20.6	11
900	6.0	22.5	23.3	11
1000	6.7	25.1	26.0	11
1200	8.2	30.2	31.3	11
1400	9.6	35.3	36.6	11
1600	11.4	40.3	41.9	11
1800	13.3	45.3	47.2	11
2000	15.3	50.2	52.4	11
2200	17.1	55.2	57.8	11
2400	19.1	60.1	63.0	11

Table 21. Statistics of differences between night radiosonde temperature data collected at Ft. Bliss and data estimated from 10-m measurements using inversion algorithm

Data differences (night) inversion algorithm - radiosonde
Jun 4 - Jun 22, 1990

Alt (m)	Temp (°C)			No.
	Mean	STDV	rms	
50	.6	1.0	1.2	11
100	1.2	1.6	2.0	11
150	1.7	2.1	2.7	11
200	1.8	2.5	3.1	11
300	1.7	2.8	3.3	11
400	1.5	2.7	3.1	11
500	1.3	2.4	2.8	11
600	1.1	2.2	2.4	11
700	1.1	2.0	2.3	11
800	1.1	2.1	2.3	11
900	1.1	1.9	2.2	11
1000	1.0	1.8	2.1	11
1200	.9	1.6	1.9	11
1400	.7	1.2	1.4	11
1600	.9	1.1	1.4	11
1800	1.2	1.1	1.6	11
2000	1.6	1.1	1.9	11
2200	1.8	1.5	2.4	11
2400	2.2	1.7	2.8	11

RMS DIFFERENCE BETWEEN MODEL
PREDICTIONS AND RADIOSONDE DATA
JUN 04 - JUN 22, 1990 (DAY)

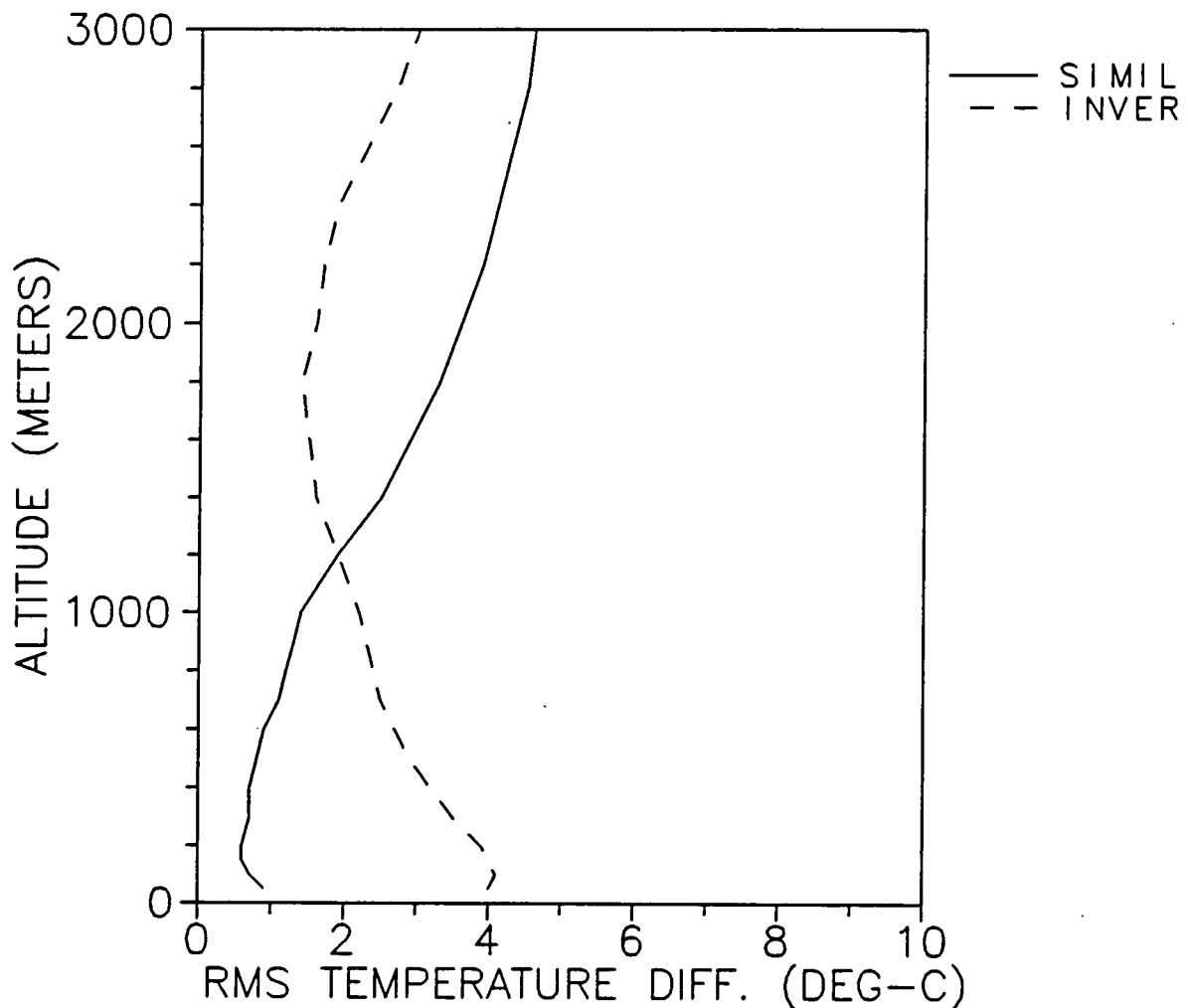


Figure 37. Rms differences between day radiosonde temperature measurements collected at Ft. Bliss and data estimated from tower measurements using Monin-Obukhov similarity and inversion algorithms.

RMS DIFFERENCE BETWEEN MODEL
PREDICTIONS AND RADIOSONDE DATA
JUN 04 - JUN 22, 1990 (NIGHT)

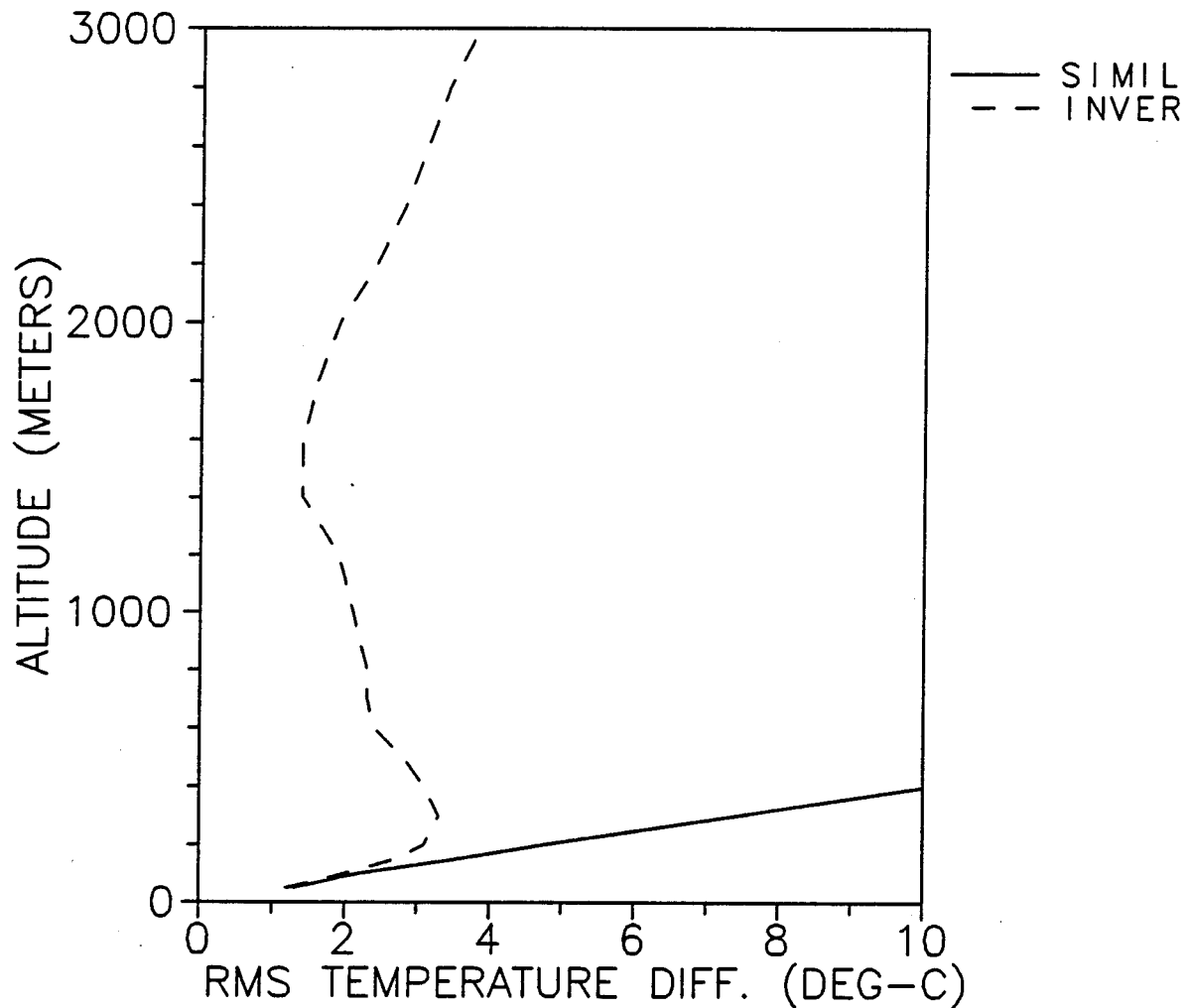


Figure 38. Rms differences between night radiosonde temperature measurements collected at Ft. Bliss and data estimated from tower measurements using Monin-Obukhov similarity and inversion algorithms.

Table 22. Statistics of differences between day radiosonde wind data collected at Champaign and data estimated from 2- and 10-m measurements using Monin-Obukhov similarity

Data differences (day) similarity - radiosonde Jul 23 - Aug 3, 1990				
Alt (m)	Wind speed (m/s)			No.
	Mean	STDV	rms	
200	.2	.9	.9	25
300	-.1	1.0	1.0	25
400	-.3	1.0	1.1	25
500	-.4	1.1	1.2	25
600	-.4	1.2	1.2	25
700	-.2	1.3	1.3	25
800	-.1	1.2	1.2	25
900	.0	1.4	1.4	25
1000	.2	1.5	1.5	25
1200	.4	1.7	1.7	25
1400	.3	1.8	1.8	25
1600	-.3	2.5	2.6	25
1800	-.7	2.9	3.0	25
2000	-.3	2.6	2.6	24
2200	.4	2.6	2.6	23
2400	.1	2.6	2.6	23
2600	-.3	2.7	2.7	23
2800	-.1	2.8	2.9	23
3000	.2	2.7	2.7	23

Table 23. Statistics of differences between day radiosonde wind data collected at Champaign and data estimated from 2- and 10-m measurements using p-profile fit

Data differences (day) p-profile - radiosonde Jul 23 - Aug 3, 1990				
Alt (m)	Wind speed (m/s)			No.
	Mean	STDV	rms	
200	2.1	1.5	2.5	25
300	2.2	1.9	2.9	25
400	2.4	1.9	3.1	25
500	2.6	2.0	3.3	25
600	3.0	2.1	3.7	25
700	3.4	2.3	4.1	25
800	3.8	2.6	4.6	25
900	4.1	2.9	5.0	25
1000	4.4	3.1	5.4	25
1200	5.0	3.5	6.1	25
1400	5.1	3.9	6.4	25
1600	4.8	4.6	6.7	25
1800	4.7	5.4	7.1	25
2000	5.4	5.4	7.6	24
2200	6.3	5.5	8.4	23
2400	6.3	5.8	8.5	23
2600	6.0	6.0	8.5	23
2800	6.4	6.2	8.9	23
3000	6.9	6.1	9.2	23

Table 24. Statistics of differences between night radiosonde wind data collected at Champaign and data estimated from 2- and 10-m measurements using Monin-Obukhov similarity

Data differences (night) similarity - radiosonde Jul 23 - Aug 2, 1990				
Alt (m)	Wind speed (m/s)			No.
	Mean	STDV	rms	
200	-.1	3.0	3.0	5
300	.3	3.3	3.3	5
400	1.1	3.9	4.0	5
500	1.7	4.5	4.8	5
600	2.0	5.5	5.8	5
700	2.4	6.4	6.9	5
800	3.1	7.4	8.0	5
900	3.9	8.2	9.0	5
1000	4.2	8.7	9.6	5
1200	4.8	9.6	10.7	5
1400	4.8	10.5	11.5	5
1600	4.6	11.2	12.1	5
1800	5.0	12.9	13.9	5
2000	6.1	15.1	16.3	5
2200	7.3	17.2	18.7	5
2400	8.0	18.7	20.4	5
2600	8.6	20.5	22.2	5
2800	8.7	23.0	24.6	5
3000	9.0	25.5	27.0	5

Table 25. Statistics of differences between night radiosonde wind data collected at Champaign and data estimated from 2- and 10-m measurements using p-profile fit

Data differences (night) p-profile - radiosonde Jul 23 - Aug 2, 1990				
Alt (m)	Wind speed (m/s)			No.
	Mean	STDV	rms	
200	2.3	2.3	3.3	5
300	3.7	4.0	5.5	5
400	5.4	5.9	8.0	5
500	6.8	7.7	10.3	5
600	8.0	9.6	12.5	5
700	9.2	11.6	14.8	5
800	10.6	13.6	17.2	5
900	12.2	15.7	19.9	5
1000	13.3	18.1	22.4	5
1200	15.3	22.2	27.0	5
1400	16.8	26.4	31.3	5
1600	18.0	30.8	35.7	5
1800	19.8	34.7	40.0	5
2000	22.3	38.7	44.6	5
2200	24.9	42.2	49.0	5
2400	27.0	45.7	53.1	5
2600	28.9	49.6	57.5	5
2800	30.3	54.1	62.0	5
3000	32.0	58.2	66.4	5

RMS DIFFERENCE BETWEEN MODEL
PREDICTIONS AND RADIOSONDE DATA
JUL 23 - AUG 03, 1990 (DAY)

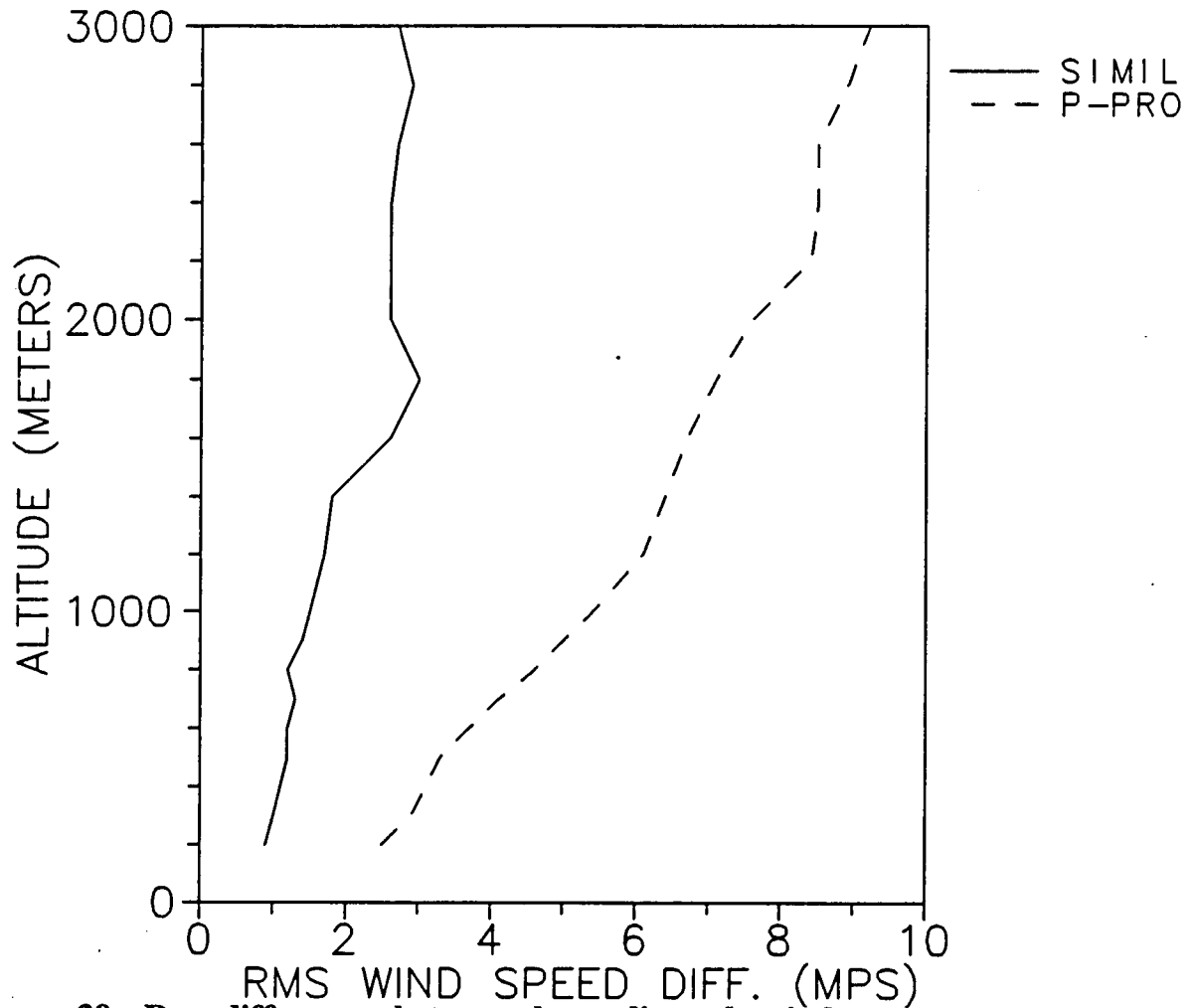


Figure 39. Rms differences between day radiosonde wind speed measurements collected at Champaign and data estimated from tower measurements using Monin-Obukhov similarity and p-profile fit.

RMS DIFFERENCE BETWEEN MODEL
PREDICTIONS AND RADIOSONDE DATA
JUL 23 - AUG 02, 1990 (NIGHT)

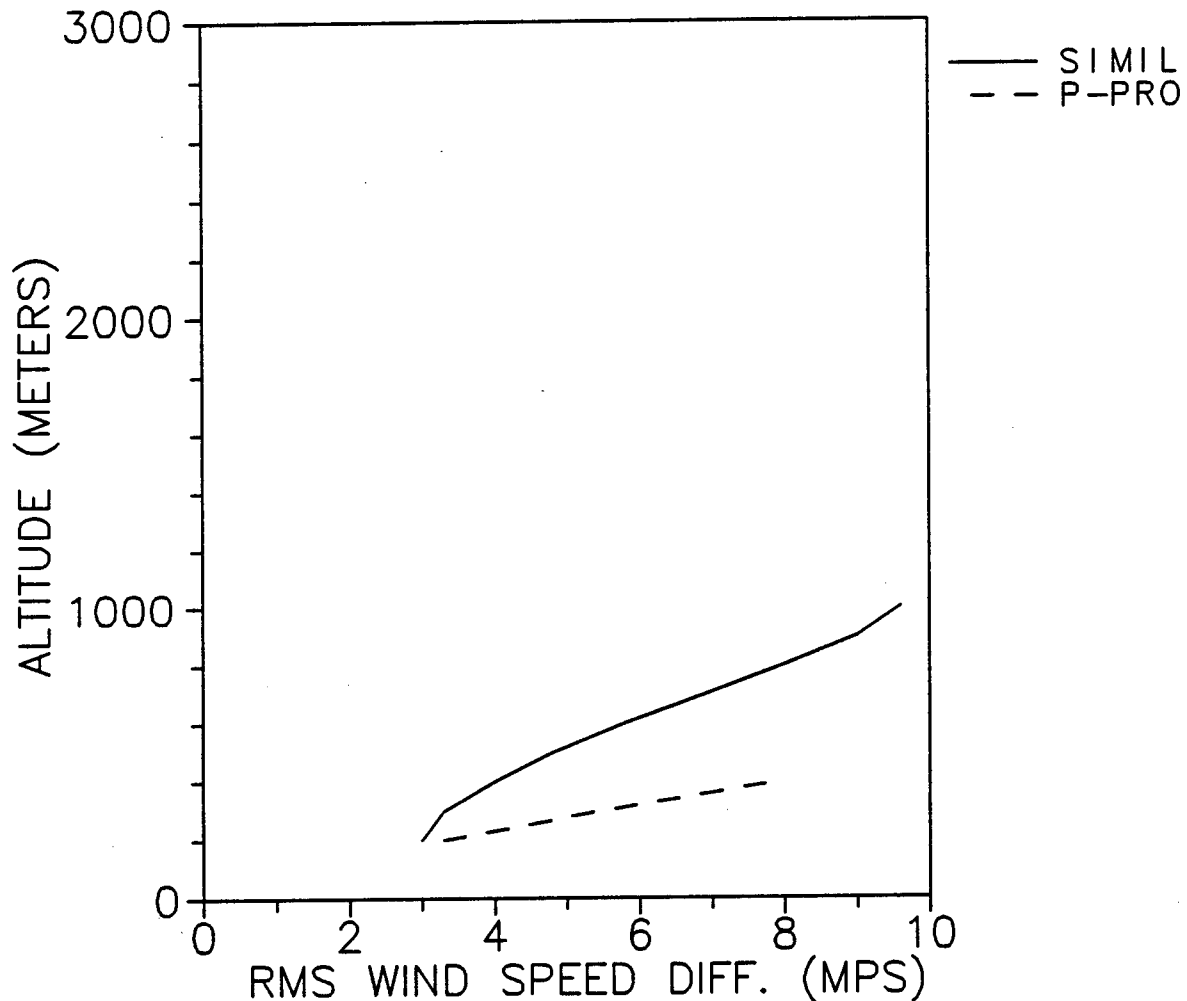


Figure 40. Rms differences between night radiosonde wind speed measurements collected at Champaign and data estimated from tower measurements using Monin-Obukhov similarity and p-profile fit.

Table 26. Statistics of differences between day radiosonde temperature data collected at Champaign and data estimated from 2- and 10-m measurements using Monin-Obukhov similarity

Data differences (day) similarity - radiosonde Jul 23 - Aug 3, 1990				
Alt (m)	Temp (°C)			No.
	Mean	STDV	rms	
50	-.9	.6	1.1	25
100	-.7	.5	.9	25
150	-.8	.5	1.0	25
200	-.9	.5	1.0	25
300	-1.1	.9	1.4	25
400	-1.2	1.0	1.6	25
500	-1.2	1.4	1.8	25
600	-1.5	1.2	1.9	25
700	-1.8	1.5	2.3	25
800	-2.0	1.6	2.5	25
900	-2.2	1.7	2.8	25
1000	-2.3	1.8	3.0	25
1200	-2.8	2.0	3.5	25
1400	-3.5	2.2	4.1	25
1600	-4.5	2.1	4.9	25
1800	-5.3	2.0	5.7	25
2000	-6.4	2.0	6.8	24
2200	-7.6	2.2	7.9	23
2400	-8.6	2.5	8.9	23

Table 27. Statistics of differences between day radiosonde temperature data collected at Champaign and data estimated from 10-m measurements using inversion algorithm

Data differences (day) inversion algorithm - radiosonde
Jul 23 - Aug 3, 1990

Alt (m)	Temp (°C)			No.
	Mean	STDV	rms	
50	-3.7	1.1	3.8	25
100	-3.6	1.2	3.8	25
150	-3.6	1.4	3.8	25
200	-3.4	1.4	3.7	25
300	-3.0	1.4	3.3	25
400	-2.6	1.3	2.9	25
500	-2.2	1.7	2.8	25
600	-2.3	.9	2.4	25
700	-2.2	.9	2.4	25
800	-2.0	.9	2.2	25
900	-2.0	.9	2.1	25
1000	-1.8	.8	2.0	25
1200	-1.7	1.0	1.9	25
1400	-1.7	1.2	2.1	25
1600	-2.0	1.2	2.3	25
1800	-2.2	1.4	2.6	25
2000	-2.7	1.7	3.2	24
2200	-3.1	2.1	3.8	23
2400	-3.6	2.4	4.3	23

Table 28. Statistics of differences between night radiosonde temperature data collected at Champaign and data estimated from 2- and 10-m measurements using Monin-Obukhov similarity

Data differences (night) similarity - radiosonde Jul 23 - Aug 2, 1990				
Alt (m)	Temp (°C)			No.
	Mean	STDV	rms	
50	-.5	.8	1.0	5
100	-1.6	2.0	2.6	5
150	-2.3	2.5	3.4	5
200	-2.9	2.7	4.0	5
300	-3.8	2.8	4.7	5
400	-4.7	3.1	5.6	5
500	-4.8	3.2	5.8	5
600	-5.0	3.4	6.0	5
700	-5.0	3.5	6.1	5
800	-5.2	3.6	6.3	5
900	-5.2	3.8	6.5	5
1000	-5.3	3.9	6.6	5
1200	-5.5	4.0	6.8	5
1400	-6.0	4.2	7.3	5
1600	-6.7	4.1	7.9	5
1800	-7.4	4.1	8.4	5
2000	-8.2	3.9	9.0	5
2200	-8.9	3.9	9.7	5
2400	-9.6	3.8	10.3	5

Table 29. Statistics of differences between night radiosonde temperature data collected at Champaign and data estimated from 10-m measurements using inversion algorithm

Data differences (night) inversion algorithm - radiosonde
Jul 23 - Aug 2, 1990

Alt (m)	Temp (°C)			No.
	Mean	STDV	rms	
50	-.1	1.2	1.2	5
100	-.6	1.4	1.5	5
150	-.9	1.7	1.9	5
200	-1.2	1.7	2.0	5
300	-1.8	1.2	2.1	5
400	-2.3	.9	2.5	5
500	-2.2	.8	2.4	5
600	-2.2	.8	2.3	5
700	-1.9	.8	2.1	5
800	-1.8	.8	1.9	5
900	-1.6	.8	1.8	5
1000	-1.4	.7	1.6	5
1200	-1.1	.8	1.4	5
1400	-1.1	1.2	1.6	5
1600	-1.3	1.4	1.9	5
1800	-1.4	1.7	2.2	5
2000	-1.7	1.9	2.5	5
2200	-1.9	2.2	2.9	5
2400	-2.1	2.4	3.2	5

RMS DIFFERENCE BETWEEN MODEL
PREDICTIONS AND RADIOSONDE DATA
JUL 23 - AUG 03, 1990 (DAY)

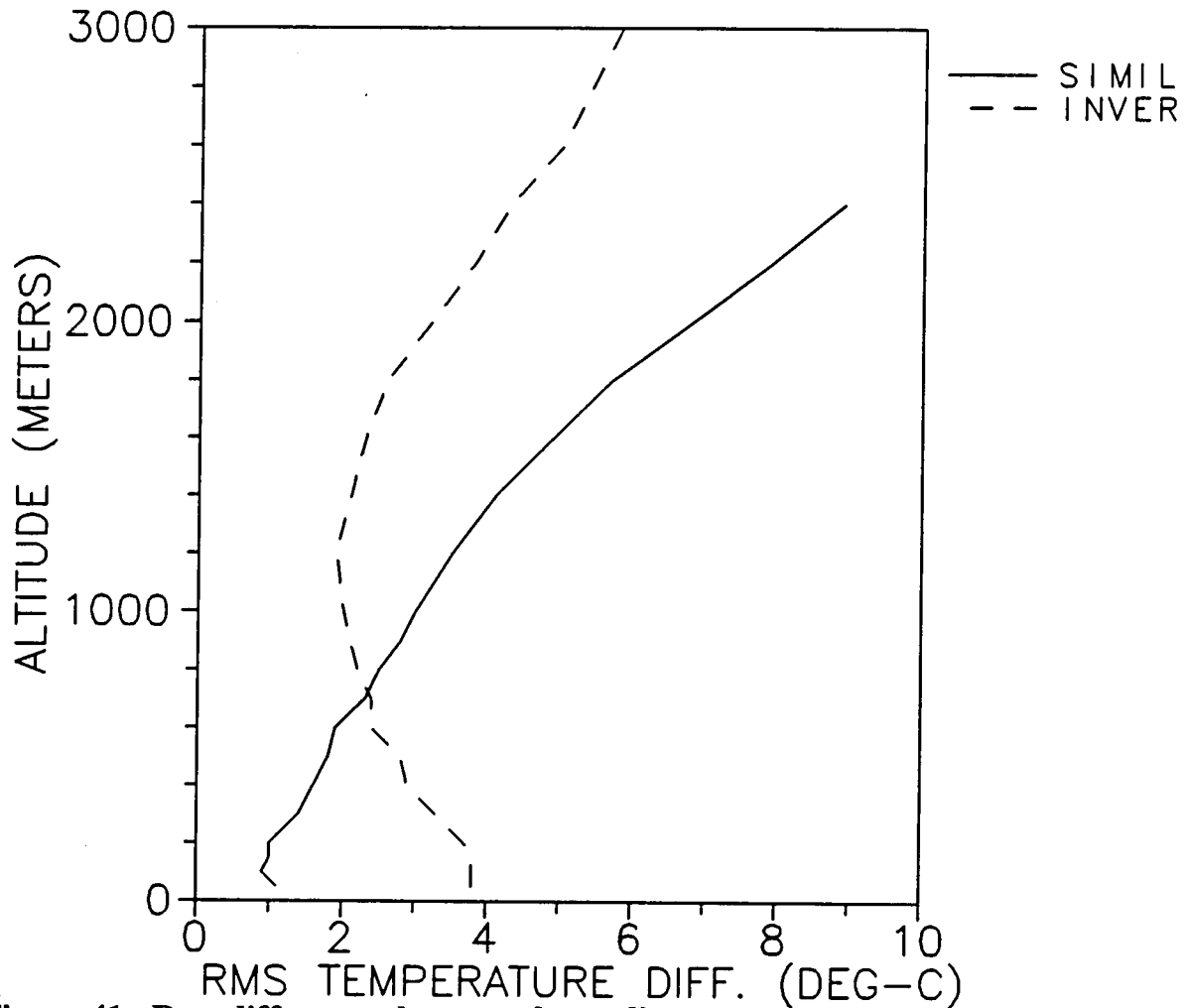


Figure 41. Rms differences between day radiosonde temperature measurements collected at Champaign and data estimated from tower measurements using Monin-Obukhov similarity and inversion algorithms.

RMS DIFFERENCE BETWEEN MODEL
PREDICTIONS AND RADIOSONDE DATA
JUL 23 - AUG 02, 1990 (NIGHT)

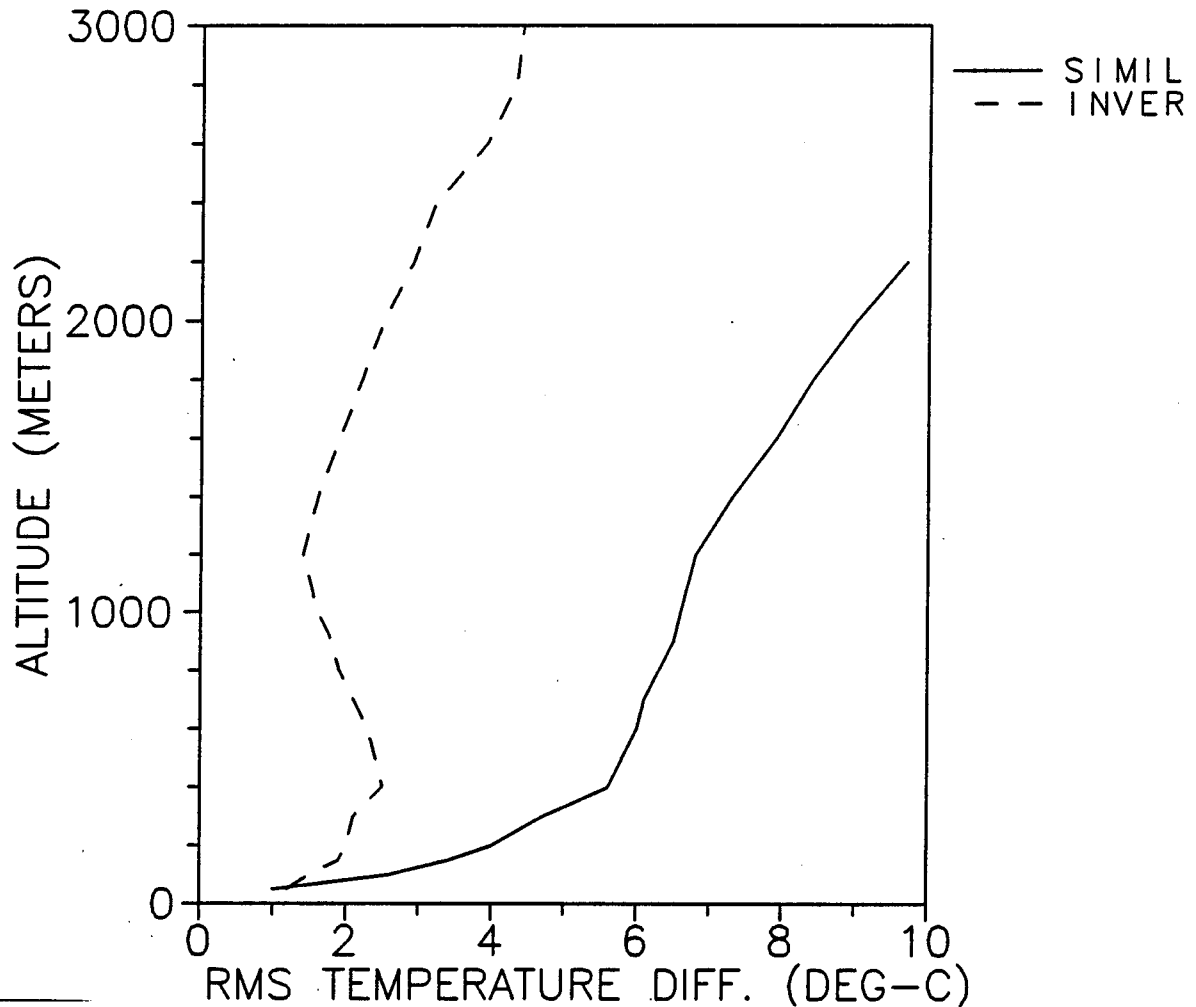


Figure 42. Rms differences between night radiosonde temperature measurements collected at Champaign and data estimated from tower measurements using Monin-Obukhov similarity and inversion algorithms.

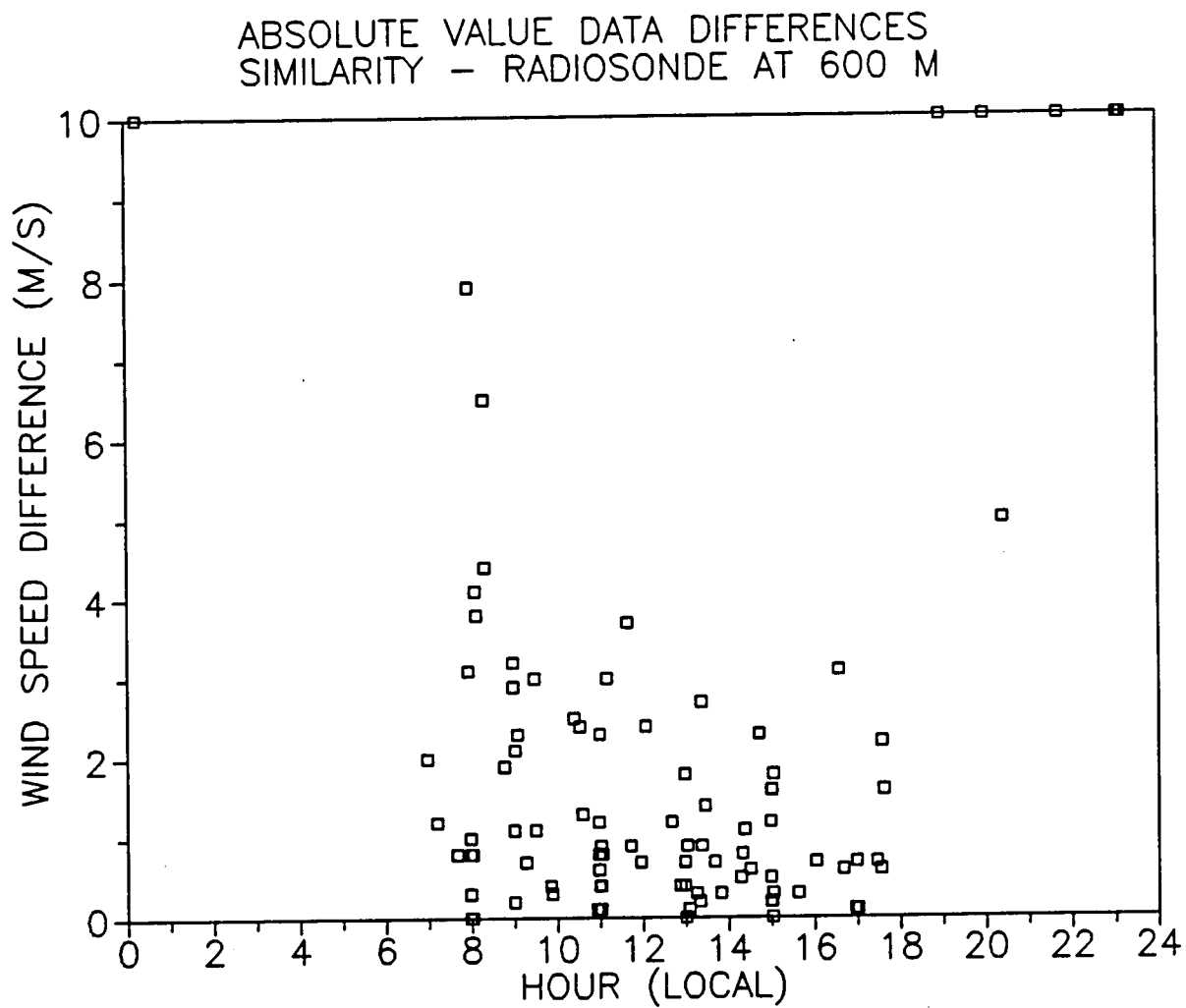


Figure 43. Absolute value of differences between radiosonde wind speed measurements and data estimated from tower measurements using Monin-Obukhov similarity.

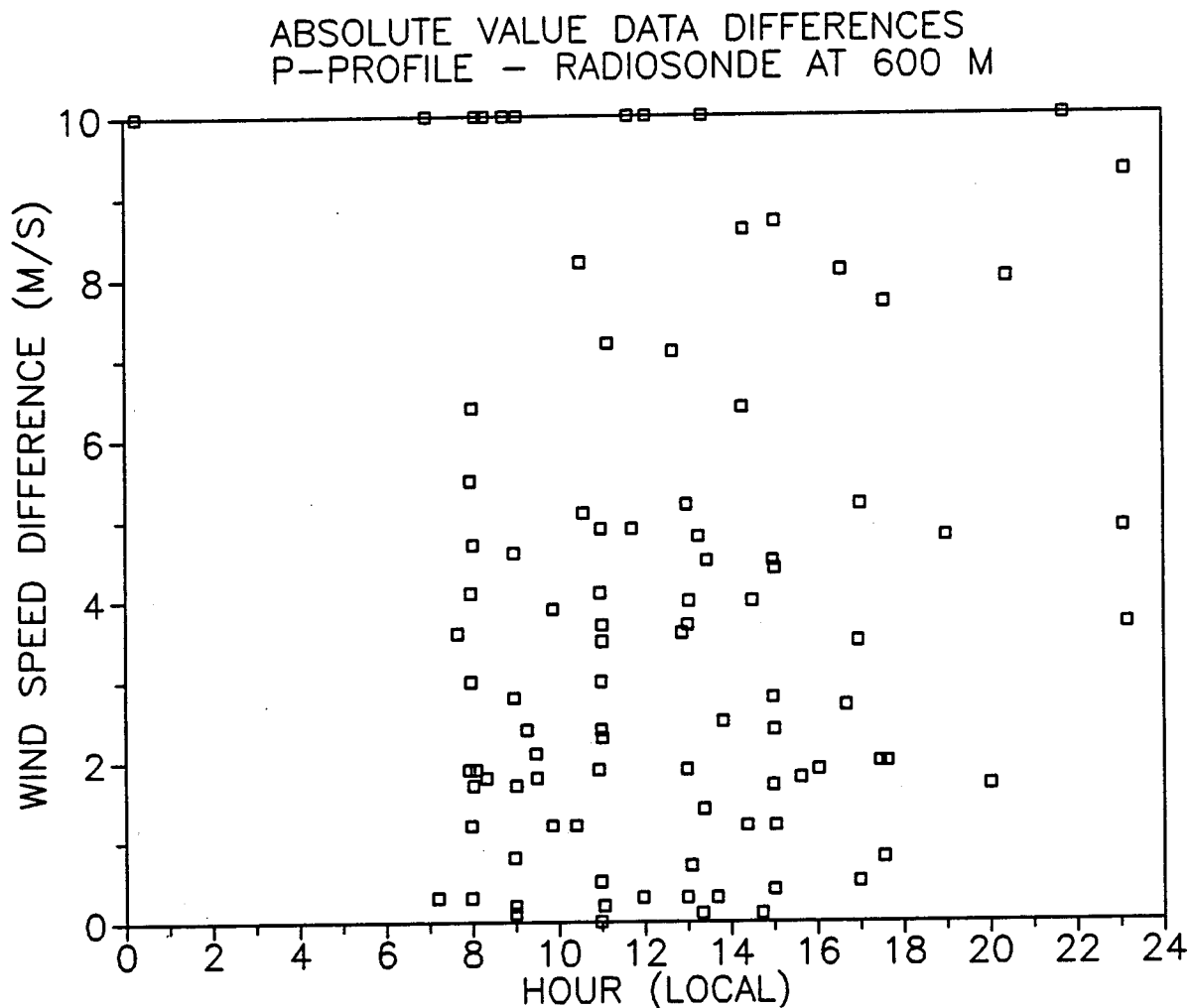


Figure 44. Absolute value of differences between radiosonde wind speed measurements and data estimated from tower measurements using p-profile.

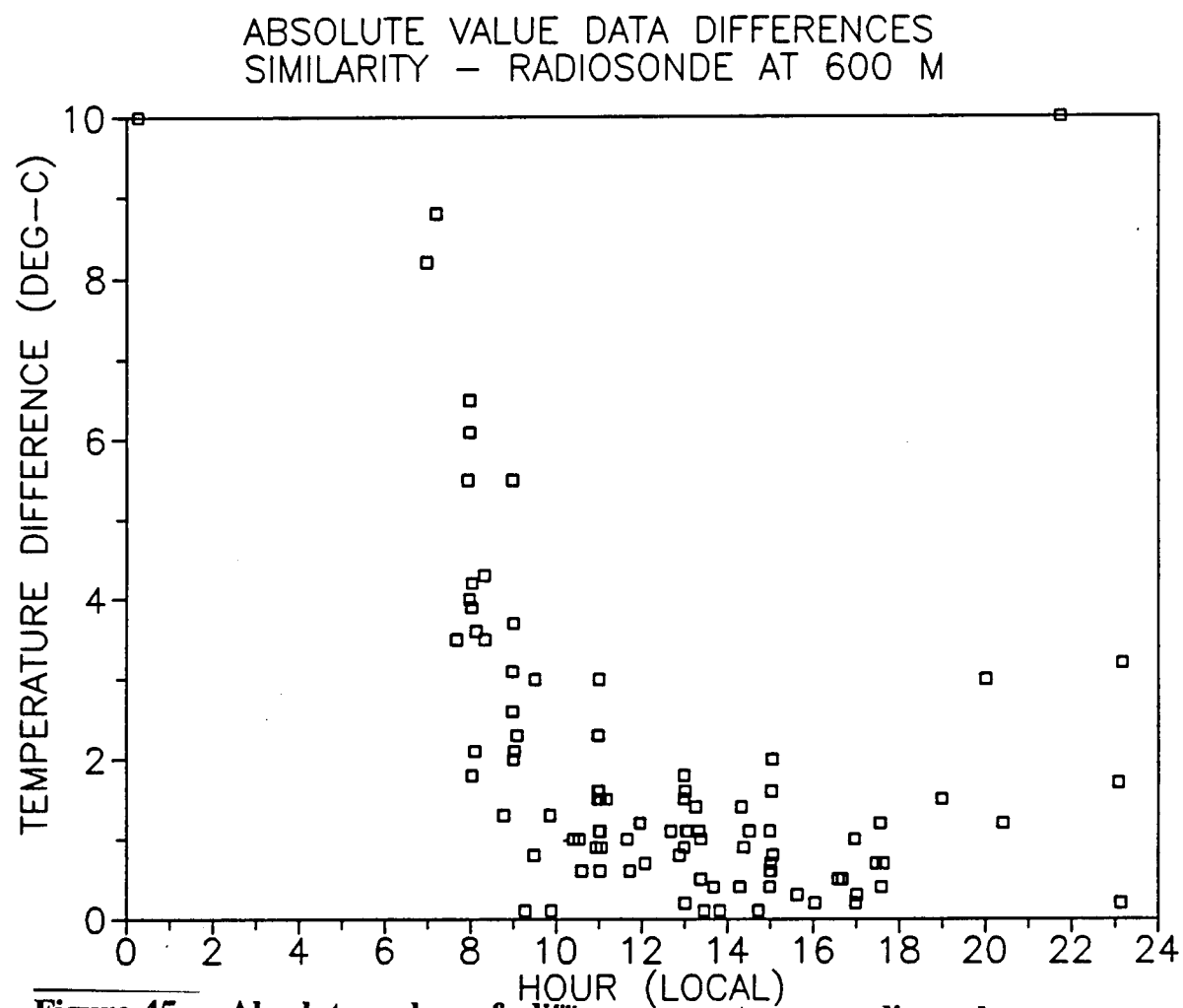


Figure 45. Absolute value of differences between radiosonde temperature measurements and data estimated from tower measurements using Monin-Obukhov similarity.

ABSOLUTE VALUE DATA DIFFERENCES
INVERSION - RADIOSONDE AT 600 M

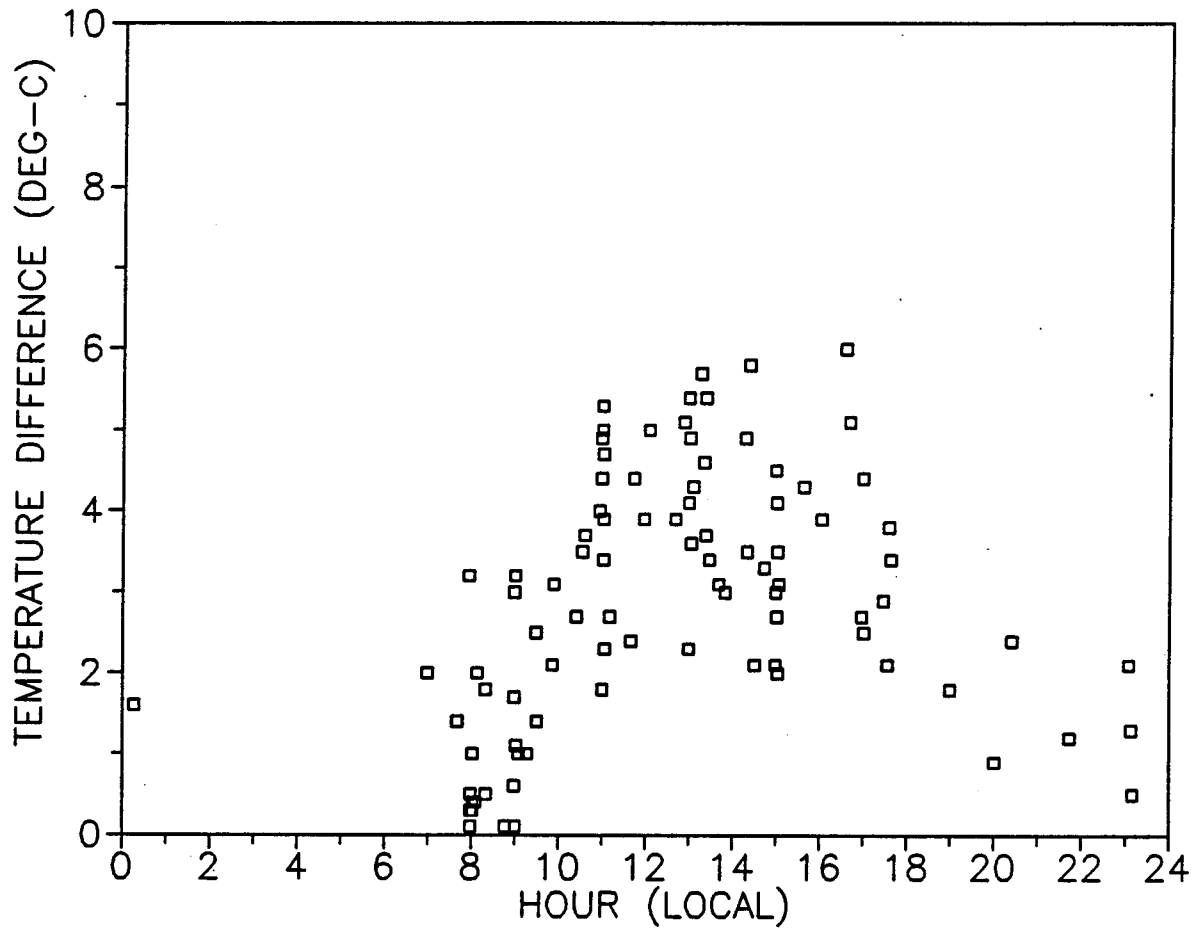


Figure 46. Absolute value of differences between radiosonde temperature measurements and data estimated from tower measurements using inversion algorithm.

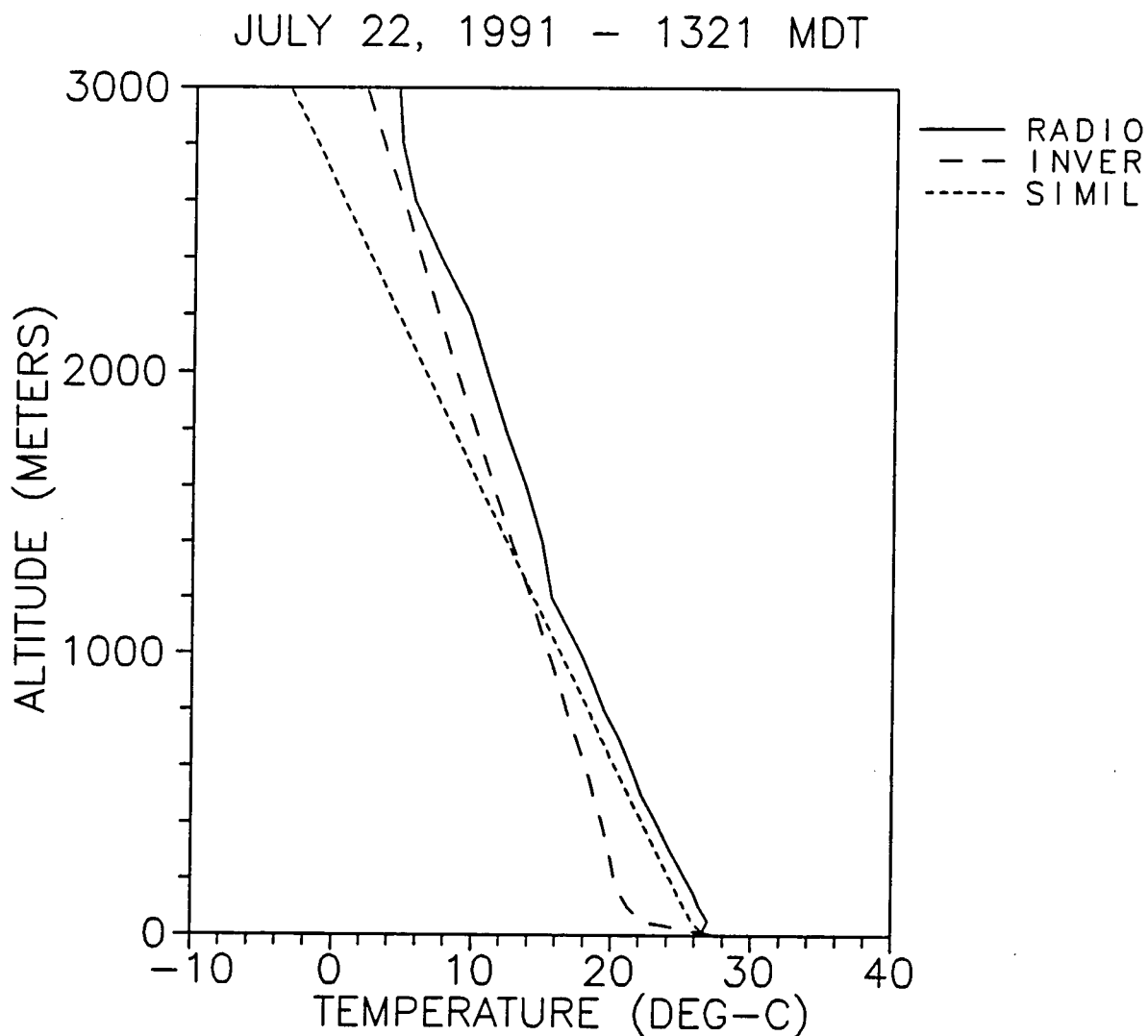


Figure 47. Comparison of temperature data collected by a radiosonde launched July 22 at 1321 MDT with values estimated from tower measurements using inversion and Monin-Obukhov similarity algorithms.

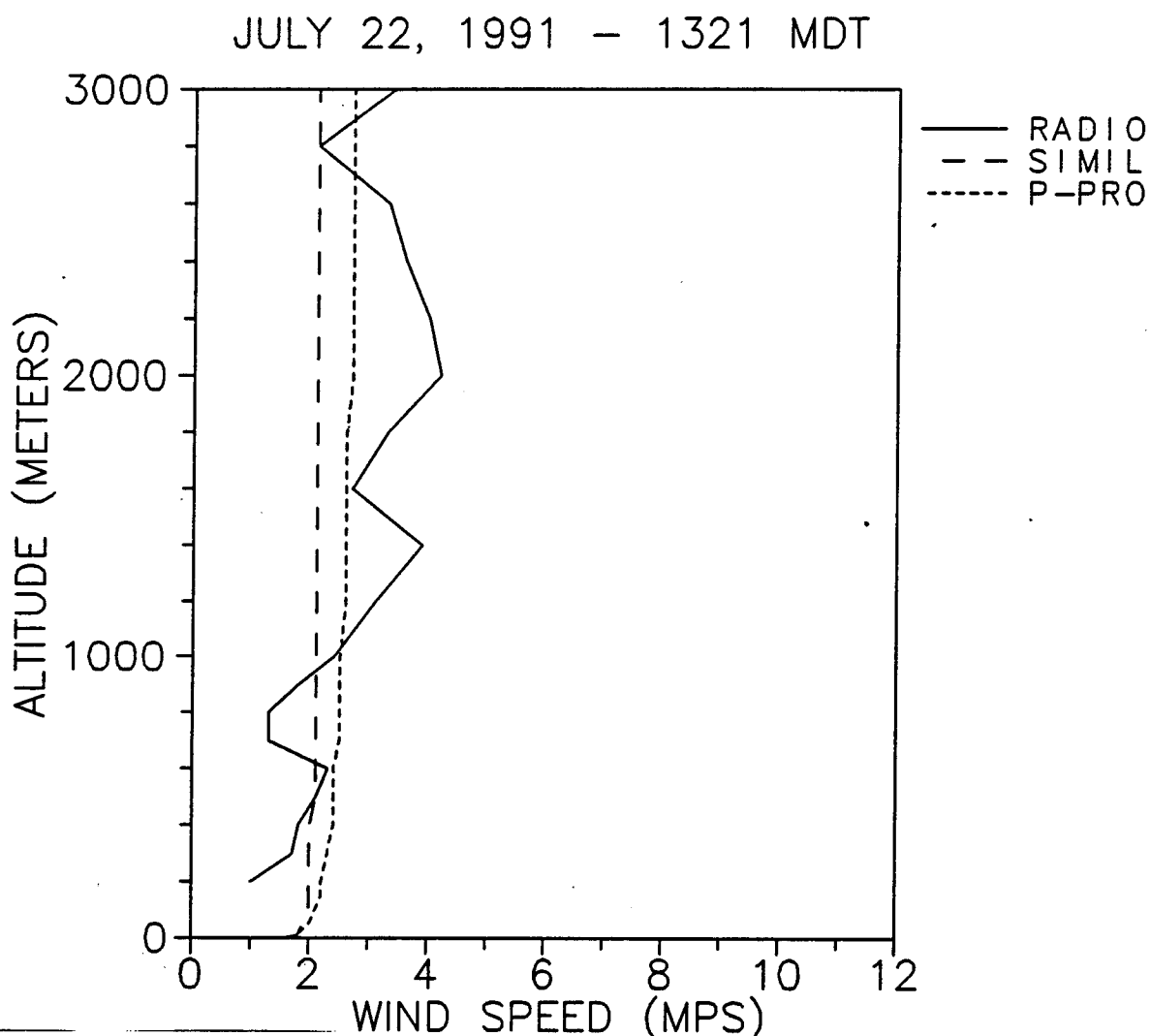


Figure 48. Comparison of wind speed data collected by a radiosonde launched July 22 at 1321 MDT with values estimated from tower measurements using Monin-Obukhov similarity and a p-profile fit.

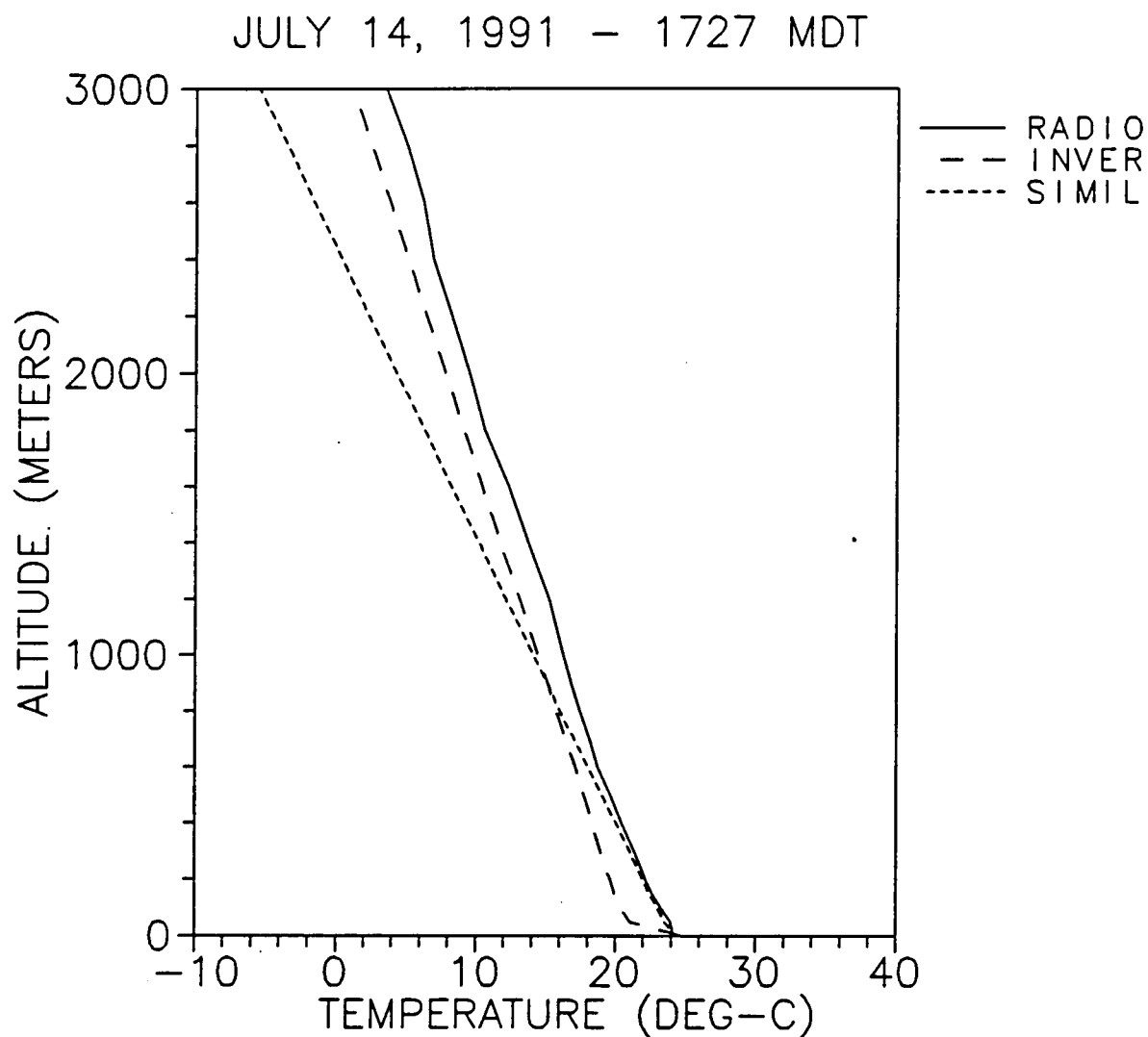


Figure 49. Comparison of temperature data collected by a radiosonde launched July 14 at 1727 MDT with values estimated from tower measurements using inversion and Monin-Obukhov similarity algorithms.

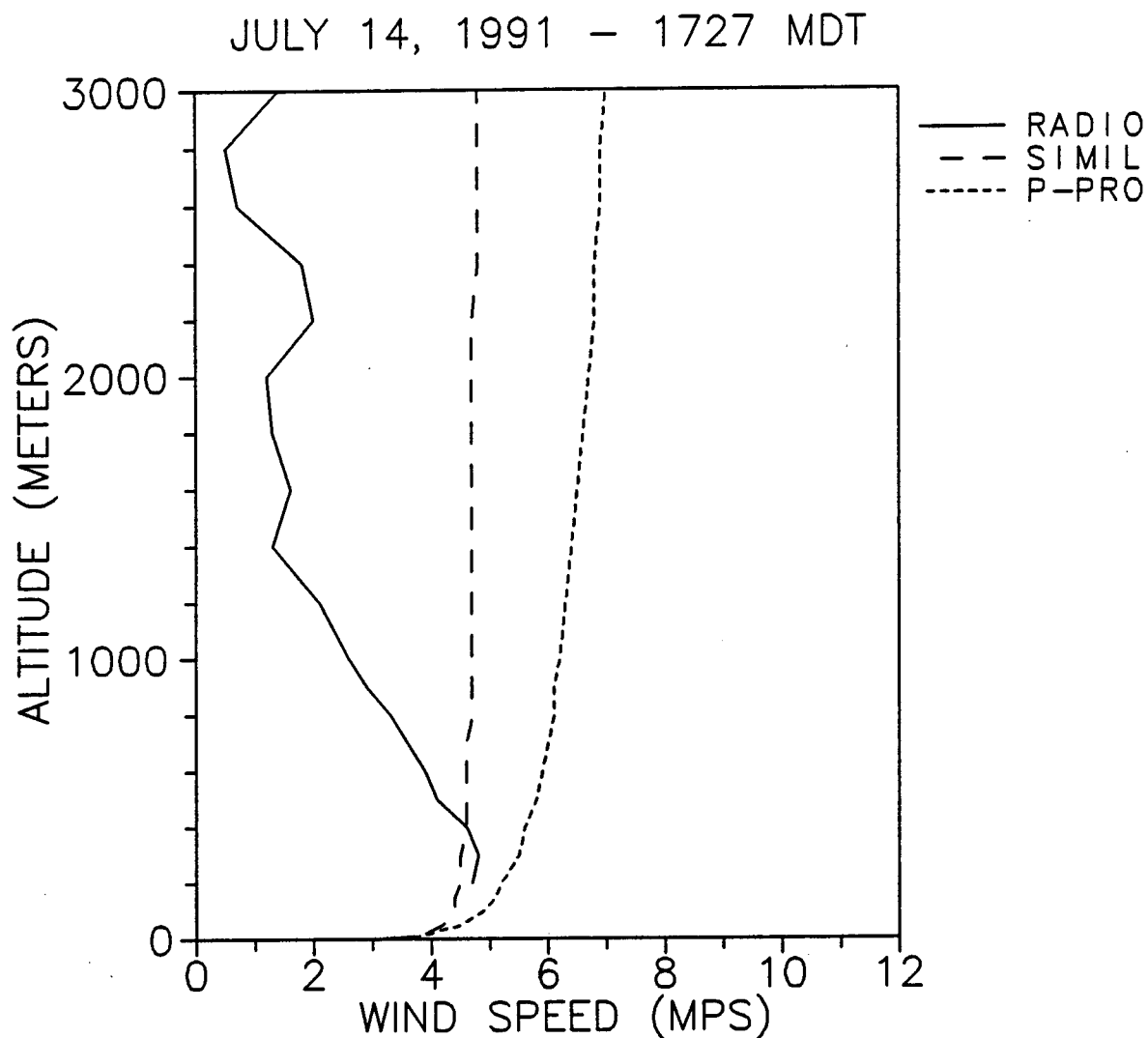


Figure 50. Comparison of wind speed data collected by a radiosonde launched July 14 at 1727 MDT with values estimated from tower measurements using Monin-Obukhov similarity and a p-profile fit.

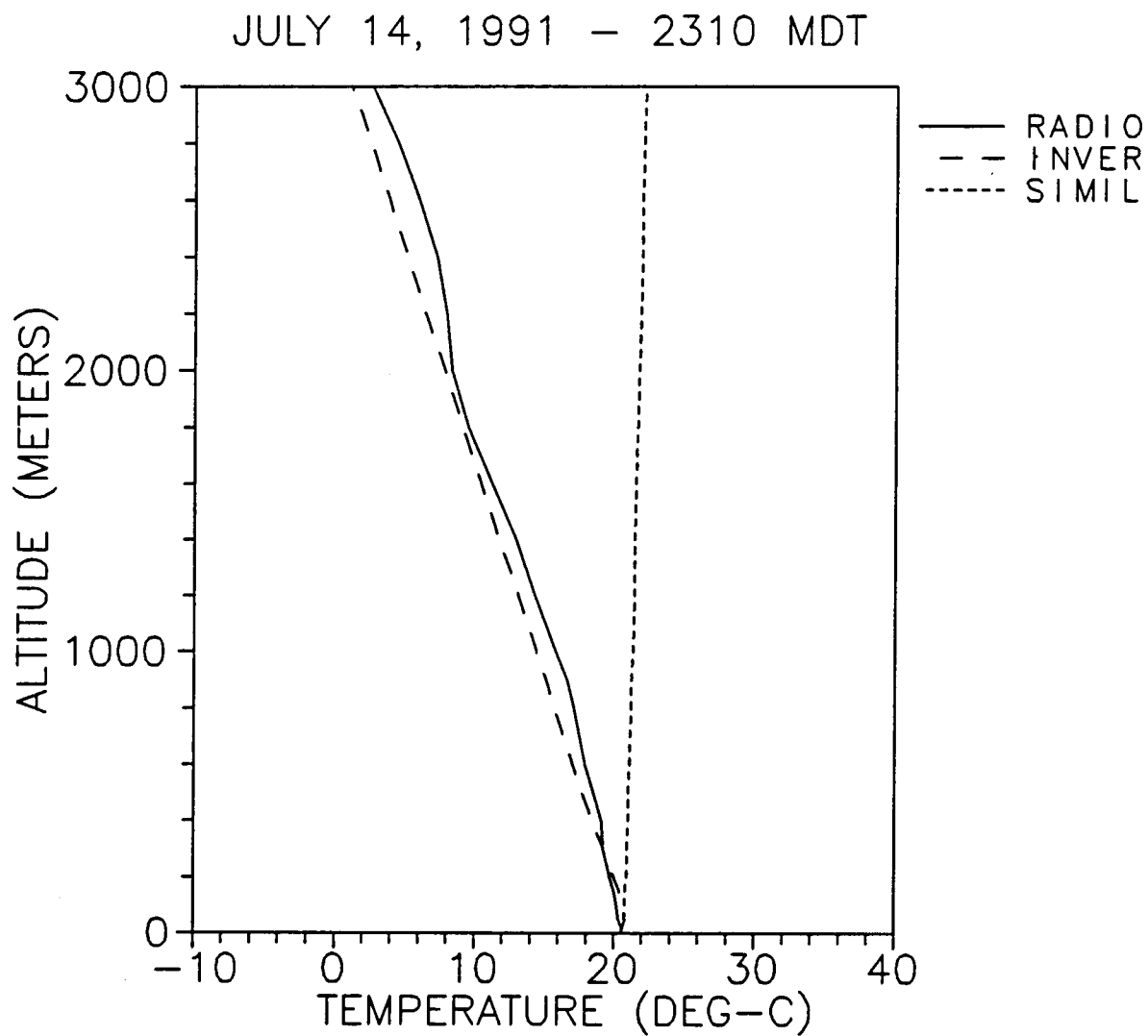


Figure 51. Comparison of temperature data collected by a radiosonde launched July 14 at 2310 MDT with values estimated from tower measurements using inversion and Monin-Obukhov similarity algorithms.

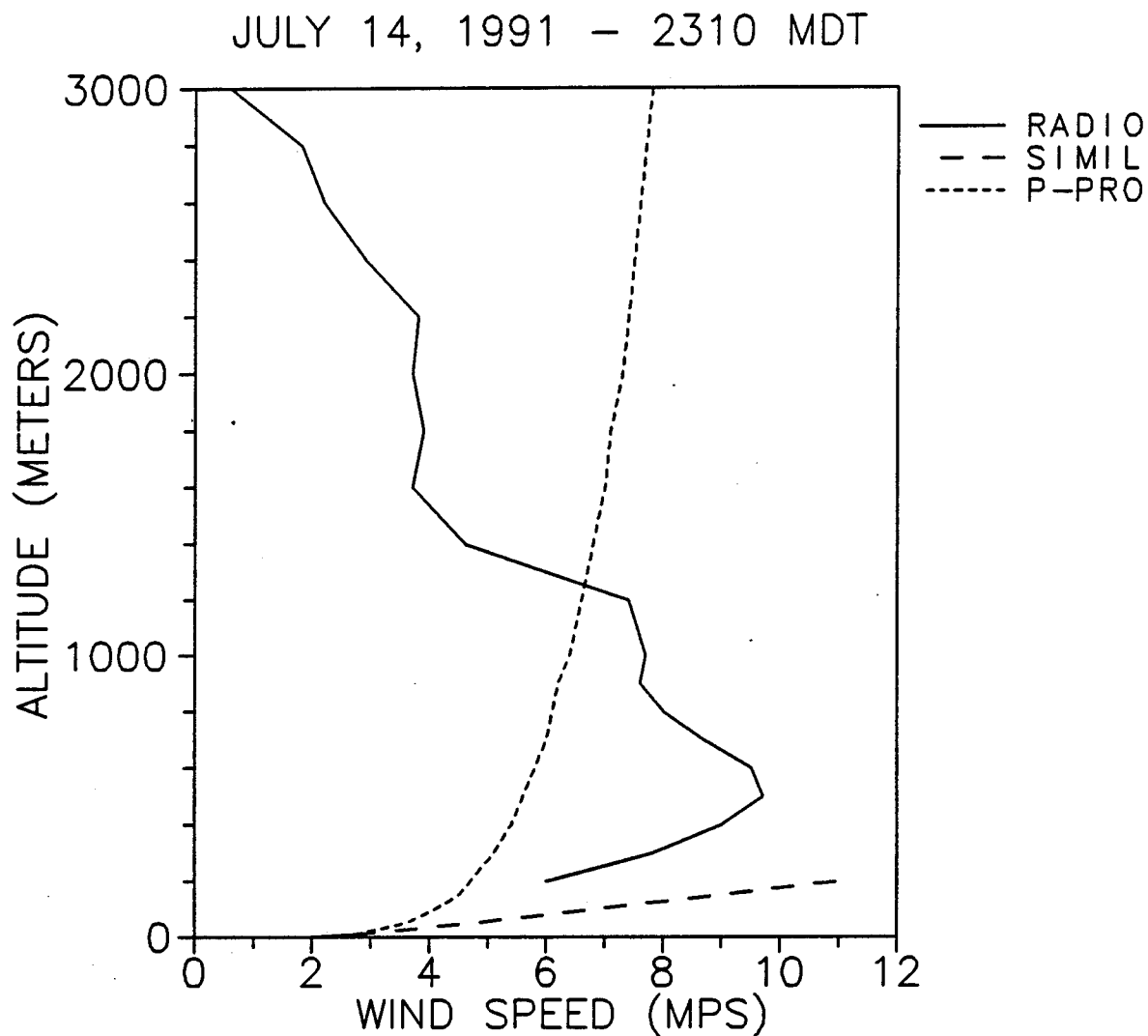


Figure 52. Comparison of wind speed data collected by a radiosonde launched July 14 at 2310 MDT with values estimated from tower measurements using Monin-Obukhov similarity and a p-profile fit.

5. Summary

Little difference was found among the predictions of the Mariah and two O'KEYPS similarity models. The statistics of the differences between measured wind speed and temperatures and data estimated by the three algorithms at 4, 16, and 30 m using 2- and 8-m tower data were almost the same for each model.

There was good agreement between the similarity model predictions at 4 and 16 m and the measured data at all times of the day. In as many as half of the night cases, no prediction was obtained because the algorithm would not converge to a solution. Predictions at 30 m agreed well with the measured data during the day, but did not agree as well at night. This diurnal variation in comparability was much more pronounced at the sodar and radiosonde measurement heights. There was good agreement up to several hundred meters above the surface between 0900 and 1900 MDT and very poor agreement outside those times between the upper-air measurements and the similarity model predictions.

Compared to the similarity predictions, the agreement between the p-profile predictions and the tower data was almost the same at 4 and 16 m and somewhat poorer at 30 m. The difference in comparabilities between the two models at the latter height was generally the same at all times of day. At the sodar and radiosonde heights, the p-profile predictions were less comparable than the similarity predictions during the day and more comparable at night. The night predictions were still considerably less comparable than the day predictions, however.

Neither the day nor night inversion algorithm estimates agreed very well with radiosonde temperature measurements within the first few hundred meters of the atmosphere. The agreement of the night inversion predictions was better than the night similarity predictions at heights above 200 m at WSMR and above 50 m at Ft. Bliss and Champaign.

References

1. Monin, A. S. and A. M. Obukhov, "Basic Regularity in Turbulent Mixing in the Surface Layer of the Atmosphere," *Trans. Geophys. Inst. (Trudy) Acad. Sci.*, USSR, 24:163-187, 1954.
2. Yaglom, A. M., "Comments on Wind and Temperature Flux Profile Relationships," *Bound.-Layer Meteor.*, 11:89-102, 1977.
3. Obukhov, A. M., "Turbulence in an Atmosphere of Non-Homogeneous Temperature," *Trans. Inst. Theor. Geophy.*, USSR, 1:95-115, 1946.
4. Kazanski, A. B. and A. S. Monin, *Izv. Akad. Nauk., S.S.S.R. Ser. Geofiz.*, Ser. 1, 79, 1956.
5. Ellison, T. H., "Turbulent Transport of Heat and Momentum from an Infinite Rough Plane," *J. Fluid Mech.*, 2:456-466, 1957.
6. Yamamoto, G., "Theory of Turbulent Transfer in Non-Neutral Conditions," *J. Meteor. Soc. Japan.*, 37:60-70, 1959.
7. Panofsky, H. A., "Determination of Stress from Wind and Temperature Measurements," *Quart. J. Roy. Meteorol. Soc.*, 89:85-94, 1963.
8. Sellers, W. D., "A Simplified Derivation of the Diabatic Wind Profile," *J. Atmos. Sci.*, 19:180-181, 1962.
9. Panofsky, H. A. and J. A. Dutton, *Atmospheric Turbulence: Models and Methods for Engineering Applications*, Wiley & Sons, New York, 1984.
10. Paulson, C. A., "The Mathematical Representation of Wind Speed and Temperature Profiles in the Unstable Atmospheric Surface Layer," *J. Appl. Meteor.* 9(12):857-861, 1970.

11. Wilson, D. K., *Reconstruction of Sound Speed Profiles from Rock Springs Meteorological Data*, Unpublished report, Pennsylvania State University, PA, 1989.
12. Rachele, H., A. Tunick and F.V. Hansen, "Mariah-A Similarity Based Method for Determining Wind, Temperature, and Humidity Profile Structure in the Atmospheric Surface Layer," To be published in *J. Appl. Meteor.* Jan/Feb 1995, 1994.
13. Frost, R., "The Velocity Profile in the Lowest 400 ft," *The Meteorological Magazine*, 76:14-17, 1947.
14. Hopfer, A. G. and A. J. Blanco, *Boundary Layer Enhancement of a Temperature and Pressure Analytic Model*, ASL-TR-0224, Army Research Laboratory, Battlefield Environment Directorate, White Sands Missile Range, NM, 1988.
15. Chintawongvanich et al. 1989.
16. Olsen, R. O., R. J. Okrasinski and F. J. Schmidlin, "Intercomparison of Upper Air Data Derived from Various Radiosonde Systems," *In Preprints: 7th Symp. on Meteor. Observations and Instrumentation*, American Meteorological Society, Boston, MA, 232-236, 1991.

Distribution

Copies

Commandant

U.S. Army Chemical School

ATTN: ATZN-CM-CC (Mr. Barnes)

Fort McClellan, AL 36205-5020

1

NASA Marshal Space Flight Center

Deputy Director

Space Science Laboratory

Atmospheric Sciences Division

ATTN: E501 (Dr. Fichtl)

Huntsville, AL 35802

1

NASA/Marshall Space Flight Center

Atmospheric Sciences Division

ATTN: Code ED-41

Huntsville, AL 35812

1

Deputy Commander

U.S. Army Strategic Defense Command

ATTN: CSSD-SL-L (Dr. Lilly)

P.O. Box 1500

Huntsville, AL 35807-3801

1

Deputy Commander

U.S. Army Missile Command

ATTN: AMSMI-RD-AC-AD (Dr. Peterson)

Redstone Arsenal, AL 35898-5242

1

Commander

U.S. Army Missile Command

ATTN: AMSMI-RD-DE-SE (Mr. Lill, Jr.)

Redstone Arsenal, AL 35898-5245

1

Commander
U.S. Army Missile Command
ATTN: AMSMI-RD-AS-SS (Mr. Anderson) 1
Redstone Arsenal, AL 35898-5253

Commander
U.S. Army Missile Command
ATTN: AMSMI-RD-AS-SS (Mr. B. Williams) 1
Redstone Arsenal, AL 35898-5253

Commander
U.S. Army Missile Command
Redstone Scientific Information Center
ATTN: AMSMI-RD-CS-R/Documents 1
Redstone Arsenal, AL 35898-5241

Commander
U.S. Army Aviation Center
ATTN: ATZQ-D-MA (Mr. Heath) 1
Fort Rucker, AL 36362

Commander
U.S. Army Intelligence Center
and Fort Huachuca
ATTN: ATSI-CDC-C (Mr. Colanto) 1
Fort Huachuca, AZ 85613-7000

Northrup Corporation
Electronics Systems Division
ATTN: Dr. Tooley 1
2301 West 120th Street, Box 5032
Hawthorne, CA 90251-5032

Commander
Pacific Missile Test Center
Geophysics Division
ATTN: Code 3250 (Mr. Battalino) 1
Point Mugu, CA 93042-5000

Commander
Code 3331
Naval Weapons Center
ATTN: Dr. Shlanta 1
China Lake, CA 93555

Lockheed Missiles & Space Co., Inc.
Kenneth R. Hardy
ORG/91-01 B/255 1
3251 Hanover Street
Palo Alto, CA 94304-1191

Commander
Naval Ocean Systems Center
ATTN: Code 54 (Dr. Richter) 1
San Diego, CA 92152-5000

Meteorologist in Charge
Kwajalein Missile Range
P.O. Box 67 1
APO San Francisco, CA 96555

U.S. Department of Commerce Center
Mountain Administration
Support Center, Library, R-51
Technical Reports
325 S. Broadway 1
Boulder, CO 80303

Dr. Hans J. Liebe
NTIA/ITS S 3
325 S. Broadway 1
Boulder, CO 80303

NCAR Library Serials
National Center for Atmos Research
P.O. Box 3000 1
Boulder, CO 80307-3000

Headquarters
Department of the Army
ATTN: DAMI-POI 1
Washington, DC 20310-1067

Mil Asst for Env Sci Ofc of
the Undersecretary of Defense
for Rsch & Engr/R&AT/E&LS
Pentagon - Room 3D129 1
Washington, DC 20301-3080

Headquarters
Department of the Army
DEAN-RMD/Dr. Gomez 1
Washington, DC 20314

Director
Division of Atmospheric Science
National Science Foundation
ATTN: Dr. Bierly 1
1800 G. Street, N.W.
Washington, DC 20550

Commander
Space & Naval Warfare System Command
ATTN: PMW-145-1G 1
Washington, DC 20362-5100

Director
Naval Research Laboratory
ATTN: Code 4110
(Mr. Ruhnke) 1
Washington, DC 20375-5000

Commandant
U.S. Army Infantry
ATTN: ATSH-CD-CS-OR (Dr. E. Dutoit) 1
Fort Benning, GA 30905-5090

USAFETAC/DNE 1
Scott AFB, IL 62225

Air Weather Service
Technical Library - FL4414 1
Scott AFB, IL 62225-5458

USAFETAC/DNE
ATTN: Mr. Glauber 1
Scott AFB, IL 62225-5008

Headquarters
AWS/DOO 1
Scott AFB, IL 62225-5008

Commander
U.S. Army Combined Arms Combat
ATTN: ATZL-CAW 1
Fort Leavenworth, KS 66027-5300

Commander
U.S. Army Space Institute
ATTN: ATZI-SI 1
Fort Leavenworth, KS 66027-5300

Commander
U.S. Army Space Institute
ATTN: ATZL-SI-D 1
Fort Leavenworth, KS 66027-7300

Commander
Phillips Lab
ATTN: PL/LYP (Mr. Chisholm) 1
Hanscom AFB, MA 01731-5000

Director
Atmospheric Sciences Division
Geophysics Directorate
Phillips Lab
ATTN: Dr. McClatchey 1
Hanscom AFB, MA 01731-5000

Raytheon Company
Dr. Sonnenschein
Equipment Division
528 Boston Post Road 1
Sudbury, MA 01776
Mail Stop 1K9

Director
U.S. Army Materiel Systems Analysis Activity
ATTN: AMXSY-CR (Mr. Marchetti) 1
Aberdeen Proving Ground, MD 21005-5071

Director
U.S. Army Materiel Systems Analysis Activity
ATTN: AMXSY-MP (Mr. Cohen) 1
Aberdeen Proving Ground, MD 21005-5071

Director
U.S. Army Materiel Systems Analysis Activity
ATTN: AMXSY-AT (Mr. Campbell) 1
Aberdeen Proving Ground, MD 21005-5071

Director
U.S. Army Materiel Systems
Analysis Activity
ATTN: AMXSY-CS (Mr. Bradley) 1
Aberdeen Proving Ground, MD 21005-5071

Director
ARL Chemical Biology
Nuclear Effects Division
ATTN: AMSRL-SL-CO 1
Aberdeen Proving Ground, MD 21010-5423

Army Research Laboratory
ATTN: AMSRL-D 1
2800 Powder Mill Road
Adelphi, MD 20783-1145

Army Research Laboratory ATTN: AMSRL-OP-SD-TP Technical Publishing 2800 Powder Mill Road Adelphi, MD 20783-1145	1
Army Research Laboratory ATTN: AMSRL-OP-CI-SD-TL 2800 Powder Mill Road Adelphi, MD 20783-1145	1
Army Research laboratory ATTN: AMSRL-SS-SH (Dr. Sztankay) 2800 Powder Mill Road Adelphi, MD 20783-1145	1
U.S. Army Space Technology and Research Office ATTN: Ms. Brathwaite 5321 Riggs Road Gaithersburg, MD 20882	1
National Security Agency ATTN: W21 (Dr. Longbothum) 9800 Savage Road Fort George G. Meade, MD 20755-6000	1
OIC-NAVSWC Technical Library (Code E-232) Silver Springs, MD 20903-5000	1

Commander
U.S. Army Research office
ATTN: DRXRO-GS (Dr. Flood) 1
P.O. Box 12211
Research Triangle Park, NC 27009

Dr. Jerry Davis
North Carolina State University
Department of Marine, Earth, and
Atmospheric Sciences 1
P.O. Box 8208
Raleigh, NC 27650-8208

Commander
U.S. Army CECRL
ATTN: CECRL-RG (Dr. Boyne) 1
Hanover, NH 03755-1290

Commanding Officer
U.S. Army ARDEC
ATTN: SMCAR-IMI-I, Bldg 59 1
Dover, NJ 07806-5000

Commander
U.S. Army Satellite Comm Agency
ATTN: DRCPM-SC-3 1
Fort Monmouth, NJ 07703-5303

Commander
U.S. Army Communications-Electronics
Center for EW/RSTA
ATTN: AMSEL-EW-MD 1
Fort Monmouth, NJ 07703-5303

Commander
U.S. Army Communications-Electronics
Center for EW/RSTA
ATTN: AMSEL-EW-D 1
Fort Monmouth, NJ 07703-5303

Commander
U.S. Army Communications-Electronics
Center for EW/RSTA
ATTN: AMSEL-RD-EW-SP 1
Fort Monmouth, NJ 07703-5206

Commander
Department of the Air Force
OL/A 2d Weather Squadron (MAC) 1
Holloman AFB, NM 88330-5000

PL/WE 1
Kirtland AFB, NM 87118-6008

Director
U.S. Army TRADOC Analysis Center
ATTN: ATRC-WSS-R 1
White Sands Missile Range, NM 88002-5502

Director
U.S. Army White Sands Missile Range
Technical Library Branch
ATTN: STEWS-IM-IT 3
White Sands Missile Range, NM 88002

Army Research Laboratory
ATTN: AMSRL-BE (Mr. Veazy) 1
Battlefield Environment Directorate
White Sands Missile Range, NM 88002-5501

Army Research Laboratory
ATTN: AMSRL-BE-A (Mr. Rubio) 1
Battlefield Environment Directorate
White Sands Missile Range, NM 88002-5501

Army Research Laboratory
ATTN: AMSRL-BE-M (Dr. Niles) 1
Battlefield Environment Directorate
White Sands Missile Range, NM 88002-5501

Army Research Laboratory
ATTN: AMSRL-BE-W (Dr. Seagraves) 1
Battlefield Environment Directorate
White Sands Missile Range, NM 88002-5501

USAF Rome Laboratory Technical
Library, FL2810 1
Corridor W, STE 262, RL/SUL
26 Electronics Parkway, Bldg 106
Griffiss AFB, NY 13441-4514

AFMC/DOW 1
Wright-Patterson AFB, OH 03340-5000

Commandant
U.S. Army Field Artillery School
ATTN: ATSF-TSM-TA (Mr. Taylor) 1
Fort Sill, OK 73503-5600

Commander
U.S. Army Field Artillery School
ATTN: ATSF-F-FD (Mr. Gullion) 1
Fort Sill, OK 73503-5600

Commander
Naval Air Development Center
ATTN: Al Salik (Code 5012) 1
Warminster, PA 18974

Commander
U.S. Army Dugway Proving Ground
ATTN: STEDP-MT-M (Mr. Bowers) 1
Dugway, UT 84022-5000

Commander
U.S. Army Dugway Proving Ground
ATTN: STEDP-MT-DA-L 1
Dugway, UT 84022-5000

Defense Technical Information Center
ATTN: DTIC-OCF 2
Cameron Station
Alexandria, VA 22314-6145

Commander
U.S. Army OEC
ATTN: CSTE-EFS 1
Park Center IV
4501 Ford Ave
Alexandria, VA 22302-1458

Commanding Officer
U.S. Army Foreign Science & Technology Center
ATTN: CM 1
220 7th Street, NE
Charlottesville, VA 22901-5396

Naval Surface Weapons Center
Code G63 1
Dahlgren, VA 22448-5000

Commander and Director U.S. Army Corps of Engineers Engineer Topographics Laboratory ATTN: ETL-GS-LB Fort Belvoir, VA 22060	1
U.S. Army Topo Engineering Center ATTN: CETEC-ZC Fort Belvoir, VA 22060-5546	1
Commander USATRADO ATTN: ATCD-FA Fort Monroe, VA 23651-5170	1
TAC/DOWP Langley AFB, VA 23665-5524	1
Commander Logistics Center ATTN: ATCL-CE Fort Lee, VA 23801-6000	1
Science and Technology 101 Research Drive Hampton, VA 23666-1340	1
Commander U.S. Army Nuclear and Chemical Agency ATTN: MONA-ZB, Bldg 2073 Springfield, VA 22150-3198	1
Record Copy	3
Total	89